CENTRO BRASILEIRO DE PESQUISAS FÍSICAS

DOCTORAL THESIS

Emerging dynamics and its application in attempts to model a quantum measurement process

Author:
Gabriel Dias CARVALHO

Supervisor:
Dr. Fernando DE MELO

A thesis submitted in fulfillment of the requirements for the degree of Doctor of Physics

in the

Quantum Information group
Coordenação de Física Teórica

August 28, 2019

"EMERGING DYNAMICS AND ITS APPLICATION IN ATTEMPTS TO MODEL A QUANTUM MEASUREMENT PROCESS"

GABRIEL DIAS CARVALHO

Tese de Doutorado em Física apresentada no Centro Brasileiro de Pesquisas Físicas do Ministério da Ciência Tecnologia e Inovação. Fazendo parte da banca examinadora os seguintes professores:

Fernando da Rocha Vaz Bandeira de Melo – Presidente/Orientador/CBPF

Gabriel Teixeira Landi - USP

Thiago Rodrigues de Oliveira - UFF

Evaldo Mendonça Fleury Curado - CBPF

Raúl Oscar Vallejos - CBPF

Rio de Janeiro, 18 de julho de 2019.

"Não sei para onde estou indo, mas sei que estou no meu caminho."

Raul Seixas

CENTRO BRASILEIRO DE PESQUISAS FÍSICAS

Abstract

Coordination Name
Coordenação de Física Teórica

Doctor of Physics

Emerging dynamics and its application in attempts to model a quantum measurement process

by Gabriel Dias CARVALHO

Quantum theory is undoubtedly a successful physics theory: it is consistent, its mathematical formalism is well founded and the laws that govern the small scale phenomena are, mostly, well described by quantum theory. However, in our daily lives we do not experience quantum phenomena. Classical physics is well enough to describe the daily world. In this thesis we use quantum information theory tools, particularly quantum channels, to contribute to the search for an answer to the question: what is the real role/importance of the impossibility of accessing all the degrees of freedom of a quantum system to emergence of the effective, "classical", realm and, parallel, the "death" of quantum features? Such impossibility is translated mathematically via a coarse-graining quantum channel. We start by developing a framework to investigate what kinds of dynamics emerge when one does not have full access to the degrees of freedom of a given system. As an application of the developed general framework, we present attempts to model a quantum measurement process: a system to be measured consisting of a qubit in a superposition interacts with a measuring apparatus consisting of a spin coherent state (first attempt) and a N qubit state (second attempt). Looking at the emerging, effective description of the apparatus, we were able to recover the superposition coefficients of the system (in both attempts). In the first attempt, we were also able to visualize the death of quantum correlations between system and apparatus and the creation of classical ones. In the second, we managed to observe the death of quantum coherences in the apparatus' effective state, obtained through the coarse-graining action. A situation akin to decoherence, although it was not necessary to evoke any interaction with the surrounding environment.

Acknowledgements

Agradeço à minha família, principalmente Joaquim, Alessandra e Mayra, pelo amor e por me darem condições de atingir meus objetivos e buscar minha felicidade. Agradeço à Fernando, meu orientador, pela amizade, orientação, oportunidades, discussões e por tantos momentos agradáveis e enriquecedores.

Agradeço aos professores e pesquisadores presentes na minha banca de qualificação do doutorado, Prof. Ruynet e Prof. Evaldo, e na defesa de tese, Prof. Gabriel Landi, Prof. Thiago Rodrigues, Prof. Raul Vallejos e novamente Prof. Evaldo. Obrigado pelas contribuições, estímulos, disponibilidade e atenção.

Agradeço à comunidade CBPF, professores, pesquisadores, funcionários e pós-graduandos. Levarei amizades e boas lembranças para toda a vida. Em especial meu grande amigo, conterrâneo e forrozeiro, Pedro. Agradeço aos colaboradores e amigos que a Física me trouxe nesses anos. Hoje me sinto muito feliz com o que faço, e muito devo a vocês.

Agradeço aos amigos cariocas, fluminenses e de outras partes do Brasil que compartilhei vivências durante minha estadia no estado do RJ. Em especial à comunidade do paraíso Lumiar e à família da minha companheira, que hoje considero também como minha família. Fui muito bem recebido e tratado com muito carinho e amor.

Agradeço aos meus grandes, bons e velhos amigos da cidade (do) Mangue, da minha amada cidade Recife. Sempre de braços abertos para me receber e trocar energias nas minhas visitas e no meu retorno. Ao meu grande amigo, conselheiro, um dos gurus profissionais, José Américo. Faltam palavras para expor o quanto já foi e continua sendo importante na minha jovem carreira.

Agradeço à quem mais me estimulou a continuar na vida de cientista e professor, certamente sem saber o quanto certos comentários, conversas e discussões foram marcantes e transformadores na minha vida. E também grande responsável pela minha escolha de filosofia de vida, a minha avó Carmem, dotada de enorme sabedoria.

Por fim, mas no hall das mais importantes figuras, agradeço demais à minha companheira (no sentido mais profundo da palavra) de aventuras, de risadas, de loucuras, Clara. Me sinto muito amado, realmente um felizardo por te ter ao meu lado :D.

Contents

List of Figures

List of Tables

Dedico ao povo Pernambucano, do litoral ao sertão, alegre e guerreiro . . .

Chapter 1

Introduction: history and motivation

1.1 Late XIX (nineteenth) and early XX (twentieth) centuries: the birth of modern physics

The nineteenth century was a period in which the humankind watched and achieved big scientific advances and inventions, responsible for a modernization never seen before and considerable improvement in the quality of life of the world population [3]. To cite key aspects, we had the industrial revolution taking place initially in Great Britain and spreading to other countries. Advances in medicine, disease prevention and the understanding of human anatomy contributed to the population growth and to a minimal health security. Urbanization intensified in several countries of the globe and slavery was greatly reduced, particularly in Brazil (1888) [3, 4].

It wasn't different in the domain of Physics. In 1873, James Clerk Maxwell (1831-1879) published his *Treatise on Electricity and Magnetism* [5], considered one of the most significant events of that century, establishing a robust theoretical underpinning to physical observations. Light, electric and magnetic effects, hitherto seen as different phenomena, were different manifestations of *electromagnetic radiation*, and were now unified in an *electromagnetic theory*.

The German physicist Heinrich Rudolf Hertz (1857-1894) was the one who, between 1886 and 1889, conduct a series of experiments that first detected effects of electromagnetic radiation, giving experimental support to the theory of Maxwell [6, 7, 8]. By the same period and working on similar experimental realizations, Hertz discovered an effect that would be one of the responsible for the birth of one of the most intriguing theories in physics just two decades latter, the *photoelectric effect* [9].

Hertz was still a child when also a German physicist called Gustav Robert Kirchhoff (1824-1887), among important contributions, studied the radiation emitted by thermal bodies. Kirchhoff was the first to state the *black-body radiation problem* and to recognize its importance [10].

Many put the black-body radiation problem and the photoelectric effect as the foundation stones for the construction and development of quantum theory [11]. The physical theories established at that time were not able to explain and understand what nature had shown in these experimental achievements.

Note that by the end of the nineteenth century, science was entering the domain of small scales in length and beginning to create mechanisms that would allow to understand the matter in its most fundamental constituents. And we can't dissociate such events from technological advances in experimental physics and changes in paradigms taking place in the world. The door to a new universe of phenomena and philosophical discussions was opening up.

But not all the scientific community seemed to realize the revolution that was underway. Lord Kelvin (1824-1907), mathematical physicist and engineer, important and respected scientist of that time, said around 1900 at the British Association for the advancement of Science something like "There is nothing new to be discovered in physics. All that remains is more and more precise measurement" [12], which is symbolic to represent the skepticism that the new changes would face.

1.1.1 A new way of looking at nature

Contemporary to Lord Kelvin's commentary is the work of the German physicist Max Planck (1858-1947) solving the black-body radiation problem [13]: how does the intensity of the electromagnetic radiation emitted by a black-body depend on the frequency of the radiation and the temperature of the body? The problem was well placed and responded experimentally, but no theory could explain so far.

After more than five years working on such problem and some unsuccessful attempts, Planck was able to explain the experimental results satisfactorily making use of an idea already considered by the Austrian physicist Ludwig Eduard Boltzmann (1844-1906) back in 1877: Boltzmann suggested that the energy levels of a physical system could be discrete [14].

Deeply suspicious of the philosophical and physical implications of such an interpretation, Planck assumed that the electromagnetic radiation could only be emitted in a *quantized* form [13]. I.e., the energy could only be a multiple of an elementary unit: $E = h\nu$. He has considered at first this assumption purely formal, and confessed that had not thought much about it. But this simple equation gave the kick-start for the development of quantum theory, and the Nobel Prize to Max Planck in 1918.

Five years latter, in 1905, the German physicist Albert Einstein (1879-1955) published a paper explaining theoretically the photoelectric effect [15]. To do so, Einstein postulated that all electromagnetic radiation can be divided into a finite number of energy quanta that are localized points in space. Translated from his own words:

> "According to the assumption to be contemplated here, when a light ray is spreading from a point, the energy is not distributed continuously over ever-increasing spaces, but consists of a finite number of 'energy quanta' that are localized in points in space, move without dividing, and can be absorbed or generated only as a whole".
>
> A. Einstein, 1905.

Currently it is known that photons cannot be sharply localized points in space, as pointed out by A. Einstein [16]. Another important contribution from the same scientist was the article about heat capacity of solids [17].

I would like to make it clear that the chronological presentation of facts, ideas and arguments that contributed to the development of quantum theory comes as an attempt to contextualize and motivate the reader. I believe that this kind of exposure creates a background that enriches and facilitates the understanding of our work. Reading and trying to understand past discussions is one of my greatest sources of learning and motivation, and I have no audacity to judge any of the arguments. Only when necessary for the understanding of our thesis work I will make comments expressing my understanding.

The contributions of Planck and Einstein were complementary and, together, gave more credibility to both; but it was not free from criticism, even from the authors themselves. In 1913, the Danish physicist Niels Henrik David Bohr (1885-1962)

adapted the atomic model of the British physicist Ernest Rutherford (1871-1937) using the ideas of quantization developed by Planck and was able to explain the spectral lines of the hydrogen atom [18], representing an important step in the consolidation of quantum theory.

In the following years, quantum theory didn't stop receiving important theoretical and experimental contributions: Stern-Gerlach experiment (1922) [19, 20, 21] showing the quantized nature of spin; the theory of matter waves (1924) from the French physicist Louis De Broglie (1891-1987) [22]; the development of matrix mechanics by Heisenberg, Born and Jordan (1926) [23, 24]; the Schrodinger's wave equation (1926) [25] and Dirac's equation (1928) [26] and the uncertainty principle by Heisenberg (1927) [27], to cite just a few.

1.2 Interpretation discussions

Although the quantum mathematical formalism was consistent and explain much of the experimental results, its implications on the way nature would behave at the Planck scale gave rise to different interpretations, leading to philosophical discussions. Some remain to this day.

It's difficult to isolate the different open topics and discussions, since they are closely related to each other. For now on, I will exhibit some ideas of different currents of thought of quantum theory from the perspective of a very intriguing topic: the *quantum measurement problem* [28].

We shall start by analyzing the Schrodinger equation, published in 1926 by the Austrian physicist Erwin Schrodinger (1887-1961) [25]:

$$i\hbar\frac{\partial}{\partial t}\left|\Psi(t)\right\rangle = H\left|\Psi(t)\right\rangle, \tag{1.1}$$

where H is the Hamiltonian operator which dictates the deterministic temporal evolution of the state vector of the system $|\Psi(t)\rangle$. Since we have here a first order linear differential equation and a linear Hilbert state space, if $|\Psi_a(t)\rangle$ and $|\Psi_b(t)\rangle$ are solutions of 1.1, any linear combination of both, for example $|\Psi_c(t)\rangle = \alpha\,|\Psi_a(t)\rangle + \beta\,|\Psi_b(t)\rangle$ also is. The probability for the system to be found in state $|\Psi_a(t)\rangle$ or $|\Psi_b(t)\rangle$ after a measurement procedure is proportional to $|\alpha|^2$ and $|\beta|^2$ (Born's rule), respectively.

This is one of the most fundamental and revolutionary principles in quantum mechanics, and well known these days as the *quantum superposition principle*. Until the time of Schrodinger's wave equation article, no one had never heard about something similar in physics. It was known from classical mechanics the superposition of waves that propagate in material media, for instance water waves, or the superposition of forces acting in a body, but in the way Schrodinger's equation suggested it sounded very strange.

To a certain extent, the conclusions that we can draw about nature's intrinsic behavior looking at the quantum superposition principle are a matter of interpretation. During the decade of 1920 a very strong way of thinking on the meaning of quantum mechanics, advocated by illustrious scientists as Niels Bohr and Werner Heisenberg, became known as the Copenhagen interpretation.

According to this group of scientists from the University of Copenhagen, while an observable of a physical system is not measured, it cannot be said that the system is in a well-defined eigenstate of the observable, but in a *superposition* of them. The act of measuring would break the superposition state leading to the reduction to

only one possible state after the measurement. This phenomenon is called the wave function collapse. Everything that quantum mechanics can predict is the probability that a measurement of a specific observable produce a specific result. In other words, once written the state vector of the system on the basis of eigenstates of an observable A, it would remain in a superposition until it interacts with, or be observed by the external world.

In 1935, A. Einstein, B. Podolsky and N. Rosen, working together at Princeton, published a paper [29] where they argue that the description of reality as given by the wave function is not complete. Consequently, according to the authors, the concepts of the quantum theory may be said to *not be* satisfactory. They used the following reality criterion: "If, without in any way disturbing the system, we can predict with certainty the value of a physical quantity, then there exists an element of physical reality corresponding to this physical quantity".

Lets understand the key aspect which led them to this conclusion. Considering two particles that interact for a finite period of time and are then separated, they expand the total wave function of the system in a series of orthogonal functions in two different ways:

$$\Psi(x_1, x_2) = \sum_{n=1}^{\infty} \psi_n(x_2) u_n(x_1) \;\; or \;\; \Psi(x_1, x_2) = \sum_{s=1}^{\infty} \phi_s(x_2) v_s(x_1), \tag{1.2}$$

where the functions $\psi_n(x_2)$ and $\phi_s(x_2)$ are eigenfunctions of momentum and position operators for the particle 2, respectively, and the functions $u_n(x_1)$ and $v_s(x_1)$ are eigenfunctions of some observable A and B for the particle 1, respectively.

Now, using the left total wave function in equation 1.2, if it were to measure the observable A for the first particle, it would be possible to gain information about the momentum of particle 2 without disturbing it. On the other hand, using the right total wave function in equation 1.2, if it were to measure the observable B for the first particle, it would be possible to gain information about the position of particle 2, again without disturbing it. But quantum theory says that these two quantities (momentum and position of particle 2) cannot have simultaneously reality. Then, the theory would not provide a complete description of the physical reality, according to the authors.

The thought experiment in the EPR paper shows strange consequences of the quantum superposition principle and the collapse of the wave function, inducing them to question the completeness of quantum theory. The theory seemed to be correct in the sense of its concordance with experimental results, but from the authors' point of view it wasn't giving a satisfactory description of reality. It is interesting to note here the beginning of the debates involving the concepts of reality, locality and entanglement, although the latter wasn't well defined at the time.

Inspired by the EPR article, also in 1935, Schrodinger published his famous cat thought experiment paper [30], showing how absurd he found the Copenhagen interpretation about the quantum superposition principle, and contributing to the good discussions that took place in those years.

The situation is quite simple. Imagine a cat inside a box with a glass tube with poison. Inside the box there is also a device that with certain probability causes the glass to break, leading to the death of the cat. Naturally, there is some nonzero probability of the glass not to break, and the cat remain alive. According to Schrodinger, the Copenhagen interpretation implies that, as long as one does not open the box, the cat remains both dead *and* alive. It wasn't his idea to defend the assumption that

a cat could really exist in such superposition, but to show how absurd the current interpretations could be when extrapolated to the macro-world.

Schrodinger's cat paper is an evincive of concern related to the coverage limits of quantum theory and its applications and consequences when extrapolated to the macro-world, the world that we experience in our daily lives. His thought experiment is used up to now in attempts of understanding alternative interpretations of quantum theory, their weaknesses, and is often evoked in discussions of the measurement problem and the *quantum-classical transition*.

The main motivation of all the research done involving this thesis is to gain insight, understand better and give some contribution to the discussion of the quantum-classical transition from the perspective of the quantum measurement problem, studying emerging dynamics from coarse-grained quantum systems and trying to model a measurement process.

Despite of the strangeness pointed out by Schrodinger, I would like to present some questions regarding the measurement process and collapse of wave function, taking advantage of the hook to introduce my understanding regarding some interpretations of the meaning of quantum theory mathematical formalism.

1.2.1 Measurements in quantum theory

Despite the strange and counter-intuitive implications of the superposition principle, its mathematical formulation is constantly tested and able to explain the experimental evidences. The task was to reconcile the greatness of states' possibilities at the underlying quantum level, guaranteed by the hugeness of Hilbert space, to our observations of just a few and well defined macroscopic classical states. Assuming that quantum mechanics talks about reality, why does the world seem classical to us despite the quantum nature of its fundamental constituents and the possibility of arbitrary superpositions at that level?

The diffraction experiment with electrons performed by Davisson and Germer in 1927 [31], supporting the wave-particle duality, kindled the debate about the fundamental importance of understanding the role of the experimentalist/observer, or in other words the interaction between the system to be measured and the world around it, in order to explain satisfactorily the acquired results.

The first to model a generic measurement process was John Von Neumann (1903-1957) in his work *Mathematical Foundations of Quantum Mechanics* (1932) [32], originally published in German. Von Neumann puts as a fundamental requirement of the scientific point of view: it must be possible to describe the subjective perception of the observer (what he call "extra-physical process") as if it were in reality in the physical world.

Suppose we would like to measure some property of a system, for example length or temperature, using a measuring apparatus. After the system-apparatus interaction, the observer must perceive the response of the measuring device to gain information about the system. One can include as the apparatus for example the measuring device up to the retina of the observer, or even up to the brain. But, at some point (and one is free to choose this boundary), one end up with "and it is perceived by the observer".

Accordingly, when modelling a measurement process we must divide the world into two parts, the observed system and the observer. In modelling the physical processes taking place on the first part, one can be arbitrarily precise. However, this is not true for the second. The boundary between them is arbitrary and can be put as deep as desired, for example inside the observer body, but it must exist in order to

have a model for a measurement process. The point is that in an experiment we can only say that an observer made a subjective observation, and never that a physical quantity has a certain value.

Following this thought, Von Neumann works on two models of measurements: premeasurement without detection and measurement with irreversible detection. In both, treating the apparatus as a quantum object. Suppose we have a system to be measured S and a measurement apparatus A initially in states $|\Psi_S\rangle = \sum_n c_n |\psi_n\rangle$ and $|\Psi_A\rangle = |a_0\rangle$, respectively. They interact with each other via a unitary evolution U:

$$|\Psi_S\rangle |\Psi_A\rangle = \sum_n c_n |\psi_n\rangle |a_0\rangle \xrightarrow{U} \sum_n c_n |\psi_n\rangle |a_n\rangle , \tag{1.3}$$

where the vectors $|a_n\rangle$ are pointer states, corresponding to macroscopic and distinguishable positions of the detector's pointer, each one related to the outcome of a measurement of the system in state $|\psi_n\rangle$.

The evolution process is attributed as premeasurement. Calculating the reduced density matrix for the system we could see that it is left in an ensemble of possible states $\sum_n |c_n|^2 |\psi_n\rangle\langle\psi_n|$, each one with probability $|c_n|^2$. As the name suggests, this process does not suffice to conclude that a measurement has been finished. Therefore, we need an additional physical process, for example some collapse mechanism, to make it clear how to account for the definite pointer positions that are perceived in a measurement.

A natural question is: why do we always perceive the pointer in a well defined position, representing a well defined apparatus state $|a_n\rangle$? This is one of the aspects that compose the quantum measurement problem, the *problem of definite outcomes*: what selects a specific well defined outcome? The second aspect is the *problem of the preferred basis*: after the system-apparatus interaction, the total final state $|\Psi_{SA}(t)\rangle$ can be written as a linear combination of basis' elements in different ways, depending on the basis chosen. That is, the expansion of the total final state is not unique. Consequently, the measured observable is not uniquely defined.

Now we can see the real importance in understanding the quantum measurement problem, or else quantum theory will not be complete. Understanding how to perform measurements will bring to science new physics, predictions to be tested. It is more than a matter of interpreting the mathematical formalism.

On the light of Copenhagen interpretation, the world is divided in two classes of systems: the underlying, small, world where the superposition principle works, and the macro, daily-life world, where the superposition principle isn't observed. The measurement consists in interacting some system which can be applied the superposition principle with one system which it cannot. In such an interpretation, the random collapse has a central role. But there are other interpretations of quantum theory that try to elucidate the measurement problem each in its own way. Lets start with the so called many-worlds interpretation [33, 34].

In some many-worlds formalism there is no distinction between systems in which the superposition principle holds or doesn't. It is universal. All the possible outcomes of a measurement actually happen; there is no collapse as understood by Copenhagen interpretation. Everything happen and is happening right now, but in different worlds. And we are not aware of all, but just one, the one which we live, experience.

Notice that the observer has a active role here, it is the one who continuously breaks the superposition of the state vector of the system, making the experience shows the result that it actually shows. It feels like a transfer of responsibility from the collapse of the wave function, the interaction, to the observer. The feeling is as

if the problem persists. Another important point is that the occurrence of all possible outcomes of a measurement together with the determinism of the Schrodinger's equation convert quantum mechanics in a fully deterministic theory.

Applied to the Schrodinger's cat thought experiment, both dead and alive cat still persist after the box is open. The initial situation with one observer and a dead and alive cat inside a box split in two new configurations: an observer looking at a dead cat and an observer looking at an alive cat, but there is no communication or interaction between the two. If we are the observer, however, we just experience one of the possibilities.

In his 1951 paper, David Bohm (1917-1992) [35, 36] suggested an interpretation of quantum theory in terms of what he called "hidden" variables. Bohm highlights that the usual quantum theory interpretation, or orthodox Copenhagen interpretation, is based on two mutually consistent assumptions that cannot be verifiable if true. They are: 1. The wave function with its probability interpretation determines the most complete possible specification of the state of an individual system; 2. The process of transfer of a single quantum from observed system to measuring apparatus is inherently unpredictable, uncontrollable, and not analyzable. To avoid assumptions that cannot be tested, he proposes to study the consequences of postulates that would contradict assumptions 1 and 2, and suggests a new interpretation.

In Bohmian mechanics, a wave function of a quantum system still evolves according to the Schrodinger's equation, but it only provides a partial description of the system. It is necessary to specify the actual positions of the particles that compose the system. Such positions evolves according to an equation which expresses the velocities of the particles in terms of the wave function. Therefore, the configuration of a system of particles evolves via a deterministic trajectory drawn by the wave function.

Believing that the wave function does not provide a complete description of physical reality, as posed in the conclusion of the EPR paper, in 1949 A. Einstein, when questioned about a theory which would give a more complete description of physical reality, remarked [37]: "the statistical quantum theory would...take an approximately analogous position to the statistical mechanics within the framework of classical mechanics". Bohmian mechanics may fit this position. Indeed, Bohm thanks Einstein for stimulating discussions in the acknowledgments of his 1951 paper.

But, how does Bohmian mechanics justify the wave function collapse? What the theory tells us about a measurement process? Those questions are answered in the second part of his 1951 paper [36].

The procedure is as follows: in a measurement process we have a system to be measured and an apparatus, which interact with each other. After the interaction, correlations are created between the both in such a way that each state of the observed system is associated with a range of states in the apparatus. The error, uncertainty in the measurement is related with a lack of definition in these correlations.

We have then what Bohm calls an *impulsive measurement*, i.e., a very strong interaction occurring in a short time interval. This is sufficient to allow neglect the system and apparatus Hamiltonian, leaving as the only relevant contribution the interaction Hamiltonian H_I.

With the objective of measuring an generic observable O in a system of particles S we must specify its coordinates positions $\vec{x}$ and also the relevant coordinates y concerning the apparatus. In order to study a concrete example, Bohm considered as the interaction Hamiltonian $H_I = cOp_y$, with c constant and p_y the momentum conjugate to y.

A key aspect of Bohmian mechanics is the role of the wave function, here called the field Ψ. In this example it is described by a function of $\vec{x}$ and y. The motion of a representative point $(\vec{x}, y)$ in its four-dimensional space, also called the *configuration space* is dictated by forces produced by the field Ψ. How to find $\Psi(\vec{x}, y, t)$? Schrodinger's wave equation.

Making the assumption of independence of system and apparatus just before the interaction and writing $\Psi(\vec{x}, y, 0) = g_0(y) \sum_q c_q \psi_q(\vec{x})$, with g_0 a packet centred in $y = 0$ with width Δy; $\psi_q(\vec{x})$ eigenfunctions of the observable O with eigenvalues q; and c_q constants, he arrived at the following equation for the field [36] at time t:

$$\Psi(\vec{x}, y, t) = \sum_q c_q \psi_q(\vec{x}) g(y - cqt). \tag{1.4}$$

As shown in equation 1.4, the interaction created correlations between the system and apparatus, visible through the presence of q in the argument of g. What does it really mean? Notice that the center of the qth packet in y space is at $y = ctq$, and consequently the separation of centers of adjacent packets is $\delta y = ct\delta q$, dependent on the product ct. In this expression is highlighted the importance of intensity and time duration of the interaction.

During the interaction between S and the apparatus, the wave function $\Psi(\vec{x}, y, t)$ becomes very complicated. Eventually, if the interaction lasts long enough, packets $g(y - cqt)$ corresponding to different values of q will cease to overlap in y direction. If we have a sufficient big product ct, the adjacent packets separation will be greater than the packets width Δy, being large enough to be classically describable.

Once coordinate y, corresponding to the apparatus, is in a region of a specific packet, it will remain within thereafter, since in the intermediate regions the probability density $|\Psi(\vec{x}, y, t)|^2$ is almost zero. In other words, after long enough the points $(\vec{x}, y)$ will stay in a region of configuration space corresponding to a specific, now fixed, q. This specific packet will determine the result of the measurement, obtained by the experimentalist when looking at the apparatus. Finally, we can replace the full wave function in equation 1.4 by a new normalized one:

$$\Psi(\vec{x}, y, t) = \psi_q(\vec{x}) g(y - cqt), \tag{1.5}$$

where q corresponds to the packet that actually contains y. In the way this example was built, actually there isn't a quantum measurement problem, and we did not need to make use of the collapse concept, as in the orthodox interpretation.

We still have to understand what is the probability of obtaining a specific measurement outcome q. According to Born's rule, it must be $|c_q|^2$. To obtain such probability, we have to integrate the probability density $|\Psi_q(\mathbf{x}, y)|^2$ over all possible values of $\mathbf{x}$ and y near the qth packet.

$$\Psi_q(\mathbf{x}, y) = c_q \psi_q(\mathbf{x}) g(y - cqt); \tag{1.6}$$

$$\Rightarrow \int_{\mathbf{x},y} |\Psi_q(\mathbf{x}, y)|^2 d\mathbf{x} dy = |c_q|^2 \int_{\mathbf{x}} |\psi_q(\mathbf{x})|^2 d\mathbf{x} \int_y |g(y - cqt)|^2 dy = |c_q|^2, \tag{1.7}$$

since $g(y - cqt)$ and $\psi_q(\mathbf{x})$ are normalized. It is just exactly the expected result.

Back to Schrodinger's cat example, but now on the light of Bohmian interpretation. Besides the wave functions corresponding to the dead cat ψ_{dead} and to the alive cat ψ_{alive}, it is also necessary to specify the position of the constituents in the configuration space, which we can denote by Q. As in the previous example, after the interaction, Q is either in the domain where ψ_{dead} is nonzero *or* in the domain where

ψ_{alive} is nonzero. These two regions no longer overlap. So the cat is either dead *or* alive, and never both, as the orthodox interpretation says. To actually know the cat state we have to make the measurement, i.e., open the box.

Despite these interesting examples, Bohmian interpretation is not unanimity within the scientific community, in particular when discussing the classical limit of Bohmian trajectories [38, 39, 40, 41]. Before going into the *Decoherence approach*, a popular theory to elucidate the quantum-classical transition and the quantum measurement problem, I would like to comment on a thought experiment posed by the Hungarian physicist Eugene Wigner (1902-1995) in 1961 that is intimately related to the measurement problem and Schrodinger's cat: *Wigner's friend* [42].

The thought experiment is about two friends, one inside (Wigner's friend) and the other outside (Wigner) of a sealed laboratory. Wigner is observing his friend making a quantum measurement in a physical system. Following quantum theory formalism, the observer and the super-observer (outside the lab) formulate a statement about the state of the measured system after the measurement. Nevertheless, depending on the interpretation the statements of the friends can contradict each other.

In his original work, Wigner propose the experiment to support his view that consciousness is necessary to complete the quantum measurement process. Suppose the friend has a system S inside the laboratory. The system is initially in a superposition state, $c_0 |0\rangle + c_1 |1\rangle$. Then with probability $|c_0|^2$ the friend will measure $|0\rangle$ and with probability $|c_1|^2$ he will measure $|1\rangle$. From the friend's point of view, the system will be or in the state $|0\rangle_S$ or in the state $|1\rangle_S$.

Wigner, outside the isolated lab, models the joint state system + friend, $S \otimes F$. From his point of view, with probability $|c_0|^2$ his friend will measure $|0\rangle_S$, and will be in state $|0\rangle_F$, and with probability $|c_1|^2$ his friend will measure $|1\rangle_S$, and will be in state $|1\rangle_F$. Therefore, in Wigner's perspective, the total state is $c_0 |0\rangle_S \otimes |0\rangle_F + c_1 |1\rangle_S \otimes |1\rangle_F$.

At the end we have Wigner assigning a superposition state to the total system and his friend experiencing a collapsed state. This is the usual, Copenhagen interpretation. In the light of many-words for example, there are many copies of Wigner's friend in different words, each one experiencing one possibility. For Wigner himself, after asking his friend about the acquired information and being conscious of his answer, the superposition is broken. Wigner's point of view opens the door to a new universe of discussions and possibilities regarding the necessity in using quantum theory to understanding complex aspects of life, consciousness and our perception of reality.

The discussions about interpretations of quantum theory concerning the quantum measurement problem, and more broadly the quantum-classical transition, are stimulating and remain until this day; not only involving pure science, but attracting researchers that work on practical problems, such as quantum engineering [43]. Even though not able to give all the expected answers nor immune to criticisms, the *decoherence approach* has fundamental importance in the debate, besides being a popular approach to explain the emergence of classicality from the quantum world [44, 39].

1.3 Decoherence approach

Objectively speaking, decoherence is the demolition of quantum coherence via interaction with the surrounding environment. In other words, environment *can* destroy

coherence. In fact, the familiar classical states of our daily experience are rare when compared to the huge number of possibilities allowed by the vastness of the Hilbert space and the superposition principle.

Imagining a quantum system and its corresponding possible states placed in contact with the external environment, not all quantum superpositions suffer the same consequences. There will be a preferred set of states that are singled out by the interaction with the environment, the so called *pointer states*, while their superpositions loose phase coherence (decohere).

This nomenclature, introduced by the polish physicist W. H. Zurek in 1981, arose from the context of quantum measurements [45]. The pointer states are associated with the pointer positions in a measurement apparatus. They are stable and remain correlated with the outcome of the measurement device after the environment interaction. This selection process of preferred states by the environment is called *environment-induced superselection*, or purely *einselection* [46].

Therefore, the monitoring of a quantum system in a superposition by the environment induces two phenomena, decoherence and einselection. Namely, the loss of quantum coherence and the selection of a set of preferred states associated with the observables monitored by the environment. The classical domain of the selected states designates the result of the two processes.

Although both may occur simultaneously with classical processes, for instance dissipation, decoherence and einselection are quantum phenomena [1]. Note that in classical physics one can always, in principle, make a measurement without disturbing the system. On the other hand, in quantum mechanics the act of measuring itself poses serious risks of redefinition in the state of the system.

As in both theoretical and experimental physics the systems of interests are mostly "isolated", the idea of emergence of classicality and loss of quantum coherence by just opening the sealed box and allowing the interaction with the environment is recent [47, 45, 46] and related with two aspects. First, it is possible and plausible to associate elements of reality with measurements outcomes; second, when a system interacts with its surrounding environment, transfer of information usually occurs.

To introduce the mathematical formalism of decoherence, lets reconsider the Von Neumann model for quantum measurements with the environment E included. We have then three parts of our composite system: the system to be measured S, the apparatus A and the environment E.

As in equation 1.3, initially $|\Psi_S\rangle = \sum_n c_n |\psi_n\rangle$, $|\Psi_A\rangle = |a_0\rangle$ and $|\Psi_E\rangle = |e_0\rangle$. The whole system unitarily evolves as following:

$$|\Psi_S\rangle |\Psi_A\rangle |\Psi_E\rangle = \left(\sum_n c_n |\psi_n\rangle\right) |a_0\rangle |e_0\rangle \rightarrow \left(\sum_n c_n |\psi_n\rangle |a_n\rangle\right) |e_0\rangle \rightarrow \sum_n |\psi_n\rangle |a_n\rangle |e_n\rangle , \tag{1.8}$$

where the environment states $|e_n\rangle$ are each one associated with the corresponding pointer state of the apparatus $|a_n\rangle$. Note that before the last step the observable of the system which will be ultimately recorded by the apparatus is not well defined. Only the interaction, generating transfer of information and correlations between apparatus-environment, remove the ambiguity in the definition of the recorded observable.

[1] Interesting questions to think about: at the quantum level, what does dissipation mean? What is the mechanism that makes us perceive it as dissipation?

We can assume that the environment is interacting predominantly with the apparatus, usually macroscopic, and in some situations with the system, usually microscopic, but the focus of attention is on the apparatus. The evolution process represented in equation 1.8 occurs as follows: the system-apparatus interaction dynamics creates stable quantum correlations between them, which is responsible for recording information about the system in the apparatus; such information can be measured by the apparatus interacting with the environment. The states $|a_n\rangle$ are then the robust preferred states superselected by the environment.

Before proceeding it is worth mention the following caveat: for two subsystems S and A a diagonal decomposition of the form $\sum_n c_n |\psi_n\rangle |a_n\rangle$ is always possible. However, there is no Schmidt decomposition in the case of three or more subsystems. Therefore, in the case of S, A and E, a decomposition of the form $\sum_n c_n |\psi_n\rangle |a_n\rangle |e_n\rangle$ is not possible. Thus, the Hamiltonian which dictates the evolution

$$\left(\sum_n c_n |\psi_n\rangle |a_n\rangle\right) |e_0\rangle \rightarrow \sum_n c_n |\psi_n\rangle |a_n\rangle |e_n\rangle \tag{1.9}$$

must have its eigenstates as direct-product states [48, 45, 46].

The interaction with the environment also cannot disturb the quantum correlations between the system state $|\psi_n\rangle$ and the corresponding apparatus state $|a_n\rangle$. In a realistic measurement process this is really difficult to happen. In fact, this idea of a robust apparatus, in the sense of indicating the state of the system, involves the definition of a measurement device. Therefore, einselection applied to the Von Neumann scheme gives an intuition of why measurement devices seem to be designed to measure just a specific physical observable.

Suppose now a situation in which we don't have a measurement apparatus, but only a system S and an environment E evolving respectively by Hamiltonian H_S and H_E and interacting via H_{int}. How can we determine the pointer states of the system, i. e., the set of states that are most robust under the influence of the environment?

In a larger number of relevant cases we have the interaction so strong that the Hamiltonian H_{int} dominates the composite evolution. In other words, the intrinsic evolution of system and environment represented by H_S and H_E are insignificant when compared to the evolution induced by the interaction. Then, the total Hamiltonian can be approximated by just the interaction Hamiltonian H_{int}.

Our objective now is to find the states $|\psi_n\rangle$ that are robust under the influence of the interaction. Namely, the states $|\psi_n\rangle$ such that the composite state system-environment, initially $|\psi_n\rangle |e_0\rangle$ at $t = 0$, remains in the product form $|\psi_n\rangle |e_n\rangle$ for all $t > 0$. Mathematically speaking, we need that

$$U_{int} |\psi_n\rangle |e_0\rangle = e^{-iH_{int}t} |\psi_n\rangle |e_0\rangle = |\psi_n\rangle |e_n\rangle , \tag{1.10}$$

where the time dependence of $|e_n\rangle$ is implicit and $\hbar = 1$.

Looking at equation 1.10 is enough to infer that the pointer states $|\psi_n\rangle$ will be given by the eigenstates of the part of the Hamiltonian H_{int} related to the Hilbert space of the system [45]. The states $|\psi_n\rangle$ will be stationary under the action of H_{int}. The approximation of the total Hamiltonian by only its interaction term is usually called *the quantum-measurement limit* [44]. In this context, we can also construct the *pointer observables* $O_S = \sum_n \psi_n |\psi_n\rangle\langle\psi_n|$; it is straightforward to see that $[O_S, H_{int}] = 0$.

Lets consider now a more concrete and didactic example, with $|\Psi_S\rangle = \sum_n c_n |x_n\rangle$ and the environment initially in the sate $|e_0\rangle$. The interaction Hamiltonian is given by $H_{int} = x \otimes E$, where x and E are operators acting on the Hilbert spaces associated with S and E, respectively. The evolution will yield

$$e^{-iH_{int}t}\sum_n c_n \left|x_n\right\rangle \left|e_0\right\rangle = \sum_n c_n \left|x_n\right\rangle e^{-ix_nEt}\left|e_0\right\rangle = \sum_n c_n \left|x_n\right\rangle \left|e_{x_n}\right\rangle . \tag{1.11}$$

Evaluating the total system-environment density matrix ρ_{SE},

$$\rho_{SE} = \Big(\sum_n c_n \left|x_n\right\rangle \left|e_{x_n}\right\rangle\Big)\sum_m c_m^* \left\langle x_m\right| \left\langle e_{x_m}\right| = \sum_{n,m} c_n c_m^* |x_n\rangle\langle x_m| \otimes |e_{x_n}\rangle\langle e_{x_m}|. \tag{1.12}$$

As we don't have access to the environment degrees of freedom, we must look to the reduced density matrix of the system ρ_S, obtained tracing out E: $\rho_S = \mathrm{Tr}_E[\rho_{SE}]$. We will leave the global level of description to go to the local level, of the system. Ending up with

$$\rho_S = \sum_{n,m} c_n c_m^* |x_n\rangle\langle x_m|\langle e_{x_n}|e_{x_m}\rangle. \tag{1.13}$$

But $\langle e_{x_n}|e_{x_m}\rangle = \langle e_0| e^{ix_nE^\dagger t}e^{-ix_mEt}|e_0\rangle$, and $\langle e_0|e_0\rangle = 1$. Then, if $x_n = x_m$, $\langle e_{x_n}|e_{x_m}\rangle = 1$, and if $x_n \neq x_m$, $\langle e_{x_n}|e_{x_m}\rangle \propto e^{\frac{-t}{\tau_d}}$, where τ_d is a characteristic decoherence timescale, which can be evaluated using values of the parameters in each model. The system reduced density matrix is then

$$\rho_S = \sum_n |c_n|^2 |x_n\rangle\langle x_n| + \sum_{n\neq m} c_n c_m^* \, C \, e^{\frac{-t}{\tau_d}}, \tag{1.14}$$

with C constant. The first factor of two in the right hand side includes the diagonal terms and can be seen as a mixture of pointer states, while the second includes those off-diagonal, the coherences. So, if we look at the composite system locally, just to the system without environment, after a sufficiently long time interacting it will decohere. The characteristic timescale is particular for each model [49, 50].

The number of possible different situations involving the energy scales of the Hamiltonians H_S, H_E and H_{int} is enormous. For instance, one can have the situation in which the environment is slow and the Hamiltonian H_S dictates the evolution of the system. Such limit is *the quantum limit of decoherence*. The pointer states will be the energy eigenstates of H_S. There is also the situation in which H_S and H_{int} contribute in equal strengths for the evolution, called *the intermediate regime*. In all of them, it is valid the rule that the pointer states are the most robust under the evolution generated by the total Hamiltonian.

1.3.1 Quantum Darwinism

Until now, we have focused our observations at the level of the system. We did not mention the observer nor his interaction with any of the subsystems S, A or E; the environment was considered just a monitoring agent. Precisely because of this last fact, information is encoded in the environment, which can be used as a resource for indirect collection of information about the system by the observer.

Indeed, analyzing measuring experiments, in some cases the observer collects information about the system looking at the environment that had interacted with it. For instance, in our daily-life we are constantly measuring the systems through the environment: the act of "seeing" an object consists of detecting the photons (light) that are scattered around the object.

Still in our daily-life example, two observers could make the measurement (act of "seeing" an object) as many times as they want, and their results would always

agree. This is a feature of the classical physics domain. Classical states are robust, usually don't get disturbed by the act of measuring and can be observed by a multiple number of observers, contributing to the notion of existence of a classical reality.

However, making measurements in a closed quantum system, in general, disturbs the state of the system. A natural question appears: how does the classical reality that we perceive emerges from the quantum realm? Notice that the decoherence formalism and the environment-induced superselection of preferred states are not sufficient to answer the above question, since they don't give us an effective (classical) description for the apparatus nor for the system. On the other hand, contribute to the understanding of why only a subset of possible states in the Hilbert space is observable.

Within this new perspective of the role of the environment, it is possible to gain information about a system without disturbing it, but investigating the environment that it has previously interacted with. We have now the environment as a witness of the system's state, or a communication channel between system and observer. The study of which kind of information about the system can be stored and proliferated by the environment in a stable manner is *the quantum Darwinism*, a recent research area that has developed quite quickly in the last decades [51, 52, 53].

Some groups [54, 55] claim that they have found that the system observable that can be most completely and redundantly (this is important for more than one observer to obtain the same result) stored in distinct subsets of the environment agrees with the pointer observable selected by the system-environment interaction.

Then, the einselected states would have their importance increased. Besides being the states less disturbed by the interaction with the environment, they also would be the states most easily found when probing environmental degrees of freedom without disturbing the system. As the same information about the pointer observables is stored in different parts of the surrounding environment, different observers could probe such pieces and agree on their findings [53]. In this sense, therefore, it would be possible to consider an effectively objective existence of the pointer states.

Now let's get into some mathematical aspects of quantum Darwinism. The density matrix approach is intuitive here. Remember that in decoherence the focus was on the system, to determine what states survive information leaks to the environment E. In quantum Darwinism the search is for information about the system that can be found out from fragments of E, considered to be initially in the state $|\Psi_E\rangle = \left|e_0^{(1)}\right\rangle \otimes \left|e_0^{(2)}\right\rangle \otimes \left|e_0^{(3)}\right\rangle .. \otimes \left|e_0^{(\mathcal{N})}\right\rangle$, with $\mathcal{N}$ the number of subsystems.

Technically speaking, while in decoherence the relevant quantity was the reduced density matrix of the system, now it will be the reduced density matrix of S including a fragment F of the environment, which in turn may include several subsystems, since we are looking for correlations between such pieces and the system:

$$\rho_{SF} = \mathrm{Tr}_{E-F}[\rho_{SE}], \tag{1.15}$$

with $E - F$ meaning tracing out the environment fragment that is not included in F. The amount of information encoded in F about S, or the degree of correlation between them, is generally quantified via the mutual information $I(S,F) = \mathcal{H}_S + \mathcal{H}_F - \mathcal{H}_{S,F}$, defined as the difference between the subsystems entropies ($\mathcal{H}_i$'s) separately and jointly.

Consider two states in S, $|\psi_1\rangle$ and $|\psi_2\rangle$, and their multiple copies printed in subsystems of E without disturbing them. Knowing the existence of the no-cloning theorem, the first question is: is this even possible? Suppose we have a superposition state $|\Psi\rangle = \alpha\,|0\rangle + \beta\,|1\rangle$ with unknown complex coefficients. To make a copy

of $|\Psi\rangle$ we take a state $|e\rangle$ and evolve the product state $|\Psi\rangle|e\rangle$ unitarily, assuming the existence of such operation. Then,

$$U(|\Psi\rangle|e\rangle) \rightarrow (\alpha|0\rangle + \beta|1\rangle)(\alpha|0\rangle + \beta|1\rangle) = \alpha^2|00\rangle + \alpha\beta|01\rangle + \beta\alpha|10\rangle + \beta^2|11\rangle \tag{1.16}$$

But by linearity of quantum mechanics,

$$U(|\Psi\rangle|e\rangle) = U\alpha|0\rangle|e\rangle + U\beta|1\rangle|e\rangle \rightarrow \alpha|00\rangle + \beta|11\rangle. \tag{1.17}$$

Since equations 1.16 and 1.17 are not equal U can not act as a *general* copy operation. This is the no-cloning theorem [56]. Now, in the quantum Darwinism context, the states imprinted in environment fragments come from the decomposition of a system state $|\Psi_S\rangle$ on a basis of a specific observable. This escapes the theorem since in this situation $|\Psi_S\rangle$ isn't an *unknown* state.

But how does this copy actually takes place? Back to the states $|\psi_1\rangle$ and $|\psi_2\rangle$ in S, they will be imprinted in the environment: $|\psi_1\rangle|e_0\rangle \rightarrow |\psi_1\rangle|e_1\rangle$ and $|\psi_2\rangle|e_0\rangle \rightarrow |\psi_2\rangle|e_2\rangle$. As this is a unitary process, it is true that

$$\langle\psi_1|\psi_2\rangle\langle e_0|e_0\rangle = \langle\psi_1|\psi_2\rangle\langle e_1|e_2\rangle, \tag{1.18}$$

with $\langle e_0|e_0\rangle = 1$. For the above equation to be true we need to have $\langle e_1|e_2\rangle = 1$ or $\langle\psi_1|\psi_2\rangle = 0$. If the first is true, the states will not be printed. If the second true, $\langle e_1|e_2\rangle$ is arbitrary and even a perfect copy $\langle e_1|e_2\rangle = 0$ is allowed.

Consequently, multiple copies of $|e_1\rangle$ and $|e_2\rangle$, perfect or not, can be imprinted on fragments of E. And more, only sets of orthogonal states can be copied, explaining the selection of a set of possible outcomes. Why pointer states are favoured? First, they survive copying. Second, only the pointer obervables can leave a redundant and robust imprint on E (mathematical proof in reference [57]). [2]

Thereby, having system S and environment E initially in states $|\Psi_S\rangle = \sum_n c_n|\psi_n\rangle$, with $\{|\psi_n\rangle\}$ eigenstates of the observable O_S; and $|\Psi_E\rangle = \left|e_0^{(1)}\right\rangle \otimes \left|e_0^{(2)}\right\rangle \otimes \left|e_0^{(3)}\right\rangle ..$, tensor product of N subsystems, the evolution takes place:

$$|\Psi_S\rangle|\Psi_E\rangle = \Big(\sum_n c_n|\psi_n\rangle\Big)\Big(\left|e_0^{(1)}\right\rangle \otimes ... \left|e_0^{(N)}\right\rangle\Big) \rightarrow \sum_n c_n|\psi_n\rangle\left|e_n^{(1)}\right\rangle \otimes \left|e_n^{(2)}\right\rangle \otimes ... \left|e_n^{(N)}\right\rangle, \tag{1.19}$$

where many copies of $|\psi_n\rangle$ were imprinted on N subsystems of E. Note that in the beginning, before the interaction, there is no correlations between system and environment, nor between environment's subsystems.

Calculating the reduced density matrix as written in 1.15,

$$\rho_{SF} = Tr_{E-F}[\sum_{n,m} c_n c_m^* |\psi_n\rangle\langle\psi_m| \otimes \Big(\left|e_n^{(1)}\right\rangle \otimes ... \left|e_n^{(N)}\right\rangle\Big)\Big(\left\langle e_m^{(1)}\right| \otimes ... \left\langle e_m^{(N)}\right|\Big)]. \tag{1.20}$$

For instance, in the case of photons as the environment (probing the system to be measured), F would represent the ones able to reach the detector, for example of our retina, while $E - F$ the photons that, though scattered by the system, are not detected. Proceeding,

$$\rho_{SF} = \sum_{n,m} c_n c_m^* |\psi_n\rangle\langle\psi_m| \otimes \left|E_n^F\right\rangle\left\langle E_m^F\right| \; C_{nm}^{E-F}, \tag{1.21}$$

[2] The concept of *redundancy* is defined as the number of disjoint subsets of the environment containing almost all information about an specific observable O present in the entire environment, and hence the maximum number of observers that can, in independent ways, find out about O in E [57].

with

$$\left|E_n^F\right\rangle \equiv \left|e_n^{(1)}\right\rangle \otimes \left|e_n^{(2)}\right\rangle ... \left|e_n^{(N_F)}\right\rangle \text{ and } C_{nm}^{E-F} = \langle E_n^{E-F}|E_m^{E-F}\rangle \equiv \prod_{k=N_F+1}^{N} \langle e_n^{(k)}|e_m^{(k)}\rangle. \tag{1.22}$$

Assuming an interaction Hamiltonian of the form $H_{int} = \sum_k O_S \otimes O_E^k$, with observables O_S and O_E^k acting on the system S and the environmental subsystem k, respectively, we have $O_S|\psi_n\rangle = \lambda_n|\psi_n\rangle$ and $\left|e_n^{(k)}\right\rangle = e^{\frac{-it\lambda_n O_E^k}{\hbar}}\left|e_0^{(k)}\right\rangle$. Thus, similar to the second term in equation 1.14, for $n \neq m$ C_{nm}^{E-F} will be typically very small as time and the number of unobserved subsystems (terms in the multiplicand) increase [57, 58]. In this limiting case, the final expression for ρ_{SF} yields:

$$\rho_{SF} = \sum_n |c_n|^2 |\psi_n\rangle\langle\psi_n| \otimes |E_n^F\rangle\langle E_n^F| = \sum_n |c_n|^2 |\psi_n\rangle\langle\psi_n| \otimes |e_n^{(1)}\rangle\langle e_n^{(1)}| ... \otimes |e_n^{(N_F)}\rangle\langle e_n^{(N_F)}|. \tag{1.23}$$

In possession of an observable acting on F, O_F, which perfectly distinguish between the orthogonal states $\left|E_n^F\right\rangle$, the state of the system after the measurement of such an observable in F will be exactly the state of S after a direct measurement of O_S:

$$O_F = \sum_i a_i O_i \equiv \sum_i a_i |E_i^F\rangle\langle E_i^F| \rightarrow \frac{Tr_F[O_i \rho_{SF} O_i]}{Tr[\rho_{SF} O_i]} = \frac{|c_n|^2 |\psi_n\rangle\langle\psi_n|}{|c_n|^2} = |\psi_n\rangle\langle\psi_n|. \tag{1.24}$$

Note that all the information about O_S is given by an indirect measurement of O_F, not disturbing directly the system S, but projecting it in an eigenstate of the observable O_S. Moreover, averaging the outcomes of measurement O_F, or tracing out F in equation 1.23, the reduced density matrix of S is a mixture of eigenstates of O_S.

To finalize this simple construction, which has served to give an intuition about the quantum Darwinism view concerning a quantum measurement process, let's comment on the assumptions made. We assumed that the interaction between system and environment, initially in a product of pure states, was sufficiently strong for the interaction Hamiltonian to dictate the evolution and that every environmental subsystem couples to the same system observable.

As the self-Hamiltonian H_S of the system is disregarded, monitoring by the environment occurs in static states of the system, selecting pointer states only by the interaction. The same behaviour is observed if H_S and H_{int} commute. In cases where those approximations are no longer valid, it can happen a suppression of the evolution dictated by H_S by the environment monitoring [57]; or the composite system can enter in the quantum-limit discussed in section 1.3 [59], where the evolution dictated by H_S is stronger than the one dictated by the interaction, for instance.

Regarding the environment, there is a huge number of possible more complicated situations: the fragments can evolve jointly or separately and interact with its neighbours or with more distant fragments. The interaction between environment subsystems can make them to get entangled and its reduced states mixed. Hence, even with the environment containing all possible information about the relevant S observable, it can become inaccessible by the observer. This is related to the assumption of system and environment initially in pure states, which we know is a rare situation in practice.

Finally, the assumption about the coupling of environmental subsystems with

only one system observable is reasonable, since typical system-environment couplings tend to depend on relative position between them. It is true, however, that may exist different environments monitoring distinct observables. In these cases, the dominant coupling will select one observable, and the others will be perceived like noise.

Considerations arise regarding the relation between the preferred selected observable by the system-environment interaction and the states of the system that are easier to infer by an observer which has only access to one subsystem of the environment. There are researchers interested in related questions, for example to which extent the Gaussian states, of much importance in the decoherence formalism, are the easiest states to infer [60].

In this context, when the available and useful environmental fragments to the observer are not contained in the set of the ones responsible for decoherence, one can still suppose that the states of S that can have information collected via the available fragments represent a coarse-grained version of the pointer states. In time, there are theorems [57] that guarantee that whenever more than one observable can be inferred redundantly from a fixed set of different fragments of E, they necessarily correspond to a coarse-grained version of a so called *maximally refined redundantly imprinted observable*.

Notice that the concept of coarse-graining here is related with the "lack of resolution", or inability to access all the information desired. This is precisely one of the key points of our work. Motivated by the measurement problem debate and with a measurement process as study object, we discuss the dynamics of a quantum system perceived by an observer not able to access all its details. This is the main subject of this thesis.

To close our brief discussion about quantum Darwinism, some recent work to illustrate the on going research: researchers are studying quantum Darwinism in the case of mixed environments [61]; also for an object illuminated by a black body [52]; studying the emergence of classical features and new correlation quantifiers [53] and the importance of redundant records for consistent histories [62], to cite a few but featured examples.

1.4 Effective dynamics

Quantum theory is undoubtedly a successful physics theory, in the sense that it is consistent, its mathematical formalism is very well founded and the laws that govern the small scale phenomena are, mostly, well described by quantum theory. It is our best description until the moment. However, in our daily lives we do not experience quantum phenomena. Classical physics is well enough to describe the daily world.

As discussed in the above sections, one of the general remaining fundamental problems in physics involves understanding how effectively classical systems and properties around us emerge from the underlying quantum domain.

To say that this problem is general is not in vain; it is possible to study the quantum-classical transition problem in several fronts, encompassing various research topics in physics, like quantum mechanics, thermodynamics and classical physics. We may understand our notion of "classicality" as an emergent concept, as something that isn't in contradiction but rather justified by the features of quantum mechanics.

As history shows, progress in science is closely related to technological advances. Therefore, the old questions concerning measurement processes and the quantum-classical transition are much more treatable. In last decades we had the revolution in the field of experimental physics and related techniques, which has allowed for the control of quantum systems with various degrees of freedom, for example the techniques of trapping and cooling ions and atoms [63, 64]. Besides that, the evolution of supercomputers and the development of numerical techniques and mathematical methods and tools provided by quantum information theory reascended the search for answers.

Thus, in this thesis we want to use quantum information theory tools, particularly quantum channels, to contribute to the search for an answer to the following question: what is the real role/importance of the impossibility of accessing all the degrees of freedom of a quantum system to the emergence of the effective, "classical", realm and, parallel, the "death" of quantum features?

There are prominent groups working on this idea. The fact that a "large" quantum system might still have pronounced quantum features - contradicting the intuition of small meaning quantum and large meaning classical [3] -, if one has access to all its degrees of freedom, was nicely shown by Prof. Časlav Brukner and his group [66, 67]. In [66] they show that a large spin length still behaves in a quantum way if one can measure all the possible values of the spin, say, in the z-direction. It is only when the measurement outcomes are coarse-grained, i.e., when we cannot resolve nearby outcomes and integrate their signal, that a classical description is obtained.

To illustrate the presence of quantum features in "large" systems, particularly entanglement, already exist theoretical works on entanglement in macroscopic objects [68, 69] and macroscopic spin ensembles [70], and experimental demonstration of entanglement in a system of 10^{12} atoms [71]. More recently, Hacker et al. created in a deterministic way entangled atom-light Schrodinger-cat states [72]. These work support our idea of coarse-grained descriptions inducing classicality.

1.5 Thesis outline

Hereafter, the thesis is organized as follows: in chapter 2 is given an introduction on quantum channels - the main used mathematical tool -, particularly the coarse-graining channels. Then, it is presented our framework to study emerging dynamics arising from coarse-grained quantum systems. The work depicted in chapter 2 is also published in PRA:
https://journals.aps.org/pra/abstract/10.1103/PhysRevA.96.032113.

In chapter 3 and appendix B are detailed our attempts to model a quantum measurement process, involving different coarse-graining channels. It is also discussed on the context of our model the decay of quantum correlations in presence of "strong coarse-graining channels" - whose meaning will become clear latter. Closing the thesis, in chapter 4 are located the conclusions and perspectives of our work, including possible applications.

[3] In fact, a physical system which is made by a large number N of constituents does not necessarily obey the rules of classical physics [65].

Chapter 2

Emerging dynamics arising from coarse-grained quantum systems

Travelling in an imaginary spacecraft as a non-interacting observer and strolling between different nature's time and length scales, we are able to experience distinct phenomena characteristic from each visited region. Different physical theories are then necessary in order to elucidate the wide variety of observed phenomena. Moreover, the transition between two theories used to explain physical phenomena occurring in, for example, successive length scales is expected to be smooth. They must be compatible in the transition zone.

However, this is usually not the case. Things are much more complicated. Physics has no general answer for the question of how does a general physical description in one scale emerge from the description in a deeper (meaning "more microscopic") scale. How does an ensemble of atoms, molecules, electrons, with a very complicated microscopic description can interact with us, in the macroscopic world, in the form of a chair or a musical instrument? What is the number of different dynamics that might emerge from the quantum world, since we do not have access to it in our daily lives? More specifically, what dynamics might emerge from a fully quantum description of a system if we are not able to resolve the system in all its details? This is the key question of this chapter.

The impossibility in resolving all the system details is translated mathematically via a coarse graining procedure. Different ways of coarse graining [73, 74, 75, 76] the description of a system are often employed in order to "zoom out" from one level and obtain an *effective description*. Coarse graining frequently appears in Statistical Physics [77], and is arguably the central tool in the renormalization method initiated by Kadanoff and Wilson [78, 79]. Nevertheless, some of these early methods are sometimes based on not so well controlled approximations or on projections, leading thus to ill-defined and/or probabilistic effective dynamics when applied to quantum systems.

In order to get a well defined coarse graining procedure, we will employ quantum information tools. More specifically, a coarse graining operation will be described by a quantum channel Λ_{CG}, giving an effective description of the system. Rewriting chapter's key question in a more concrete way (see figure 2.1): given a system represented by a density matrix state ψ_0 evolving by the unitary map $\mathcal{U}_t$ ($\psi_t = \mathcal{U}_t(\psi_0) = U_t(\psi_0)U_t^\dagger$) what is the dynamics Γ_t induced by a coarse graining Λ_{CG}?

The theory of quantum channels, which describes the most general transformations that can be applied to a system [80, 81, 82], became well established in the last decades [83, 84]. This was accompanied and supported by the formalization and development of a theory for quantum correlations and by efficient descriptions

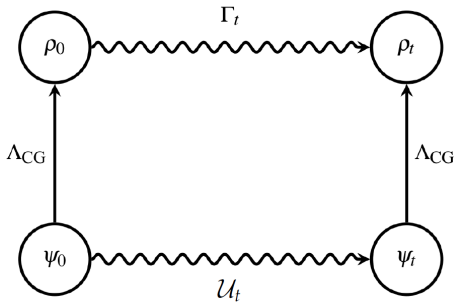

FIGURE 2.1: **Coarse graining induced dynamics.** Schematic diagram representing the different levels of description connected by a coarse graining. Given an initial state of the system ψ_0, its evolution, $\mathcal{U}_t$, and a coarse graining map Λ_{CG}, we want to determine what is the induced dynamics Γ_t, and its properties, such that $\Gamma_t \circ \Lambda_{CG}(\psi_0) = \Lambda_{CG} \circ (U_t(\psi_0)U_t^\dagger)$.

of many-body quantum systems [84]. Working together with other scientists and employing some of these tools, we tried to obtain effective descriptions of quantum systems and their dynamics, answering the questions asked in the above paragraphs [85].

2.1 Quantum channels

Let's start the discussion by studying quantum channels and reviewing some of its important properties. Consider an evolution in the Schrodinger picture of quantum mechanics described by a map $\Lambda : \mathcal{L}(\mathcal{H}_D) \to \mathcal{L}(\mathcal{H}_d)$, where $\mathcal{H}_D$ and $\mathcal{H}_d$ are Hilbert spaces assigned to a D-dimensional and d-dimensional quantum systems, respectively, and $\mathcal{L}(\mathcal{H}_i)$ the set of all linear operators acting on the Hilbert space $\mathcal{H}_i$.

If Λ describes a physically meaningful evolution, meaning that acting on density matrices it returns a valid density matrix, it should fulfill three conditions. The first one is *linearity*: for all operators ρ_A and $\rho_B \in \mathcal{L}(\mathcal{H}_D)$ and $c \in \mathbb{C} : \Lambda(c\rho_A + \rho_B) = c\Lambda(\rho_A) + \Lambda(\rho_B)$. It is easy to perceive the importance of such property. Suppose two friends Alice and Bob share a bipartite pure state ψ, and Alice has a physical device which is characterized by a non-linear map Λ_{nl} on density operators. Namely, there exists a convex decomposition of Alice's reduced state $\psi_A = \sum_i \lambda_i \rho_i$ such that $\sum_i \lambda_i \Lambda_{nl}(\rho_i) \neq \Lambda_{nl}(\sum_i \lambda_i \rho_i)$.

If Bob leaves his reduced state untouched and Alice applies Λ_{nl}, her state will be given by $\Lambda_{nl}(\psi_A)$. However, if Bob applies an instrument [80] in order to prepare ρ_i on Alice's side with probability λ_i, her state will be $\sum_i \lambda_i \Lambda_{nl}(\rho_i)$. By the non-linear character of Alice's device, she can distinguish if Bob applies in his subsystem a linear map or not, with probability of success bigger than one half. That is, by looking at her local system she can gain information about what Bob applied in his reduced density matrix, implying a locality breakdown.

Aware of the importance of linearity, the second is the *trace preserving* condition. The operation Λ has to map density matrices (trace one) onto density matrices, and we must guarantee that probabilities are conserved under the channel action. Then, for all $\rho \in \mathcal{L}(\mathcal{H}_D) : Tr[\Lambda(\rho)] = Tr[\rho]$.

Finally, we demand *complete positivity*. Suppose we have a global system composed of two parts, with total Hilbert space $\mathcal{H}_D \otimes \mathcal{H}_z$, so that the evolution of the total system is described by $\Lambda \otimes \mathbb{1}_z$, with $\mathbb{1}_z$ representing the identity map in the Hilbert space $\mathcal{H}_z$. Positivity of Λ alone is not sufficient, $\Lambda \otimes \mathbb{1}_z$ should again be a

positive map for all dimensions z. This guarantees that even if the channel acts only on a subsystem of the whole, states are mapped onto states.

We call *quantum channel* a map that fulfills the three above conditions. Quantum channels are the most general framework in which general input-output relations are described within quantum mechanics. One can parametrize and represent such a channels in various ways, for example in terms of a bipartite quantum state, leading to the state-channels duality introduced by Jamiolkowski and Choi [86, 87, 88], or as the reduced dynamics of a larger (unitarily evolving) system as expressed by the theorems of operator sum representation (Kraus representation), Stinespring, and Neumark (for POVM's) [89, 90, 91]. In our work we use Kraus and Stinespring representations, and I'll focus here on these two.

Let's begin with a theorem for Kraus representation.

Theorem 1 ***(Kraus representation)*** *A linear map $\Lambda : \mathcal{L}(\mathcal{H}_D) \to \mathcal{L}(\mathcal{H}_d)$ is a quantum channel if and only if there exists a finite set of linear operators $\{K_i\}_{i=1}^N$, with each $K_i : \mathcal{H}_D \to \mathcal{H}_d$ known as a Kraus operator, such that $\forall \psi \in \mathcal{L}(\mathcal{H}_D)$:*

$$\Lambda(\psi) = \sum_{i=1}^{N} K_i \psi K_i^\dagger \text{ with } \sum_{i=1}^{N} K_i^\dagger K_i = \mathbb{1}_D.$$

This decomposition has the following properties:

1. Normalization: Λ is trace preserving iff $\sum_{i=1}^N K_i^\dagger K_i = \mathbb{1}_D$ and unital[1] iff $\sum_{i=1}^N K_i K_i^\dagger = \mathbb{1}_D$.

2. Kraus rank[2] r: The number of Kraus operators in a minimal representation. In general, the number of Kraus operators is unlimited, but it is always possible to find a minimal representation; i. e., to characterize a quantum channel $\Lambda : \mathcal{L}(\mathcal{H}_D) \to \mathcal{L}(\mathcal{H}_d)$ with a set of Kraus operators with at most $D.d$ elements (maximal number in this minimal representation), as this is the number of generators for the map. So, $r \leq D.d$.

   If we want to find r for a given quantum channel Λ, we have to use the corresponding Choi state ρ_Λ,

   $$\rho_\Lambda = \mathbb{1}_D \otimes \Lambda(|\phi^+\rangle\langle\phi^+|), \tag{2.1}$$

   where $|\phi^+\rangle$ is the maximally entangled state, $D \times D$-dimensional. The Kraus rank r is given by the rank of matrix $\rho_\Lambda \in \mathcal{L}(\mathcal{H}_D \otimes \mathcal{H}_d)$. That's why $r \leq D.d$.

3. Freedom: Two sets of linearly independent Kraus operators $\{K_j\}$ and $\{K'_l\}$ represent the same map Λ iff there is a unitary U so that $K_j = \sum_l U_{jl} K'_l$, where a possibly smaller set is padded with zeros.

This more general type of evolution allows for describing processes where there is a loss of information about the system, with pure states evolving to mixed ones. It is worth noticing that quantum channels generalize the evolution of a quantum

[1] In abstract algebra, a unital map is a map Λ which preserves the identity element: $\Lambda(\mathbb{1}) = \mathbb{1}$.

[2] The rank of a matrix is the dimension of the vector space spanned by its columns, or rows. Analogously, the maximum number of independent columns, or rows. Note that the Kraus rank is related to the quantum channel representation, and therefore it is *not* related, in general, with just one specific matrix K_j.

system, with the unitary evolution being a particular channel in which $d = D$ and with a single Kraus operator, namely the unitary U_t itself. The Kraus representations of a completely positive map Λ and its dual Λ^* are related via interchanging $K_j \leftrightarrow K_j^\dagger$. Moreover, $\Lambda = \Lambda^*$ iff there is a representation with Hermitian Kraus operators.

Notice a simple consequence of the Kraus representation $\Lambda(\rho) = \sum_i^{r'} K_i \rho K_i^\dagger$: we can construct an isometry $V^\dagger := \sum_i^{r'} K_i \otimes |i\rangle$, with $|i\rangle$ any orthonormal basis in $\mathbb{C}^{r'}$, r' at least the Kraus rank of Λ, and $VV^\dagger = \sum_j K_j^\dagger K_j = \mathbb{1}_D$, reflecting the trace preserving condition. Then, the following theorem holds by construction.

Theorem 2 ***(Stinespring representation)*** *Let $\Lambda : \mathcal{L}(\mathcal{H}_D) \to \mathcal{L}(\mathcal{H}_d)$ be a completely positive linear map. Then for every $r' \geq r$ (recall that $r \leq D.d$) there is a $V^\dagger : \mathbb{C}^D \to \mathbb{C}^d \otimes \mathbb{C}^{r'}$ such that*

$$\Lambda(\rho) = Tr_{r'}[V^\dagger \rho V], \quad \forall \rho \in \mathcal{L}(\mathcal{H}_D).$$

V is an isometry (i.e., $VV^\dagger = \mathbb{1}_D$) iff Λ is trace preserving.

PROOF: Since $\Lambda(\rho) = \sum_i^{r'} K_i \rho K_i^\dagger = \sum_i^{r'} (\mathbb{1}_d \otimes \langle i|) V^\dagger \rho V (\mathbb{1}_d \otimes |i\rangle) = Tr_{r'}[V^\dagger \rho V]$.

On the other way,

$$Tr_{r'}[V^\dagger \rho V] = Tr_{r'}[(\sum_i^{r'} K_i \otimes |i\rangle)\rho(\sum_j^{r'} K_j^\dagger \otimes \langle j|)] = Tr_{r'}[\sum_{i,j}^{r'} K_i \rho K_j^\dagger \otimes |i\rangle\langle j|] = \sum_i K_i \rho K_i^\dagger.$$

The auxiliary space $\mathbb{C}^{r'}$ is sometimes called in the literature as dilation space [80]. Note that the same way in which we constructed $V^\dagger$ from the set of Kraus operators can be useful to obtain the latter from $V^\dagger$ as $K_i = (\mathbb{1}_d \otimes \langle i|)V^\dagger$. As r is the smallest number of Kraus operators, it is also the smallest possible dimension for a representation of the form shown in the theorem 2. Dilations with $r' = r$ are called minimal. From the unitary freedom in the choice of Kraus operators (theorem 1) we obtain that, for minimal dilations, $V^\dagger$ is unique up to the unitary freedom $V^\dagger \to (\mathbb{1}_d \otimes U)V^\dagger$.

For a good description of open quantum systems, so as to our purpose in describing coarse graining operations, and to obtain well defined equations of motion (we intend to find them in a future work - see "Conclusions and Perspectives"), the following operational way to describe quantum channels turn the approach simpler.

Theorem 3 ***("Open-system representation")*** *[80] Let $\Lambda : \mathcal{L}(\mathcal{H}_D) \to \mathcal{L}(\mathcal{H}_d)$ be a completely positive and trace-preserving linear map. Then there exists an auxiliary Hilbert space $\mathcal{H}_r$, with dimension $r \leq d$, and a unitary U acting on $\mathcal{H}_D \otimes \mathcal{H}_r \otimes \mathcal{H}_d$ such that*

$$\Lambda(\rho) = Tr_{Dr}[U(\rho \otimes |0\rangle\langle 0| \otimes |0\rangle\langle 0|)U^\dagger].$$

PROOF: Starting from $Tr_{r'}[V^\dagger \rho V]$, we can choose $r' = Dr$. In this way we can embed V into a unitary which acts on a tensor product and write $V^\dagger = U(\mathbb{1}_D \otimes |00\rangle\langle 00|)$ for $|00\rangle\langle 00| \in \mathcal{L}(\mathcal{H}_r) \otimes \mathcal{L}(\mathcal{H}_d)$.

Why "Open-system representation" with quotation marks? A common approach in the case of open quantum systems consists of coupling the system to an environment, which is initially in the state $|00\rangle\langle 00|$ for instance, let them evolve jointly according to a unitary U and finally disregard (trace out) environmental degrees of freedom, as one has no control over them. Here, however, the system and environment roles are unclear. As we want to allow for channels with different input-output

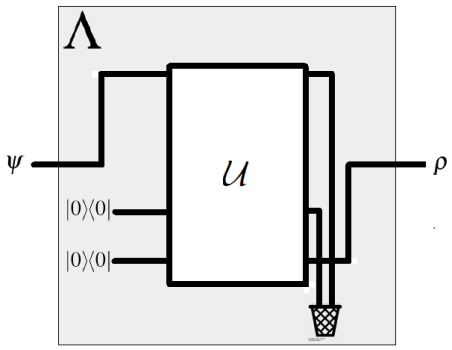

FIGURE 2.2: **Operational interpretation of a quantum channel.** The input and output states are depicted by density matrices ψ and ρ, respectively.

dimensions, the partial trace is taken over the auxiliary system ($\mathcal{H}_r$) and also over the factor encoding the system initial state (see figure 2.2).

Again, the representations of theorem 1 and theorem 3 are completely equivalent, $U(\mathbb{1}_D \otimes |0\rangle \otimes |0\rangle) = \sum_{i=1}^{D} \sum_{j=1}^{r} |i\rangle \otimes |j\rangle \otimes K_{ij}$, with U an unitary acting on $\mathcal{L}(\mathcal{H}_D \otimes \mathcal{H}_r \otimes \mathcal{H}_d)$. Note that the auxiliary system is necessary as to accommodate quantum channels which require a number of Kraus operators bigger than D, or one will not even be able to write the corresponding unitary. Indeed, for a quantum channel with a set of Kraus operators $\{K_i\}_{i=1}^{N}$, we take the dimension of $\mathcal{H}_r$ as $r = N/D$. If N is not divisible by D, we take r as the next natural number after $\frac{N}{D}$ and must find an equivalent set of Kraus operators with Dr elements, $\{K_i'\}_{i=1}^{Dr}$. For instance, suppose we have a system with $D = 3$ dimensions and a quantum channel with 4 Kraus operators. We need an auxiliary basis corresponding to $r = 2$ (right-hand side of the above expression) and a new set of Kraus operators with 6 elements to construct the unitary.

Given a general introduction about quantum channels, in the next section are presented some properties of one specific kind of them, the coarse graining channels.

2.1.1 Coarse graining channels

In our daily descriptions of the world, we only use a small fraction of the variables needed for a complete description of the systems we interact with. Our daily perception of the world are highly coarse grained. Coarse graining in classical physics is made natural by our limited powers of observation and computation. The same is true in quantum mechanics, but in the latter a coarse graining procedure shall be described as a *reduced description* obtained by the *action of a quantum channel*. Roughly speaking, descriptions are named coarse grained when some fine details of the underlying model are smoothed out, or replaced by average behaviours.

A reduced description of a quantum physical system which we aren't able to resolve in detail is obtained by means of the action of a quantum channel $\Lambda_{CG} : \mathcal{L}(\mathcal{H}_D) \to \mathcal{L}(\mathcal{H}_d)$, with $D > d$. After the action of Λ_{CG}, we have the output density matrix as an *effective state* of the system.

Consider the diagram represented in figure 2.3, similar to the one in figure 2.1, extended to give a better understanding of the coarse graining action. As the reader can see, three levels of description are considered: the lower level, which sometimes we call "microscopic level"; the intermediate level - this one just a mathematical abstraction to elucidate the coarse graining action, detailed in the next paragraph; and

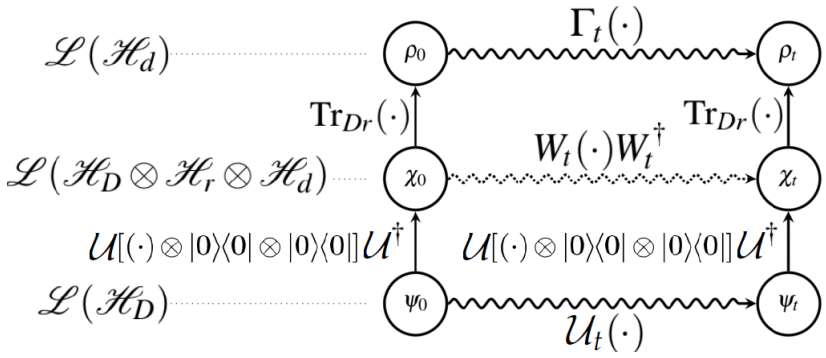

FIGURE 2.3: **The distinct levels and dynamics induced by the coarse graining.**

the upper level, which sometimes we call "macroscopic level". It's important to stress that quantum mechanics is assumed to be valid in all levels, the terminology "microscopic" and "macroscopic" come to facilitate the understanding.

Assume we do not have access to all degrees of freedom of a quantum system described by the density matrix $\psi_0 \in \mathcal{L}(\mathcal{H}_D)$. Operationally, applying the coarse graining channel means: i) to couple the state $|00\rangle\langle 00|$ to ψ_0, increasing the dimension of the system; ii) apply the coarse graining unitary U on the new total system. At this point we have the density matrix $\chi_0 = U(\psi_0 \otimes |00\rangle\langle 00|)U^\dagger \in \mathcal{L}(\mathcal{H}_D \otimes \mathcal{H}_r \otimes \mathcal{H}_d)$. The unitary U is responsible for the interaction between the system and the auxiliary states, mixing the degrees of freedom. We can divide the total system in two parts. One part belonging to $\mathcal{H}_d$ and the other to $\mathcal{H}_D \otimes \mathcal{H}_r$, which does not prevent them from being correlated[3]. Completing the coarse graining procedure, iii) trace out the degrees of freedom which we don't have control over or aren't interested in $(\mathcal{H}_D \otimes \mathcal{H}_r)$, giving the effective state $\rho_0 \in \mathcal{L}(\mathcal{H}_d)$. Notice that the coarse graining channel Λ_{CG} can be applied at any time of the microscopic dynamics.

To proceed, it's worth remembering the questions we want to answer: what's the effective/induced dynamics perceived in the "macroscopic level" Γ_t? What properties Γ_t must have such that $\Gamma_t \circ \Lambda_{\mathrm{CG}}(\psi_0) = \Lambda_{\mathrm{CG}} \circ (U_t(\psi_0)U_t^\dagger)$? The latter condition guarantees that if one evolves ψ_0, in the microscopic level, and then apply Λ_{CG}, one ends with the same state ρ_t that would be obtained if had applied the coarse graining in ψ_0 and then evolved it via Γ_t.

The above construction and our framework (presented in the next section) apply for any coarse graining quantum channel. But, to build concrete examples we need to choose a specific coarse graining map. To motivate and justify our choice, consider a typical optical lattice experiment [1]. In these experiments, a periodic oscillating potential is constructed by counter-propagating light beams and individual atoms are trapped in each potential minimum. In the deep Mott insulator regime hyperfine levels of each atom act as a qubit, and neighbouring qubits interact with each other via a Heisenberg-like Hamiltonian. The measurement of each atom is made via a fluorescence technique: the atoms are shone with a laser in a way that if an atom is in the state $|1\rangle$, lots of light is scattered; if in the state $|0\rangle$, no light is scattered. In order to resolve the light coming from each atom, a powerful lens is necessary, and only recently a single-atom resolution was accomplished [1].

For simplicity, lets consider the case with only two atoms. In this example, our lens is not good enough as to resolve the light coming from each atom (figure 2.4)

[3] In theory of open quantum systems, they are usually related to system and environment, but this is not the case here.

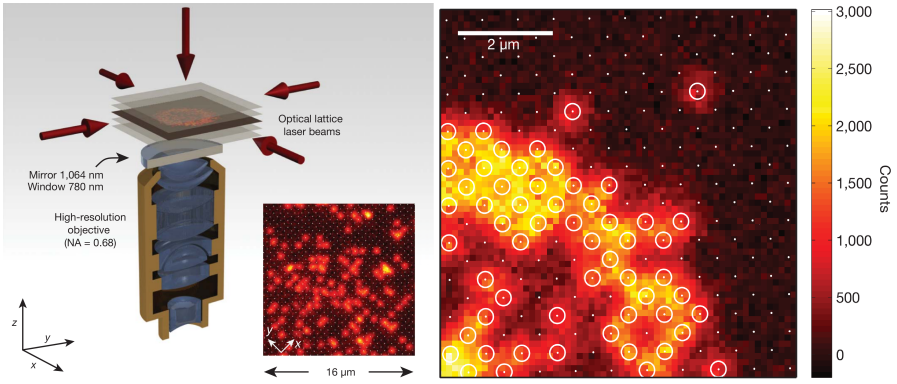

FIGURE 2.4: **Experiment illustrating the blurred detector [1].**

and the amount of light coming from a single atom is sufficient to saturate our detector. In this situation, the states $|01\rangle$ and $|10\rangle$ cannot be distinguished. Besides that, having two excitation, $|11\rangle$, or one excitation, $|01\rangle$ or $|10\rangle$, leads to the same signal. In such conditions, to describe the experiment with two atoms an effective description is already enough. This experimental conditions suggest the coarse graining presented in Table 2.1.

$$\Lambda_{CG}(|00\rangle\langle 00|) = |0\rangle\langle 0| \qquad \Lambda_{CG}(|01\rangle\langle 00|) = \frac{|1\rangle\langle 0|}{\sqrt{3}}$$
$$\Lambda_{CG}(|00\rangle\langle 01|) = \frac{|0\rangle\langle 1|}{\sqrt{3}} \qquad \Lambda_{CG}(|01\rangle\langle 01|) = |1\rangle\langle 1|$$
$$\Lambda_{CG}(|00\rangle\langle 10|) = \frac{|0\rangle\langle 1|}{\sqrt{3}} \qquad \Lambda_{CG}(|01\rangle\langle 10|) = 0$$
$$\Lambda_{CG}(|00\rangle\langle 11|) = \frac{|0\rangle\langle 1|}{\sqrt{3}} \qquad \Lambda_{CG}(|01\rangle\langle 11|) = 0$$

$$\Lambda_{CG}(|10\rangle\langle 00|) = \frac{|1\rangle\langle 0|}{\sqrt{3}} \qquad \Lambda_{CG}(|11\rangle\langle 00|) = \frac{|1\rangle\langle 0|}{\sqrt{3}}$$
$$\Lambda_{CG}(|10\rangle\langle 01|) = 0 \qquad \Lambda_{CG}(|11\rangle\langle 01|) = 0$$
$$\Lambda_{CG}(|10\rangle\langle 10|) = |1\rangle\langle 1| \qquad \Lambda_{CG}(|11\rangle\langle 10|) = 0$$
$$\Lambda_{CG}(|10\rangle\langle 11|) = 0 \qquad \Lambda_{CG}(|11\rangle\langle 11|) = |1\rangle\langle 1|$$

TABLE 2.1: **Coarse graining for a blurred and saturated detector**. Kraus operators can be easily obtained by a quantum process tomography. With the Kraus operators, one can find the corresponding unitary U.

Note that as the detector does not distinguish between the states $|01\rangle$, $|10\rangle$, and $|11\rangle$, there can be no coherence in this subspace. To give a better intuition, consider the following experimental perspective: a photon sent to a Mach-Zehnder interferometer. After the first 50/50 beam splitter, we have a superposition state meaning the photon took the lower arm of the interferometer and the photon took the upper arm. We can assign to these the states $|01\rangle$ and $|10\rangle$, respectively. Once we distinguish the two arms of the interferometer, we can insert a glass plate in one of them in order to visualize interference after the second beam splitter. Decreasing the distance between the two arms, at some point we will no longer be able to place the

plate in just one. The interference pattern will be lost.

The $1/\sqrt{3}$ factors are necessary to make Λ_{CG} trace preserving and completely positive. These factors signals that coherences in the effective description might decrease, but they do not necessarily vanish. This can be readily seen by evaluating the action of Λ_{CG} over a general two-qubits pure state $|\psi\rangle = \sum_{i,j=0}^{1} c_{ij}\,|ij\rangle$, which gives:

$$\Lambda_{CG}(|\psi\rangle\langle\psi|) = \begin{pmatrix} |c_{00}|^2 & c_{00}\frac{c_{01}^*+c_{10}^*+c_{11}^*}{\sqrt{3}} \\ c_{00}^*\frac{c_{01}+c_{10}+c_{11}}{\sqrt{3}} & |c_{01}|^2+|c_{10}|^2+|c_{11}|^2 \end{pmatrix}.$$

This effective state accounts for the statistics of all possible measurements that can be carried out by the detector here modelled. It is thus the description that really matters for this experimental condition, not carrying inaccessible information.

2.2 Coarse-graining induced dynamics

Having in mind the discussions of the previous sections, it is time to address the central question of this chapter: what dynamics might emerge from a fully quantum description if we are not able to resolve the system in all its details? We look for an effective map Γ_t which makes the diagram in figure 2.1 consistent. The induced dynamics then emerges from a coarse grained description of the underlying dynamics.

In order to obtain the induced dynamics Γ_t acting on the effective state $\rho_0 = \Lambda_{CG}(\psi_0)$, we generalize the procedure suggested by Štelmachovič and Bužek in [92]. The authors proposed to write the states of system and environment as the tensor product of its local parts plus a correlation term. Despite the fact that here we do not have such splitting between system and environment, the action of the coarse-graining unitary U_{CG}, now identified by CG, represented in the extended diagram (figure 2.3) suggests the following decomposition:

$$\chi_0 = (\omega_0 \otimes \rho_0) + (\chi_0 - \omega_0 \otimes \rho_0)\,, \tag{2.2}$$

where $\chi_0 = U_{CG}(\psi_0 \otimes |0\rangle\langle 0| \otimes |0\rangle\langle 0|)U_{CG}^\dagger \in \mathcal{L}(\mathcal{H}_D \otimes \mathcal{H}_r \otimes \mathcal{H}_d)$; $\rho_0 = \Lambda_{CG}(\psi_0) = Tr_{Dr}(\chi_0) \in \mathcal{L}(\mathcal{H}_d)$ and $\omega_0 = Tr_d(\chi_0) \in \mathcal{L}(\mathcal{H}_D \otimes \mathcal{H}_r)$. Equation 2.2 is equivalent to Štelmachovič and Bužek decomposition in the intermediate (and abstract) level $\mathcal{H}_D \otimes \mathcal{H}_r \otimes \mathcal{H}_d$, with the last term now representing the correlation between the degrees of freedom which can be assessed and those that cannot.

We can rewrite equation 2.2 as:

$$\psi_0 \otimes |0\rangle\langle 0| \otimes |0\rangle\langle 0| = U_{CG}^\dagger(\omega_0 \otimes \rho_0)U_{CG} + U_{CG}^\dagger(\chi_0 - \omega_0 \otimes \rho_0)U_{CG}. \tag{2.3}$$

Now, applying $U_{CG}.(U_t \otimes \mathbb{1} \otimes \mathbb{1})(\cdot)(U_t^\dagger \otimes \mathbb{1} \otimes \mathbb{1}).U_{CG}^\dagger$ on both sides of equation 2.3 and tracing over Dr, we end up with

$$\begin{aligned} Tr_{Dr}(U_{CG}(U_t(\psi_0)U_t^\dagger \otimes |0\rangle\langle 0| \otimes |0\rangle\langle 0|)U_{CG}^\dagger) = Tr_{Dr}(W_t(\omega_0 \otimes \rho_0)W_t^\dagger) \\ + Tr_{Dr}(W_t(\chi_0 - \omega_0 \otimes \rho_0)W_t^\dagger), \end{aligned} \tag{2.4}$$

where $W_t = U_{CG}.(U_t \otimes \mathbb{1} \otimes \mathbb{1}).U_{CG}^\dagger$ act as the unitary evolution operator in the level $\mathcal{H}_D \otimes \mathcal{H}_r \otimes \mathcal{H}_d$, i. e., $\chi_t = W_t\chi_0 W_t^\dagger$ (see figure 2.3). Note that what we have in the

left hand side of equation 2.4 is $\Lambda_{CG} \circ (U_t(\psi_0)U_t^\dagger)$, which is equal to ρ_t (just choose the bottom path in figures 2.1 and 2.3).

To ensure consistency, $\rho_t = \Gamma_t(\rho_0)$, and equation 2.4 becomes

$$\Gamma_t(\rho_0) = \sum_{i,j} M_{ij}\rho_0 M_{ij}^\dagger + Tr_{Dr}\left(W_t\left(\chi_0 - \omega_0 \otimes \rho_0\right) W_t^\dagger\right), \tag{2.5}$$

with $M_{ij} = \sqrt{p_j}(\langle\phi_i| \otimes \mathbb{1})W_t(|\phi_j\rangle \otimes \mathbb{1})$, where we employed the spectral decomposition $\omega_0 = \sum_j p_j|\phi_j\rangle\langle\phi_j|$. This is the dynamics that emerges if one is not able to resolve all the details of the underlying system. Notice that the effective channel Γ_t is generated by the underlying evolution U_t, the coarse-graining unitary U_{CG} and the underlying initial state ψ_0.

Equation 2.5 is composed by two terms: the first term displays a Kraus form (theorem 1), with $\{M_{ij}\}$ the corresponding set of effective Kraus operators; the second one represents the evolution of the correlations between accessible and non-accessible degrees of freedom. For a better understanding of the latter, consider the Bloch representation of χ_0, ρ_0 and ω_0:

$$\begin{aligned}
\chi_0 &= \frac{1}{Drd}(\mathbb{1}_{Dr} \otimes \mathbb{1}_d + \mathbb{1}_{Dr} \otimes \vec{\alpha}.\vec{\sigma}_d + \vec{\beta}.\vec{\sigma}_{Dr} \otimes \mathbb{1}_d + \sum_{i,j} \theta_{ij}\sigma_{Dr}^{(i)} \otimes \sigma_d^{(j)});\\
\rho_0 &= \frac{1}{d}(\mathbb{1}_d + \vec{\alpha}.\vec{\sigma}_d);\\
\omega_0 &= \frac{1}{Dr}(\mathbb{1}_{Dr} + \vec{\beta}.\vec{\sigma}_{Dr}),
\end{aligned} \tag{2.6}$$

where the $\sigma_q^{(i)}$ are the $q \times q$ generalized Pauli matrices, $\vec{\sigma}_q = (\sigma_q^{(1)}, \sigma_q^{(2)}, \ldots, \sigma_q^{(q^2-1)})^T$; $\vec{\alpha} \in \mathbb{R}^{d^2-1}$ and $\vec{\beta} \in \mathbb{R}^{(Dr)^2-1}$ are the Bloch vectors of ρ_0 and ω_0, respectively. The $((Dr)^2 - 1)(d^2 - 1)$ coefficients $\theta_{ij} \in \mathbb{R}$ fix the correlation between accessible and non-accessible degrees of freedom.

Defining the correlation matrix $[\Theta]_{ij} = (\theta_{ij} - \beta_i\alpha_j)/Drd$, the evolution of the coarse grained state can be written as:

$$\Gamma_t(\rho_0) = \sum_{i,j} M_{ij}\rho_0 M_{ij}^\dagger + \sum_{i,j} \Theta_{ij} Tr_{Dr}\left(W_t\sigma_{Dr}^{(i)} \otimes \sigma_d^{(j)} W_t^\dagger\right). \tag{2.7}$$

It can be verified that $\sum_{i,j} M_{ij}^\dagger M_{ij} = \mathbb{1}_d$:

$$\begin{aligned}
\sum_{i,j} M_{ij}^\dagger M_{ij} &= \sum_{i,j} \sqrt{p_j}(\langle\phi_j| \otimes \mathbb{1}_d)W_t^\dagger(|\phi_i\rangle \otimes \mathbb{1}_d)\sqrt{p_j}(\langle\phi_i| \otimes \mathbb{1}_d)W_t(|\phi_j\rangle \otimes \mathbb{1}_d)\\
&= \sum_j p_j(\langle\phi_j| \otimes \mathbb{1}_d)W_t^\dagger(\sum_i |\phi_i\rangle\langle\phi_i| \otimes \mathbb{1}_d)W_t(|\phi_j\rangle \otimes \mathbb{1}_d)\\
&= \sum_j p_j(\langle\phi_j| \otimes \mathbb{1}_d)W_t^\dagger W_t(|\phi_j\rangle \otimes \mathbb{1}_d)\\
&= \sum_j p_j(\langle\phi_j| \otimes \mathbb{1}_d)(U_{CG}^\dagger.(U_t^\dagger \otimes \mathbb{1} \otimes \mathbb{1}).U_{CG})(U_{CG}.(U_t \otimes \mathbb{1} \otimes \mathbb{1}).U_{CG}^\dagger)(|\phi_j\rangle \otimes \mathbb{1}_d)\\
&= \sum_j p_j(\langle\phi_j|\phi_j\rangle \otimes \mathbb{1}_d) = \mathbb{1}_d.
\end{aligned} \tag{2.8}$$

And that $Tr_d\left(Tr_{Dr}\left(W_t\sigma_{Dr}^{(i)}\otimes\sigma_d^{(j)}W_t^\dagger\right)\right)=0$, as W_t is unitary and the (generalized) Pauli matrices are traceless:

$$\begin{aligned} Tr_d\left(Tr_{Dr}\left(W_t\sigma_{Dr}^{(i)}\otimes\sigma_d^{(j)}W_t^\dagger\right)\right) &= Tr_d\left(Tr_{Dr}\left(\sigma_{Dr}^{(i)}\otimes\sigma_d^{(j)}W_t^\dagger W_t\right)\right) \\ &= Tr_d\left(Tr_{Dr}\left(\sigma_{Dr}^{(i)}\otimes\sigma_d^{(j)}\right)\right) \\ &= Tr_d(\sigma_d^{(j)})Tr_{Dr}(\sigma_{Dr}^{(i)})=0. \end{aligned} \tag{2.9}$$

These guarantee that $Tr_d(\Gamma_t(\rho_0))=1$ for all times. The structure of this type of evolution is very similar to the one describing open quantum systems when system and environment are initially correlated [93, 92].

Let's consider the situation described in section 2.1.1: atoms in neighbouring wells of an optical lattice being measured by a blurred and saturated detector. Suppose that two atoms in such situation are initially represented by a two-qubit pure state $|\psi_0\rangle=\sum_{i,j=0}^{1}c_{ij}|ij\rangle$ and interacting via the Hamiltonian $H=\hbar J\sigma_z\otimes\sigma_z$. At a latter time t, the state $|\psi_0\rangle$ evolves to:

$$|\psi_t\rangle=(c_{00}|00\rangle+c_{11}|11\rangle)e^{-iJt}+(c_{01}|01\rangle+c_{10}|10\rangle)e^{iJt}. \tag{2.10}$$

The effective state at time t can be evaluated via $\rho_t=\Lambda_{CG}(\psi_t)$, and it gives us a matrix very similar to the one evaluated in section 2.1.1:

$$\rho_t=\begin{pmatrix} |c_{00}|^2 & c_{00}\frac{e^{-2iJt}(c_{01}^*+c_{10}^*)+c_{11}^*}{\sqrt{3}} \\ c_{00}^*\frac{e^{2iJt}(c_{01}+c_{10})+c_{11}}{\sqrt{3}} & |c_{01}|^2+|c_{10}|^2+|c_{11}|^2 \end{pmatrix}.$$

Figure 2.5 shows the evolution of the purity, $Tr(\rho_t^2)$, as a function of time for the concrete example in which $J=1$ rad/s and all coefficients c_{ij} in $\psi_0=|\psi_0\rangle\langle\psi_0|$ are all equal: $c_{ij}=\frac{1}{2}$ for $i,j\in\{0,1\}$. One can see that the purity oscillates with time; i. e., the state alternates between pure (when equal to 1) and mixed. Remember that in the underlying level the system is pure for all times, although this is not the way our detector observes the effective system.

Another key point to stress is that changing the coefficients c_{ij}, besides changing the state ρ_t (as the reader can see in the matrix representation above), might also change the effective channel Γ_t. This fact become clear if we look at the Kraus operators M_{ij} in the first term of equation 2.5, which came from the spectral decomposition of $\omega_0=Tr_d(\chi_0)$. The same is true for the correlation matrix Θ_{ij} in equation 2.7. In other words, by changing the input ρ_0 the effective channel Γ_t may change. Let's clarify this point and explore some properties of Γ_t in the next section.

2.2.1 Properties of the effective dynamics

So far, the exact dependence of Γ_t with ψ_0 is unclear. Equation 2.7 doesn't make explicit how the channel depends on the underlying state ψ_0. In this section, making use of the Bloch representation for ψ_0 (equation 2.11 below), we are going to clarify this dependence and study the domain, the positivity and complete positivity of Γ_t. In order to do that, we are going to try to answer two important questions: i) how do we change the effective channel Γ_t for a fixed effective input state ρ_0? And ii) how to change the effective input state keeping Γ_t fixed?

Let

$$\psi_0=\frac{1}{D}(\mathbb{1}+\vec{\gamma}_0.\vec{\sigma}_D) \tag{2.11}$$

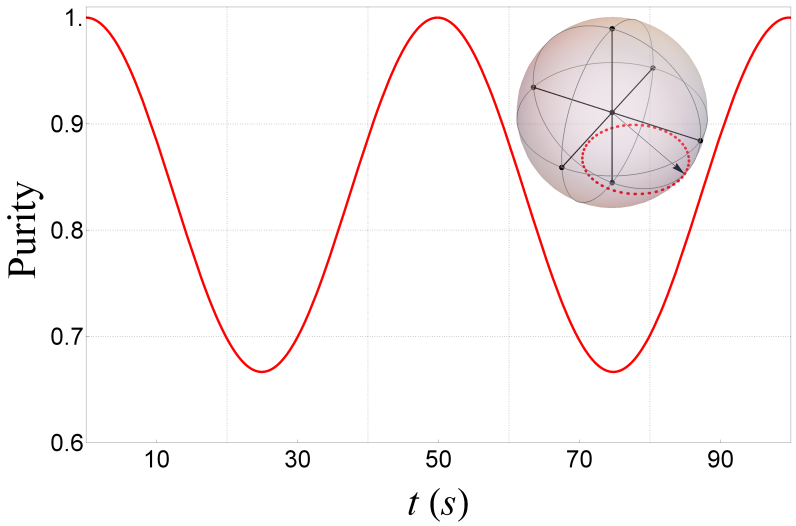

FIGURE 2.5: **Effective evolution as seen by a blurred-saturated detector.** The plot shows an oscillatory behaviour for the purity of the effective state. The inset shows the effective state trajectory in the Bloch sphere.

and

$$\rho_0 = \frac{1}{d}(\mathbb{1} + \vec{\alpha_0}.\vec{\sigma}_d) \tag{2.12}$$

be the Bloch decomposition for ψ_0 and ρ_0 with $\vec{\gamma_0} \in \mathbb{R}^{D^2-1}$ and $\vec{\alpha_0} \in \mathbb{R}^{d^2-1}$ their Bloch vectors, respectively. After the action of a fixed coarse-graining channel in an underlying state ψ_0, the components of ρ_0's $(= \Lambda_{CG}(\psi_0))$ Bloch vector $\vec{\alpha_0}$ are obtained via the linear equations written below (see equation 2.12):

$$\begin{cases} \alpha_{0_1} &= \text{Tr}[\Lambda_{\text{CG}}(\psi_0(\vec{\gamma_0}))\sigma_d^{(1)}]; \\ \alpha_{0_2} &= \text{Tr}[\Lambda_{\text{CG}}(\psi_0(\vec{\gamma_0}))\sigma_d^{(2)}]; \\ \vdots \quad \vdots & \qquad \vdots \\ \alpha_{0_{d^2-2}} &= \text{Tr}[\Lambda_{\text{CG}}(\psi_0(\vec{\gamma_0}))\sigma_d^{(d^2-2)}]; \\ \alpha_{0_{d^2-1}} &= \text{Tr}[\Lambda_{\text{CG}}(\psi_0(\vec{\gamma_0}))\sigma_d^{(d^2-1)}]. \end{cases} \tag{2.13}$$

Seeking to understand well the properties of Γ_t, it is convenient to evoke a geometrical approach. In the $(D^2-1)-$dimensional space of Bloch vectors $\vec{\gamma_0}$, which for now on we will call "γ-space", equations 2.13 represents hyper-planes whose intersection depicts the effective state ρ_0.

Since we are dealing with a coarse-graining map, with $D > d$, the set of equations 2.13 is under-determined, meaning that we can have more than one state ψ_0 leading to the same effective state ρ_0. In the γ-space, this many-to-one mapping is visualized as a hyper-surface of possible solutions.

With the help of figure 2.6 A), and considering fixed the underlying evolution and the coarse graining channel, it can be seem that changes in ψ_0 that represent movements in the intersection of the hyper-planes won't affect the effective state ρ_0. However, such changes can induce modifications in ω_0 and Θ_{ij}, since both have information about $\vec{\gamma}$, and consequently in Γ_t. Figure 2.7 shows a simple example of fixing ρ_0 and changing the effective channel.

Now that we have the first question answered, lets turn to the following: how do we change the effective input state ρ keeping Γ_t fixed? Changing the effective state

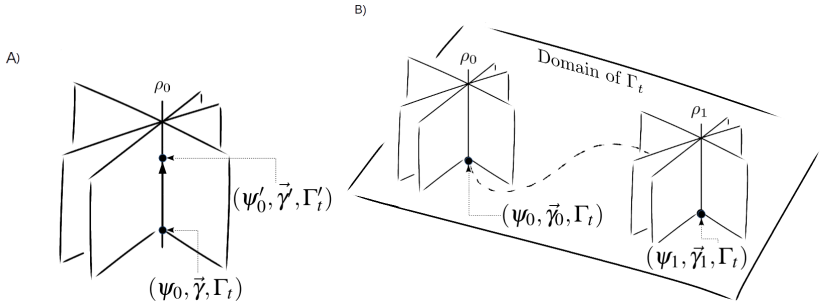

FIGURE 2.6: **The γ-space, and the effects of changing the underlying state.** The intersection between the hyper-planes defines the effective state. A non point-like region reflects the fact that many underlying states lead to the same effective state. A) The left panel shows a change in the underlying state that does not change the effective state ρ_0. This change may, nevertheless, have impact on the effective channel. B) Changing the underlying state such that its Bloch vector $\vec{\gamma}$ moves normally to the hyper-planes changes only the effective state, preserving the effective channel. The region obtained by such normal displacement of the Bloch vector defines the domain of an effective channel.

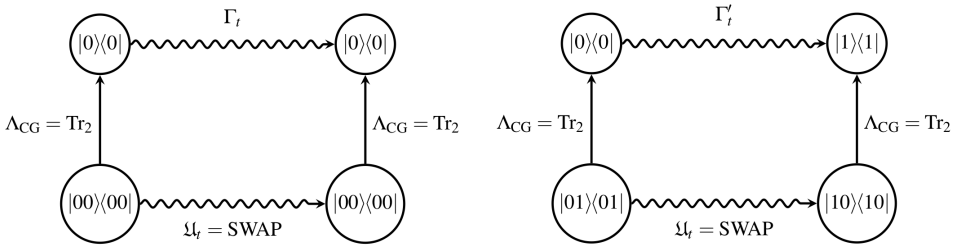

FIGURE 2.7: **Simple example of fixing ρ_0 and changing the effective channel.** For the case where we fix the unitary mapping as the *SWAP*, i.e., $U_t |ij\rangle = SWAP |ij\rangle = |ji\rangle$, and the coarse graining as the usual partial trace on the second component, we see that different underlying states generate different effective channels. The fact that the emergent channels cannot be the same is clear, as if that was the case the same input would lead to two different outputs.

ρ is a consequence of changes in α_i's. Moving the α_i's means, geometrically, to move the hyper-planes in the γ-space. After a specific movement, the hyper-planes will intersect all together in a new different position, representing another effective state.

As shown in figure 2.6 A), moving $\vec{\gamma}$ in the intersection of the hyper-planes, parallel to it, may change the channel. Therefore, in order to keep the channel fix and change only the effective state, we must move $\vec{\gamma}$ outside the intersection, perpendicular to it, as depicted in figure 2.6 B).

The reader may be wondering if the movement depicted in 2.6 B), outside the intersection, and consequently in the α's, won't modify ω_0 or Θ. In fact, it will. But this change in the Kraus operators and the correlation matrix is only due to the change in the input $\rho(\alpha)$ of the effective channel Γ_t. One can rewrite the dynamical equation 2.7 in order to clarify this dependence on the Bloch vector of ρ, α:

$$\Gamma_t(\rho(\alpha)) = \sum_{i,j} M_{ij}(\alpha)\rho(\alpha)M_{ij}^{\dagger}(\alpha) + \zeta(\alpha), \tag{2.14}$$

with $\zeta(\alpha) = \sum_{i,j}\Theta_{ij}(\alpha)Tr_{Dr}(W_t\sigma_{Dr}^{(i)} \otimes \sigma_d^{(j)}W_t^{\dagger})$ the correlation term.

At this time we already know what means to fix the input state ρ_0 and to fix the channel Γ_t. Let's study its properties, beginning with its domain. Our effective channel Γ_t, as mentioned before, is generated by the underlying state ψ_0, the coarse graining Λ_{CG}, which also fixes the hyper-planes in the γ-space through 2.13, and the underlying evolution $U_t(\cdot)U_t^{\dagger}$. Therefore, $\rho_0 = \Lambda_{CG}(\psi_0)$ is our first element of the domain, and starting point.

Consider now two states ρ_0 and ρ_1 in the γ-space, represented by different regions of intersection of hyper-planes. The states $\rho_0 = \Lambda_{CG}(\psi_0)$ and $\rho_1 = \Lambda_{CG}(\psi_1)$ undergo the action of the same channel Γ_t if the two points in the γ-space corresponding to the underlying states ψ_0 and ψ_1 can be connected via the relation:

$$\vec{\gamma}_1 = \vec{\gamma}_0 + \sum_{i}^{d^2-1} c_i\vec{n}_i, \tag{2.15}$$

where $c_i \in \mathbb{R}$ and the vector $\vec{n}_i$ is the normal vector of the i-th hyper-plane, defined only by the coarse graining. This condition guarantees that $\vec{\gamma}_1$, Bloch vector of ψ_1, can be reached from $\vec{\gamma}_0$, Bloch vector of ψ_0 and our initial point in γ-space, by moving it perpendicular to the hyper-planes; therefore not changing the effective channel Γ_t. The domain of Γ_t is then given by all $\rho = \Lambda_{CG}(\psi)$ generated from ψ, with Bloch vector $\vec{\gamma}$, for which there exists coefficients $c_i \in \mathbb{R}$ such that an equation like 2.15 is satisfied.

Equation 2.15 implies that the domain of Γ_t is convex. Let's see: consider $\rho_A = \Lambda_{CG}(\psi_A)$ and $\rho_B = \Lambda_{CG}(\psi_B)$ in the domain of Γ_t. This means that exists coefficients $\{c_{Ai}\}$ and $\{c_{Bi}\}$ such that the Bloch vectors of ψ_A and ψ_B can be written as $\vec{\gamma}_A = \vec{\gamma}_0 + \sum_i^{d^2-1} c_{Ai}\vec{n}_i$ and $\vec{\gamma}_B = \vec{\gamma}_0 + \sum_i^{d^2-1} c_{Bi}\vec{n}_i$, respectively, with c_{Ai} and $c_{Bi} \in \mathbb{R}$. The convex combination of ψ_A and ψ_B, $\psi = p\psi_A + (1-p)\psi_B$ with $p \in [0,1]$, has a Bloch vector $\vec{\gamma}_0 + \sum_i^{d^2-1}(pc_{Ai} + (1-p)c_{Bi})\vec{n}_i$ and $\Lambda_{CG}(\psi) = p\rho_A + (1-p)\rho_B$, which is the convex combination of ρ_A and ρ_B and is also in the domain of Γ_t. Then, the domain of Γ_t is convex.

What about the positivity of Γ_t? As one can see in equation 2.14, our dynamics does not have a Kraus form (theorem 1). This means that, if we consider $\Gamma_t : \mathcal{D}(\mathcal{H}_d) \to \mathcal{D}(\mathcal{H}_d)$, with $\mathcal{D}(\mathcal{H}_d)$ the set of all density matrices acting in $\mathcal{H}_d$, Γ_t is not completely positive and we cannot guarantee that it is even positive. However, as explained above, not all the states of $\mathcal{D}(\mathcal{H}_d)$ are in the domain of Γ_t. And we can

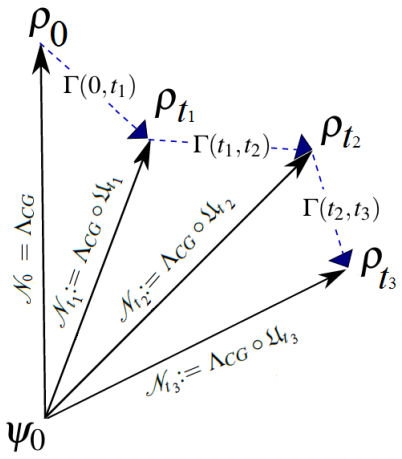

FIGURE 2.8: **Recovering strict complete positivity for the effective channel.** One way to obtain a family of CP effective channels is to require the channel $\mathcal{N}_{t_k} = \Lambda_{CG} \circ \mathcal{U}_{t_k}$ to be CP-divisible.

guarantee the positivity of the channel in its domain, just using the consistence of the diagram in figure 2.3: $\Gamma_t(\rho_0) = \Gamma_t \circ \Lambda_{CG}(\psi_0) = \Lambda_{CG} \circ (U_t(\psi_0)U_t^\dagger)$. In the last term we are applying two positive channels on ψ_0, making the first term, and also Γ_t, positive in all its domain.

We have to be careful when studying the complete positivity of Γ_t, since it isn't all the extensions of effective states ρ into $\rho' \in \mathcal{D}(\mathcal{H}_d \otimes \mathcal{H}_z)$, $\mathcal{H}_z$ an auxiliary Hilbert space, that are possible. The possible extensions for $\rho = \Lambda_{CG}(\psi)$ are those that can be obtained from states $\Psi \in \mathcal{D}(\mathcal{H}_D \otimes \mathcal{H}_z)$, such that $Tr_z(\Psi) = \psi$. This guarantees that $Tr_z((\Lambda_{CG} \otimes \mathbb{1}_z)(\Psi)) = \rho$ and that ψ generates the channel Γ_t. Note that the extension has to come from the underlying level. As we do not have control of all system degrees of freedom, not all the states in the upper level can be generated. The complete positivity is then guaranteed by the same arguments as the positivity (consistence of the diagram in figure 2.3), and the set of states Ψ is the set of effective complete positivity for Γ_t.

We can still re-obtain strict complete positivity if we demand the composite channel $\mathcal{N}_t := \Lambda_{CG} \circ \mathcal{U}_t$, with $\mathcal{U}_t(\cdot) = U_t(\cdot)U_t^\dagger$ to be CP-divisible (CP meaning completely positive) [94], as shown in figure 2.8. If that is the case, the definition of CP-divisible channels requires $\mathcal{N}_{t_k} = \Gamma_{(t_k,t_j)} \circ \mathcal{N}_{t_j}$ for all $t_k \geq t_j$ to be completely positive, with $\Gamma_{(t_k,t_j)}$ representing the effective channel from time t_k to time t_j. This shows a connection between the theory of coarse-graining maps and the theory of non-Markovian maps [94, 95].

2.2.2 Effective Distance Increase

We know from Physics that the discrimination between two unknown quantum states cannot be improved by any further processing of the states [84]. This fact is reflected in a common property of quantum channels (theorem 1): the distance between two input states cannot increase. Mathematically, let $\Upsilon : \mathcal{L}(\mathcal{H}_d) \to \mathcal{L}(\mathcal{H}_d)$ be a quantum channel and ψ and ψ' states in $\mathcal{L}(\mathcal{H}_d)$. Then, $||\Upsilon(\psi) - \Upsilon(\psi')||_1 \leq ||\psi - \psi'||_1$, where the 1-norm distance is defined as $||A||_1 := Tr(\sqrt{A^\dagger A})$.

Looking at equation 2.5 one can see that the effective channel Γ_t is not, in general, in Kraus form. A natural question then arises: It is possible for us to have $||\Gamma_t(\rho_0) - \Gamma_t(\rho_0')||_1 \geq ||\rho_0 - \rho_0'||_1$? We already know by intuition that the distance between the

effective states in the upper level of the dynamics cannot be greater than the distance between the underlying states. Since we do not have access to all degrees of freedom in the underlying level, how would we be able to distinguish it better than if we had full information about it? It's prohibited, and simple to check.

Let $\rho_0 = \Lambda_{CG}(\psi_0)$ and $\rho_0' = \Lambda_{CG}(\psi_0')$ be effective states in $\mathcal{L}(\mathcal{H}_d)$ with respective evolved states $\rho_t = \Gamma_t(\rho_0)$ and $\rho_t' = \Gamma_t(\rho_0')$. Then,

$$\begin{aligned} ||\rho_t - \rho_t'||_1 &= ||\Lambda_{CG}(\psi_t) - \Lambda_{CG}(\psi_t')||_1; \\ &\leq ||\psi_t - \psi_t'||_1; \qquad (2.16) \\ &= ||\mathcal{U}_t(\psi_0) - \mathcal{U}_t(\psi_0')||_1; \\ &\leq ||\psi_0 - \psi_0'||_1 \qquad (2.17) \end{aligned}$$

The last inequality turns into an equality in the case of a unitary mapping $\mathcal{U}_t$, i.e, $\mathcal{U}_t(.) = U_t(.)U_t^\dagger$ for some unitary U_t.

The above expressions doesn't prevent an increasing in distance between effective states. In fact, the answer for the question made two paragraphs above is yes, it is! It is possible to have an increase in distance between the effective states undergoing the same effective channel in comparison with the distance between the effective states before the evolution take place ($t = 0$).

Let's consider an example of such distance increase, taking advantage of the geometric description presented in section 2.2.1. Consider as the coarse-graining quantum channel the one describing the blurred and saturated detector (figure 2.1) and two two-qubits states ψ_0 and ψ_0', which generate the same effective channel Γ_t. In the γ-space of Bloch vectors, the coarse-graining map fixes the normal vectors $\vec{n}_i$ of the hyper-planes. Rewriting the linear system 2.13 in this case, where $\Lambda_{CG} : \mathcal{L}(\mathcal{H}_4) \to \mathcal{L}(\mathcal{H}_2)$,

$$\begin{cases} \alpha_{0_1} &= \mathrm{Tr}[\Lambda_{CG}(\psi_0(\vec{\gamma}_0))\sigma_2^{(1)}] = \mathrm{Tr}[\Lambda_{CG}(\psi_0(\vec{\gamma}_0))\sigma_x]; \\ \alpha_{0_2} &= \mathrm{Tr}[\Lambda_{CG}(\psi_0(\vec{\gamma}_0))\sigma_2^{(2)}] = \mathrm{Tr}[\Lambda_{CG}(\psi_0(\vec{\gamma}_0))\sigma_y]; \\ \alpha_{0_3} &= \mathrm{Tr}[\Lambda_{CG}(\psi_0(\vec{\gamma}_0))\sigma_2^{(3)}] = \mathrm{Tr}[\Lambda_{CG}(\psi_0(\vec{\gamma}_0))\sigma_z]. \end{cases} \qquad (2.18)$$

Above we have three hyper-plane equations in the γ-space of Bloch vectors corresponding to the states $\in \mathcal{L}(\mathcal{H}_4)$. In the left hand side, the α_{0_i}'s are the coefficients of the Bloch vector $\vec{\alpha_0}$ (eq. 2.12). Detailing the expressions we will be able to extract the three corresponding normal vectors, required to find a state ψ_0' so that ρ_0' evolves under the same effective channel Γ_t. For such, we should write the state ψ_0 in its Bloch decomposition (eq. 2.11), which gives

$$\begin{cases} \alpha_{0_1} &= \mathrm{Tr}[\frac{\Lambda_{CG}(\mathbb{1}_4)\sigma_x}{4} + \sum_{i=1}^{15} \frac{\gamma_{0_i}\Lambda_{CG}(\sigma_{4_i})\sigma_x}{4}]; \\ \alpha_{0_2} &= \mathrm{Tr}[\frac{\Lambda_{CG}(\mathbb{1}_4)\sigma_y}{4} + \sum_{i=1}^{15} \frac{\gamma_{0_i}\Lambda_{CG}(\sigma_{4_i})\sigma_y}{4}]; \\ \alpha_{0_3} &= \mathrm{Tr}[\frac{\Lambda_{CG}(\mathbb{1}_4)\sigma_z}{4} + \sum_{i=1}^{15} \frac{\gamma_{0_i}\Lambda_{CG}(\sigma_{4_i})\sigma_z}{4}]. \end{cases} \qquad (2.19)$$

The matrices σ_{4_i} are the 4×4 Gell-Mann matrices, a generalized representation for the Pauli matrices. Then, the i-component of the normal vector to the first hyper-plane, for example, is given by $\frac{\mathrm{Tr}[\Lambda_{CG}(\sigma_{4_i})\sigma_x]}{4}$. For the second and the third hyper-planes, σ_x is changed by σ_y and σ_z, respectively. Thus, the normal vectors $\vec{n}_i$ are

$$\begin{cases} \vec{n}_1 &= \{\frac{1}{2\sqrt{3}}, \frac{1}{2\sqrt{3}}, 0, \frac{1}{2\sqrt{3}}, 0, 0, 0, 0, 0, 0, 0, 0, 0, 0, 0\}; \\ \vec{n}_2 &= \{0, 0, 0, 0, 0, 0, \frac{1}{2\sqrt{3}}, \frac{1}{2\sqrt{3}}, 0, \frac{1}{2\sqrt{3}}, 0, 0, 0, 0\}; \\ \vec{n}_3 &= \{0, 0, 0, 0, 0, 0, 0, 0, 0, 0, 0, 0, \frac{1}{2}, \frac{1}{2\sqrt{3}}, \frac{1}{2\sqrt{6}}\}. \end{cases} \tag{2.20}$$

Notice that the normal vectors are completely determined by the coarse-graining channel, regardless of the initial microscopic state ψ_0. In order to see the effect of increasing in distance (or distinguishability) between states with respect to the trace norm, we are free to choose ψ_0 and $\psi_0^{'}$, provide that they generate the same effective channel Γ_t. For such, it must exist real numbers c_i such that the corresponding Bloch vectors $\vec{\gamma}_0$ and $\vec{\gamma}_0^{'}$ satisfy the relation $\vec{\gamma}_0^{'} = \vec{\gamma}_0 + \sum_{i=1}^{3} c_i \vec{n}_i$. It is satisfied for example if we pick

$$\begin{cases} \vec{\gamma}_0 &= \{0, 0, 0, 0, 0, 0, 0, 0, 0, 0, 0, 0, 0, 0, 0\}; \\ c_1 &= 0,72; \\ c_2 &= 2; \\ c_3 &= 1,035; \\ \vec{\gamma}_0^{'} &= \{\frac{3\sqrt{3}}{25}, \frac{3\sqrt{3}}{25}, 0, \frac{3\sqrt{3}}{25}, 0, 0, \frac{1}{\sqrt{3}}, \frac{1}{\sqrt{3}}, 0, \frac{1}{\sqrt{3}}, 0, 0, \frac{207}{400}, \frac{69\sqrt{3}}{400}, \frac{69\sqrt{\frac{3}{2}}}{400}\}. \end{cases} \tag{2.21}$$

The states ψ_0 and ψ_0' can be obtained using equation 2.11 and information of 2.21, allowing us to calculate $||\psi_0 - \psi_0'||_1$ and also $||\rho_0 - \rho_0'||_1$, using that $\rho_0 = \Lambda_{CG}(\psi_0)$. In order to evaluate $||\rho_t - \rho_t'||_1$, with $\rho_t = \Gamma_t(\rho_0)$, we need to know the underlying dynamics $\mathcal{U}(.)$ governed by the Hamiltonian H. The underlying dynamics together with the coarse-graining channel $\Lambda_{CG}(.)$ and the initial state ψ_0 will specify the effective channel $\Gamma_t(.)$. Relation 2.15 guarantees that ρ_0 and ρ_0' are under the action of the same channel.

We studied two situations with different Hamiltonians. First, an Ising Hamiltonian $H = \hbar J \sigma_z \otimes \sigma_z$. Figure 2.9 A) shows how the distance $||\rho_t - \rho_t'||_1$ evolve in time. Note that, despite the oscillation, $||\rho_0 - \rho_0'||_1 \geq ||\rho_t - \rho_t'||_1$ for all times. If we switch on a transverse field, the Hamiltonian becomes $H = \hbar J \sigma_z \otimes \sigma_z + \hbar\Omega(\sigma_x \otimes \mathbb{1} + \mathbb{1} \otimes \sigma_x)$ and the evolution of the distance between the effective states is shown in figure 2.9 B). The reader can see that the distance $||\rho_t - \rho_t'||_1$ can go beyond $||\rho_0 - \rho_0'||_1$ for some specific times, opening a myriad of opportunities.

Immediate questions arise when we come across this result, for instance: which kind of dynamics or microscopic Hamiltonians could cause this effect? What kind of coarse-grainings channels? What pairs of initial microscopic states? It is possible to predict quantitatively this effect? Could it be a sign of chaos emergence? Is it possible to find bounds? In the concluding chapter we talk about a tool, namely *quantum master equations*, that can help us in dealing with these questions.

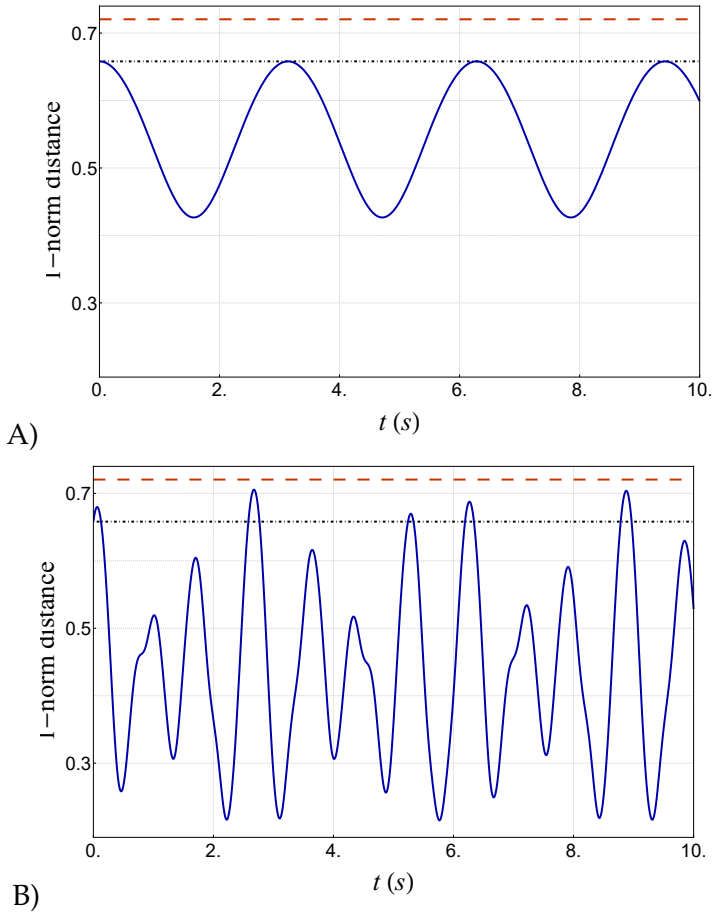

FIGURE 2.9: **Distance increase for the effective dynamics.** In the above plots $||\rho_t - \rho'_t||_1$, $||\psi_0 - \psi'_0||_1$, and $||\rho_0 - \rho'_0||_1$ are represented, respectively by the blue-continuous line, red-dashed line, and the black-dot-dashed line. Contrary to the usual contractive property of quantum channels, on the effective level the distance between two states undergoing the same process may increase. This increase is, however, upper-bounded by the distance between the underlying states (red-dashed line). A) The underlying interaction is dictated by the Hamiltonian $H = \hbar J \sigma_z \otimes \sigma_z$. We see that the distance oscillates, increasing for some time intervals. Nevertheless, in this case, we always have $||\rho_0 - \rho'_0||_1 \geq ||\rho_t - \rho'_t||_1$. B) The underlying evolution is dictated by the Hamiltonian $H = \hbar J \sigma_z \otimes \sigma_z + \hbar\Omega(\sigma_x \otimes \mathbb{1} + \mathbb{1} \otimes \sigma_x)$, and we set $J = 1$ rad/s and $\Omega = 3$ rad/s. In this case we see that $||\rho_t - \rho'_t||_1$ can even go beyond $||\rho_0 - \rho'_0||_1$.

Chapter 3

Modeling a quantum measurement process

Until now, we set out a historical discussion concerning the development of quantum theory, motivating and building a background for the remaining of this thesis. In chapter 2 we investigated emerging dynamics experienced by an observer due to its inability in resolving all the degrees of freedom of a system of interest. Making use of the approach presented in the previous chapter, here we try to model a quantum measurement process involving a system and an apparatus. As will be clear in chapter 4, this is only one of several possible situations to which the formalism of chapter 2 can be applied.

Currently, nature's best description is given by quantum mechanics. According to quantum theory, to every system we assign a quantum state ψ, and its evolution is dictated by Schrodinger's equation [96]. As Schrodinger himself realized, if we take this postulate to our macroscopic and everyday world, we quickly run into paradoxical situations – for example the possibility of an alive-and-dead cat [30]. Not only we do not observe quantum effects on macroscopic systems, but also we do not employ the full quantum description for such systems. In fact, our everyday life experiences heavily rely on effective (macroscopic) descriptions which are far less complex than their underlying quantum characterization (microscopic).

The quantum-classical transition then requires two things to happen: first, that quantum features, like superposition and entanglement, must fade away; second, that an effective description of the macroscopic system must emerge from its quantum description. These issues become more prominent in the measuring process of a microscopic system [97, 39, 98]. In such a situation we interact a system like a single atom, whose description is given by quantum mechanics, with a macroscopic measuring apparatus, for which a classical description is more suitable. The two realms, quantum and classical, meet in such situation. Much like in the Schrodinger's cat scenario, we do not expect to observe an entangled state between the atom and the apparatus. Also, for the measuring apparatus to be of any use, we should observe the apparatus' pointer in a well defined position, and not on a superposition of possible classical values. That amounts for the apparatus to be described by its effective classical description. How are these traits obtained if we depart from a fully quantum description? In other words, how do we reconcile our classical description of the measuring process with the fact that intrinsically both the system being measured and the measuring apparatus are mostly well described by quantum theory?

Traditionally, these questions are addressed by the formalism of decoherence [50, 99, 100], which appeals to the unavoidable interaction between system+apparatus and the environment to explain the diminishing of quantum features. Nevertheless, this approach only cares for local observables and does not explain how the effective

description of the apparatus emerges from its quantum mechanics many-body state. Without that, quantum properties of the apparatus could still be observed.

The fact that a large quantum system might still have pronounced quantum features, if one has access to all its degrees of freedom, was nicely shown by Brukner and his group [66, 67]. In [66] they show that a large spin length still behaves in a quantum way if one can measure all the possible values of the spin, say, in the z-direction. It is only when the measurement outcomes are coarse-grained, i.e., when we cannot resolve nearby outcomes and integrate their signal, that a classical description is obtained.

The approach devised by Brukner's group, however, is not dynamical, in the sense that it applies a coarse graining procedure directly on the measurement outcomes. Inspired by such results, we, at Quantum Information Group at CBPF (qig@CBPF) in collaboration with researchers from the Federal University of Minas Gerais (UFMG) and Federal University of Pernambuco (UFPE), developed a framework that applies a coarse graining procedure directly on the many-body system [85], as described in chapter 2. In this way we can obtain both the effective description of the system and its effective dynamics. Our framework then combines the dynamical aspects of the decoherence approach, with the coarse graining procedure devised by Brukner's group.

The aim of the present chapter is thus to use the developed tools to analyze the effective dynamics of a quantum measurement process. In this way we hope to shed light on one of the most intriguing points of the quantum formalism, the *measurement problem* [101].

Given the generality of quantum channels, in subsection 2.1.1 we used them to construct well-defined deterministic coarse-grainings. A *coarse-graining map* is then a quantum channel Λ_{CG} which maps states from $\mathcal{L}(\mathcal{H}_D) \to \mathcal{L}(\mathcal{H}_d)$ with $D > d$. Physically speaking, the coarse-graining operation defines a partition of the system into accessible and non-accessible degrees of freedom, and then selects only the accessible ones.

The dimension of this accessible part can be much smaller than the dimension of the whole system, rendering a less complex description of the system, i.e., an effective system. In this way, a coarse graining operation is related to a given experimental situation: if all the microscopic details can be observed, then no coarse graining is necessary. On the other hand, if one cannot resolve all the details of the system, the effective description that can be measured corresponds to the coarse-grained state. This is similar to what was described in [66], but this time at the level of the systems.

In section 2.2 we determined the properties of the effective evolution $\Gamma_t : \mathcal{L}(\mathcal{H}_d) \to \mathcal{L}(\mathcal{H}_d)$, which is induced by the underlying evolution $\mathcal{U}_t$, the initial state ψ_0, and the coarse graining Λ_{CG}. In other words, we determined the effective evolution Γ_t which fulfills the consistence relation $\Gamma_t \circ \Lambda_{\mathrm{CG}}(\psi_0) = \Lambda_{\mathrm{CG}} \circ \mathcal{U}_t(\psi_0)$. See figure 2.1. With such formalism at hand, now we are going to apply it to a quantum measurement process.

3.1 Quantum measurement process

The measurement process within quantum mechanics, i.e., using a quantum description for both system and measurement apparatus, was first spelled out by Von Neumann [32]. Revisiting it, suppose that a system S is in a state $|\chi\rangle \in \mathcal{H}_{d_S}$ and a scientist wants to measure an observable $J \in \mathcal{L}(\mathcal{H}_{d_S})$ with corresponding eigenvectors and eigenvalues $|j\rangle$ and $j \in \mathbb{R}$ (assumed non-degenerated), respectively.

It is possible to write the initial system state as $|\chi\rangle = \sum_j c_j |j\rangle$, with $c_j \in \mathbb{C}$ such that $\sum_j |c_j|^2 = 1$. To perform the measurement, the scientist couples the system to the measurement apparatus A, which is in its idle state $|x_0\rangle \in \mathcal{H}_{d_A}$ representing the measurement pointer at position x_0. Observe that for a real quantum measurement situation we have $d_A \gg d_S$. The two systems interact via an unitary operation $U_{SA} : \mathcal{L}(\mathcal{H}_{d_S}) \otimes \mathcal{L}(\mathcal{H}_{d_A}) \to \mathcal{L}(\mathcal{H}_{d_S}) \otimes \mathcal{L}(\mathcal{H}_{d_A})$, which ideally is such that:

$$|\psi_0\rangle \equiv |\chi\rangle |x_0\rangle = \left(\sum_j c_j |j\rangle\right) |x_0\rangle \xrightarrow{U_{SA}} |\psi_t\rangle \equiv \sum_j c_j |j\rangle |x_0 - \alpha j\rangle , \tag{3.1}$$

with $\alpha \in \mathbb{R}$ some proportionality constant. Assuming that the pointer positions at the measurement apparatus are distinguishable, $\langle x_0 - \alpha i | x_0 - \alpha j\rangle = \delta_{ij}$, it will be at position $x_0 - \alpha j$ with probability $|c_j|^2$. However, the composed state of system+apparatus has not a well defined position for the pointer after the interaction. Indeed we get an entangled state between the system and apparatus, a situation akin to Schrodinger's cat [30].

At this point the decoherence program invokes the coupling to an environment E, which initial state is $|\phi_0\rangle$. The measurement dynamics is then changed to:

$$\begin{aligned} |\chi\rangle |x_0\rangle |\phi_0\rangle = \left(\sum_j c_j |j\rangle\right) |x_0\rangle |\phi_0\rangle &\xrightarrow{U_{SA}} \sum_j c_j |j\rangle |x_0 - \alpha j\rangle |\phi_0\rangle \\ &\xrightarrow{U_{SAE}} \sum_j c_j |j\rangle |x_0 - \alpha j\rangle |\phi_j\rangle , \end{aligned} \tag{3.2}$$

where U_{SAE} describes the interaction with the environment. As we can not control the environmental degrees of freedom, they are traced out and, using that $\langle \phi_i | \phi_j \rangle = \delta_{ij}$, we are left with

$$\sum_j |c_j|^2 |j\rangle\langle j| \otimes |x_0 - \alpha j\rangle\langle x_0 - \alpha j|.$$

This state indeed represents an incoherent mixture of product states of the system and measurement apparatus, i.e., only classical correlations are present. Nevertheless, for each value of j we have a *quantum* state for the apparatus. An effective description for the measurement apparatus is thus not obtained by such formalism, and, as such, still depends on a fully quantum description of the apparatus.

In order to tackle this issue, we intend to model the resolution of the measurement apparatus in order to design a coarse graining operation $\Lambda_{\mathrm{CG}} : \mathcal{L}(\mathcal{H}_{d_A}) \to \mathcal{L}(\mathcal{H}_{d'_A})$, with $d_A > d'_A$. Such coarse graining encompasses the decoherence approach, in the sense that it can be used even in closed quantum systems. After the interaction between the system and apparatus, the action of the coarse graining on the apparatus is as follows:

$$\begin{aligned} |\psi_t\rangle\langle\psi_t| &= \sum_{jk} c_j c_k^* |j\rangle\langle k| \otimes |x_0 - \alpha j\rangle\langle x_0 - \alpha k| \\ &\xrightarrow{\mathbb{1}\otimes\Lambda_{\mathrm{CG}}} \rho_t \equiv \sum_{jk} c_j c_k^* |j\rangle\langle k| \otimes \Lambda_{\mathrm{CG}}(|x_0 - \alpha j\rangle\langle x_0 - \alpha k|). \end{aligned} \tag{3.3}$$

For a suitably constructed coarse graining map Λ_{CG}, we expect that the larger the difference $d_A - d'_A$, the smaller will be the contribution of the off-diagonal terms $\Lambda_{\mathrm{CG}}(|x_0 - \alpha j\rangle\langle x_0 - \alpha k|)$, with $j \neq k$. In the limit of a macroscopic detector, $d_A -$

$d'_A \to \infty$, we should obtain

$$|\psi_t\rangle\langle\psi_t| = \sum_{jk} c_j c_k^* |j\rangle\langle k| \otimes |x_0 - \alpha j\rangle\langle x_0 - \alpha k| \xrightarrow{\mathbb{1}\otimes\Lambda_{CG}} \rho_t \approx \sum_j |c_j|^2 |j\rangle\langle j| \otimes \omega_j; \quad (3.4)$$

with $\omega_j \equiv \Lambda_{CG}(|x_0 - \alpha j\rangle\langle x_0 - \alpha j|)$ the effective state of the apparatus when we measure j, such that $Tr(\omega_j \omega_k) = \delta_{jk}$.

Using the techniques developed in chapter 2, we want to obtain not only the effective final state of the measurement, but also the effective dynamics $\Gamma_t : \mathcal{L}(\mathcal{H}_{d_S} \otimes \mathcal{H}_{d'_A}) \to \mathcal{L}(\mathcal{H}_{d_S} \otimes \mathcal{H}_{d'_A})$ induced by the coarse graining Λ_{CG}, the underlying dynamics $\mathcal{U}_t(\cdot) = U_{AB}(\cdot)U_{AB}^\dagger$, and by the initial state $\psi_0 = |\chi_0\rangle\langle\chi_0| \otimes |x_0\rangle\langle x_0|$. Very much like in Fig. 2.1, the consistency for such dynamics now implies

$$\Gamma_t \circ (\mathbb{1} \otimes \Lambda_{CG})(|\chi_0\rangle\langle\chi_0| \otimes |x_0\rangle\langle x_0|) = (\mathbb{1} \otimes \Lambda_{CG}) \circ \mathcal{U}_t(|\chi_0\rangle\langle\chi_0| \otimes |x_0\rangle\langle x_0|). \quad (3.5)$$

In this way, we will be able to describe the whole measurement process for different levels of coarse graining, i.e., different values of $d_A - d'_A$.

3.2 Detailing our proposal

The general objective of this chapter is to apply the tools of quantum information, more specifically those related to quantum channels and the ones developed in previous chapters [85], in order to analyze a quantum measurement process. While the construction in [85] is general and somewhat abstract, here we want to specialize to a concrete scenario of a quantum measurement. To do that, I will describe now the step-by-step procedure.

First we need to devise an exemplary system and measurement apparatus. For instance, as the system to be measured we can take a spin 1/2 system (a qubit), and as the measuring apparatus a system with N qubits. The system+apparatus interaction will then be crafted as to act like a measurement of a system's observable (see Eq. 3.1).

Another possibility to be tested for measurement apparatus is a system with large angular momentum, as used in Ref. [66]. In such a case, the initial state of the apparatus can be taken as a spin-coherent state, and the interaction can be a conditional displacement (a rotation for spin-coherent systems) – this is the situation placed in section 3.3 and appendix B.

Once the system-apparatus microscopic model is fixed, we need to construct and characterize a physically consistent coarse graining channel Λ_{CG}. In [85], and also in chapter 2, we give an example of a coarse graining channel that illustrates a blurred-and-saturated detector. It is an elucidating and didactic example, but to study the measurement process we need a more realistic coarse graining map.

Recently in the literature [102], it was proposed a coarse graining map from a spin-J system to a spin-1/2 system (from qudits to qubits). This can be directly applied to the model for which the measurement apparatus is represented by a large angular momentum system. This coarse graining, differently from the one proposed in [85], has the advantage that it preserves the rotation symmetry. As such, the effective dynamics can be easily computed – if at the underlying level we have a conditional rotation, then at the effective level we expect to obtain also a conditioned rotation.

Inspired by the constructions in [85, 102], we try to obtain a well-defined coarse graining channel to act on the measuring apparatus. Besides describing the lack of

resolution of a measurement apparatus, the coarse graining has to give an effective description of the apparatus, and to transform the entanglement between system and apparatus into classical correlations.

The next step is then to apply the coarse graining channel, in correspondence with the formalism developed in [85], in order to study the quantum measurement process. We will determine the effective evolution which is induced by the coarse graining Λ_{CG}, the underlying evolution $\mathcal{U}_{SA}$ and the combined initial state $|\chi_0\rangle\langle\chi_0| \otimes |x_0\rangle\langle x_0|$. Like in [85], the effective dynamics is to be constructed observing the consistency in 3.5. This means that the effective evolution of the effective state $(\mathbb{1} \otimes \Lambda_{CG})(|\chi_0\rangle\langle\chi_0| \otimes |x_0\rangle\langle x_0|)$ must be the same as to evolve the underlying system, and then apply the coarse graining map. Once this is done, we will pursue the equation of motion for the effective state, i.e., a Lindblad-like equation. This, as suggested in [85], might be a non-linear equation for coarse-grained times.

The coarse graining defined in [102] maps systems of dimension d_A always to two-dimensional systems. Ideally, however, it would be interesting to design a coarse graining map such that it could map a system with an arbitrary dimension d_A to an effective system with arbitrary dimension d'_A, with the only constraint that $d_A > d'_A$. This would allow us to go deeper in the analysis by studying different levels, $d_A - d'_A$, of coarse graining of a quantum system. Pictorially speaking, this would allow us to observe the apparatus in different levels of "zoom out". Thus, we would be able to go from the microscopic and highly detailed underlying level of the apparatus, up to its macroscopic and effective description.

We expect that these process will be responsible by the emergence of the classical features of the system, and that it will be more and more evident as we approach the "macroscopic" description. To analyze that, we also intend to, for instance, observe how the amount of entanglement between system and apparatus get smaller for larger difference $d_A - d'_A$, while the purely classical correlations rise up.

Until the end of this chapter two different modeling attempts are presented, and one more is shown in appendix B. The numbering of the attempts is in chronological order. The main difference between them is in the coarse-graining channels involved in the calculations, while the mathematical procedure is basically the same (explained in section 3.1).

3.3 Model 1: coarse-graining preserving rotation symmetry

A beautiful theory-experiment paper published by Serge Haroche and others in 1992 [103] is the most responsible for the design of the model that is described in this section and in section 3.4. The authors use atoms, one by one passing through a cavity, to reconstruct the photon number distribution of an oscillatory field present within it.

When applied to an initial bosonic coherent field, the intermediate steps of the measuring sequence by the atoms produce quantum superpositions of classical fields, Schrodinger cat states. The Hamiltonian is such that an atom passing through the cavity induces a displacement (or rotation) in the phase space of the coherent state in one direction or the other conditioned to the states of the atom, which act as a qubit – for instance in a superposition of states $|e\rangle$ (excited) and $|g\rangle$ (ground).

They were also able to visualize the death of quantum coherences via decoherence inspecting the Wigner function corresponding to the field state [103] – the interference pattern seen previously is lost. The decay of quantum properties happens on account of the photon losses from the cavity to the surrounding environment.

We have here a very similar situation but with some differences. We will use an atomic coherent state in order to gain information about a qubit in a superposition state. Our first objective is to recover the coefficients c_0 and c_1 of the qubit superposition. Our second objective is to visualize the death of quantum features, but without evoking the decoherence formalism. The main responsible for this effect will be a coarse-graining channel, which mathematically translates our inability in accessing all the degrees of freedom of a given system. So that, to define a good physically motivated coarse-graining will be our biggest challenge.

We then begin our attempts to model a quantum measurement process using the coarse-graining channel introduced in [102]:

$$\Lambda_{CG}(\Psi) = \frac{1}{2}\left(\mathbb{1} + \frac{1}{j}\sum_{i=1}^{3} \langle J_i \rangle_\Psi \, \sigma_i\right), \tag{3.6}$$

where J_i $(i = 1,2,3)$ are the three Cartesian angular momentum components, the generators of SU(2) rotations around the x, y, and z axes, in the d-dimensional Hilbert space $\mathcal{H}_d$ [102]. The denominator j is the largest eigenvalue of J_i $(d = 2j+1)$ and $\langle J_i \rangle_\Psi = \mathrm{Tr}[J_i \, \Psi]$ denotes its expectation value evaluated on the state Ψ.

The coarse-graining channel maps a state Ψ in $\mathcal{L}(\mathcal{H}_d)$ to an effective state $\rho = \Lambda_{CG}(\Psi)$ in $\mathcal{L}(\mathcal{H}_2)$. Unable to access Ψ in all its details, we are left with an effective description. Since in our modelling the channel will act on the measurement device – as explained in section 3.2 –, here represented by a spin coherent state, a property of the channel is convenient: it preserves rotation symmetry. As posed by the authors in [102], this was their main motivation to use the channel. Although a good physical motivation to use it is lacking, it allowed us to get beautiful results, including analytical expressions.

The work done by Haroche in [103] and the channel in 3.6 together guided our choice of a spin coherent state for the measuring apparatus. Why? They are minimum-uncertainty states, the closest to "classical states" [2]. In the three dimensional spin coherent state's space, we can visualize them as localized regions, making the visualization of the dynamics more intuitive (figure 3.2).

Consider as the system to be measured a qubit initially in a state

$$|\chi_0\rangle = c_0 \, |0\rangle + c_1 \, |1\rangle \, , \tag{3.7}$$

with $c_i \in \mathbb{C}$, and the apparatus initially in a spin coherent state. Knowing that a coherent state $|\theta, \phi\rangle$ is obtained by a rotation of the *Dicke state* $|-j\rangle$, the eigenvector associated with the lowest eigenvalue of J_z, two cases will be considered here for the apparatus' initial state $|x_0\rangle$: $(i)\,|x_0\rangle = |-j\rangle \equiv |0,\phi\rangle$ and $(ii)\,|x_0\rangle = \left|\frac{\pi}{2},\phi\right\rangle = R_{\frac{\pi}{2},\phi}\,|-j\rangle$. The rotation operator is given by $R_{\theta,\phi} \equiv e^{-i\theta\vec{n}\cdot\vec{J}}$, $\theta \equiv \omega t$ the rotation angle and ϕ setting the axis $\vec{n} = (\sin\phi, -\cos\phi, 0)$ around which the rotation occurs (see figure 3.1).

We have then our total initial state in the (i) case

$$|\psi_0\rangle = |\chi_0\rangle \otimes |x_0\rangle = (c_0 \, |0\rangle + c_1 \, |1\rangle) \otimes |-j\rangle \, . \tag{3.8}$$

The interaction between system and apparatus plays an important role. It is the responsible for generating entanglement between the parts and also for what we will call here the *conditioned rotation*. The interaction Hamiltonian is given by $H = \hbar\omega \, \sigma_z \otimes \vec{n} \cdot \vec{J}$, with ω meaning frequency, σ_z the Pauli matrix in the z-direction, $\vec{J}$ the angular momentum vector of operators and the unit vector $\vec{n} = (\sin\phi, -\cos\phi, 0)$

(see figure 3.1). Individual Hamiltonians of system and apparatus will not be considered. The state of the system is written on the basis of the eigenvectors of σ_z: $\sigma_z |0\rangle = +1 |0\rangle$ and $\sigma_z |1\rangle = -1 |1\rangle$.

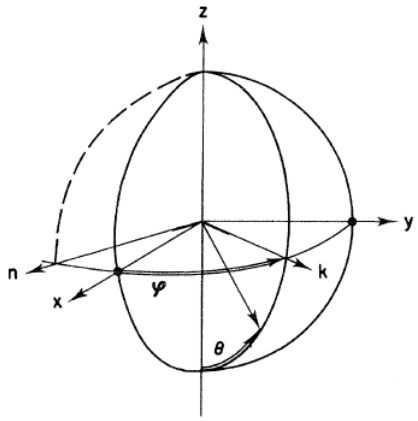

FIGURE 3.1: **Definition of the rotation $R_{\theta,\phi}$ in angular momentum space.** Rotations on the state $|-j\rangle \equiv |0,\phi\rangle$, localized in the south pole, give us the coherent states $|\theta,\phi\rangle$. Figure from [2].

Therefore, the evolved total state $|\psi_t\rangle = U_t |\psi_0\rangle = e^{\frac{-itH}{\hbar}} |\psi_0\rangle$ is equal to

$$|\psi_t\rangle = c_0\, e^{-it\omega\, \mathbb{1}\otimes\vec{n}\cdot\vec{J}} |0\rangle |-j\rangle + c_1\, e^{+it\omega\, \mathbb{1}\otimes\vec{n}\cdot\vec{J}} |1\rangle |-j\rangle\,, \tag{3.9}$$

since the states $|0\rangle$ and $|1\rangle$ are eigenstates of the σ_z operator with eigenvalues $+1$ and -1, respectively. Equation 3.9 shows that the qubit states $|0\rangle$ and $|1\rangle$ induce rotations in the counterclockwise and clockwise directions, respectively, in the apparatus: $e^{-it\omega\vec{n}\cdot\vec{J}} |-j\rangle = R_{\theta,\phi} |-j\rangle \equiv |\theta,\phi\rangle$ and $e^{+it\omega\vec{n}\cdot\vec{J}} |-j\rangle = R_{-\theta,\phi} |-j\rangle \equiv |-\theta,\phi\rangle$ – the temporal dependence will be implicit on θ. Notice that the definition of the direction of rotation is *conditioned* to the eigenvalues of σ_z; in other words, to the qubit state.

In order to view geometrically the dynamics of interaction and the difference between the two cases (i) and (ii), consider the three-dimensional spheres in figure 3.2: the apparatus is initially placed in the "south pole" (i) and in the "equator" (ii). When the system+apparatus interaction is turned on, we have a superposition of two possibilities for the apparatus (red areas representing "positions" of the coherent state): rotations by θ and $-\theta$ angles are induced, weighted by c_0 and c_1, respectively. In figure 3.2 the red areas will run the circumference in blue, each in a direction, clockwise and counterclockwise.

This is how the apparatus acquires information about the system to be measured. The two possible directions of rotations are weighted by c_0 and c_1. The probability of finding the apparatus effective state in one of the superposition possibilities after a measurement contains information about c_0 and c_1. Their values can be recovered looking at such probabilities. This is precisely what we will do: measuring magnetization (σ_z) in the apparatus' effective state after the coarse-graining channel, we will have two possible outcomes, 1 and -1, each one keeping information of one coefficient c_i. We will be able to reconstruct c_0 and c_1.

We can then rewrite the total system-apparatus entangled state $|\psi_t\rangle$ (3.9) as

$$|\psi_t\rangle = c_0 |0\rangle |\theta,\phi\rangle + c_1 |1\rangle |-\theta,\phi\rangle\,. \tag{3.10}$$

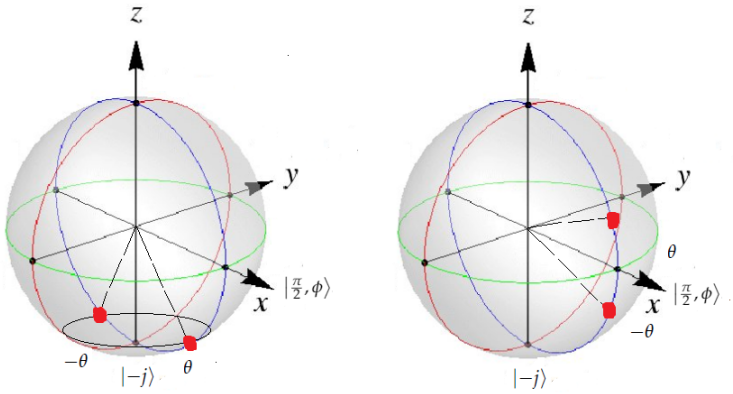

FIGURE 3.2: **Induced dynamics by the Hamiltonian** H. On the left, $(i)\,|x_0\rangle = |-j\rangle$; on the right, $(ii)\,|x_0\rangle = |\frac{\pi}{2},\phi\rangle$. The red areas represent the "positions" of the possibilities for the apparatus' state after a "time" $\theta = \omega t$.

It's better from now on to work on the formalism of density matrices, since we are interested in studying correlations and populations. Let $D = 2d$ be the dimension of the total system+apparatus state. We define $\mathcal{L}(\mathcal{H}_D)$ as the set of all linear operators acting on $\mathcal{H}_D$, and $\mathcal{D}(\mathcal{H}_D) = \{\Psi \in \mathcal{L}(\mathcal{H}_D)|\ \Psi \geq 0, \mathrm{Tr}(\Psi) = 1\}$ the convex set containing all the possible states (density matrices) of the total system. For the total state $\Psi_t = |\psi_t\rangle\langle\psi_t|$,

$$\begin{aligned}\Psi_t = {} & |c_0|^2|0\rangle\langle 0| \otimes |\theta,\phi\rangle\langle\theta,\phi| + c_0c_1^*|0\rangle\langle 1| \otimes |\theta,\phi\rangle\langle -\theta,\phi| \\ & + c_1c_0^*|1\rangle\langle 0| \otimes |-\theta,\phi\rangle\langle\theta,\phi| + |c_1|^2|1\rangle\langle 1| \otimes |-\theta,\phi\rangle\langle -\theta,\phi|.\end{aligned} \tag{3.11}$$

Realize that once interacting, the dynamics represented in figure 3.2 will continue indefinitely. The spin coherent states will keep circular trajectories on the generalized sphere representing the total angular momentum space. It is important to highlight two points: first, the overlap of two coherent states $|\langle\theta,\phi|\theta',\phi\rangle|^2 = \cos(\frac{\Theta}{2})^{4j}$, with Θ the angle between them. In our effective description, as we are mapping states from $d = 2j+1$ to $j = \frac{1}{2}$, the overlap between the coherent states increases. It is important to keep this in mind in order to understand that there will be times in the dynamics that the two contributions for the coherent state will be indistinguishable. In those moments, therefore, no information can be acquired.

The second point refers to the time required by the coherent states to complete a full period and restart the cycle in the sphere (figure 3.2). The coarse-graining preserves rotation symmetry, which means that the angular velocities of the coherent state in its original and effective description will be the same. However, the linear velocities to travel through arc lengths will be different, smaller for the effective description, since it is related to the radius of the trajectory and this, in turn, with the dimension $d = 2j+1$. This means that, comparing the linear velocities just before and after the coarse-graining channel, for increasing values of j, the effective description will become slower and slower in comparison with the original. In the limit $j \to \infty$, it will be necessary an infinity time for a cycle in the sphere (figure 3.2) to be completed.

Assuming we aren't able to access the measuring apparatus in all its details but only via an effective state which shall we call $\rho_A \in \mathcal{L}(\mathcal{H}_2)$, we should apply on it the coarse graining channel Λ_{CG}, responsible for translating such disability mathematically. As we also do not have access to the system to be measured, we should apply

the map $\mathbb{1} \otimes \Lambda_{CG}(\cdot)$ in the total state 3.11.

$$\begin{aligned}\Rightarrow \rho_t = \mathbb{1} \otimes \Lambda_{CG}(\Psi_t) = |c_0|^2 |0\rangle\langle 0| \otimes \Lambda_{CG}(|\theta,\phi\rangle\langle\theta,\phi|) + c_0 c_1^* |0\rangle\langle 1| \otimes \Lambda_{CG}(|\theta,\phi\rangle\langle -\theta,\phi|) \\ + c_1 c_0^* |1\rangle\langle 0| \otimes \Lambda_{CG}(|-\theta,\phi\rangle\langle\theta,\phi|) + |c_1|^2 |1\rangle\langle 1| \otimes \Lambda_{CG}(|-\theta,\phi\rangle\langle -\theta,\phi|).\end{aligned} \tag{3.12}$$

In order to find ρ_t and then $\rho_A = \mathrm{Tr}_S(\rho_t)$, with the help of equation 3.6 we must evaluate $\Lambda_{CG}(|\theta,\phi\rangle\langle\theta,\phi|)$, $\Lambda_{CG}(|\theta,\phi\rangle\langle -\theta,\phi|)$, $\Lambda_{CG}(|-\theta,\phi\rangle\langle\theta,\phi|)$ and $\Lambda_{CG}(|-\theta,\phi\rangle\langle -\theta,\phi|)$. For such, it is convenient to rewrite the coarse-graining channel in equation 3.6 in terms of Dicke states.

$$\Rightarrow \Lambda_{CG}(\Psi) = \frac{1}{2}\Big(\mathbb{1} + \frac{1}{j}\,\mathrm{Tr}[J_x\,\Psi]\,\sigma_x + \frac{1}{j}\,\mathrm{Tr}[J_y\,\Psi]\,\sigma_y + \frac{1}{j}\,\mathrm{Tr}[J_z\,\Psi]\,\sigma_z\Big). \tag{3.13}$$

Considering each term,

$$\mathrm{Tr}[J_z\,\Psi] = \sum_m \langle m|\,\Psi\,J_z\,|m\rangle = \sum_m \hbar m\,\langle m|\,\Psi\,|m\rangle\,; \tag{3.14}$$

$$\begin{aligned}\mathrm{Tr}[J_x\,\Psi] &= \sum_m \langle m|\,\Psi\,\frac{1}{2}(J_+ + J_-)\,|m\rangle = \sum_m (\langle m|\,\Psi\,\frac{J_+}{2}\,|m\rangle + \langle m|\,\Psi\,\frac{J_-}{2}\,|m\rangle) \\ &= \sum_m \frac{\hbar}{2}\Big([(j-m)(j+m+1)]^{\frac{1}{2}}\,\langle m|\,\Psi\,|m+1\rangle \\ &+ [(j+m)(j-m+1)]^{\frac{1}{2}}\,\langle m|\,\Psi\,|m-1\rangle\Big);\end{aligned} \tag{3.15}$$

$$\begin{aligned}\mathrm{Tr}[J_y\,\Psi] &= \sum_m \langle m|\,\Psi\,\frac{1}{2i}(J_+ - J_-)\,|m\rangle = \sum_m (\langle m|\,\Psi\,\frac{J_+}{2i}\,|m\rangle - \langle m|\,\Psi\,\frac{J_-}{2i}\,|m\rangle) \\ &= \sum_m \frac{\hbar}{2i}\Big([(j-m)(j+m+1)]^{\frac{1}{2}}\,\langle m|\,\Psi\,|m+1\rangle \\ &- [(j+m)(j-m+1)]^{\frac{1}{2}}\,\langle m|\,\Psi\,|m-1\rangle\Big).\end{aligned} \tag{3.16}$$

The coarse-graining channel then becomes

$$\begin{aligned}\Lambda_{CG}(\Psi) = \frac{1}{2}\Big\{\mathbb{1} + \frac{\hbar}{j}\sum_m \big\{|0\rangle\langle 0|\,m\,\langle m|\,\Psi\,|m\rangle - |1\rangle\langle 1|\,m\,\langle m|\,\Psi\,|m\rangle \\ + |0\rangle\langle 1|[(j+m)(j-m+1)]^{\frac{1}{2}}\,\langle m|\,\Psi\,|m-1\rangle \\ + |1\rangle\langle 0|[(j-m)(j+m+1)]^{\frac{1}{2}}\,\langle m|\,\Psi\,|m+1\rangle\,\big\}\Big\}.\end{aligned} \tag{3.17}$$

Let's start by calculating $\Lambda_{CG}(|\pm\theta,\phi\rangle\langle\pm\theta,\phi|)$, which encompasses $\Lambda_{CG}(|\theta,\phi\rangle\langle\theta,\phi|)$ and $\Lambda_{CG}(|-\theta,\phi\rangle\langle -\theta,\phi|)$.

$$\begin{aligned}\Rightarrow \Lambda_{CG}(|\pm\theta,\phi\rangle\langle\pm\theta,\phi|) = \frac{1}{2}\Big\{\mathbb{1} + \frac{\hbar}{j}\sum_m \big\{|0\rangle\langle 0|\,m\,\langle m|\pm\theta,\phi\rangle\,\langle\pm\theta,\phi|m\rangle \\ - |1\rangle\langle 1|\,m\,\langle m|\pm\theta,\phi\rangle\,\langle\pm\theta,\phi|m\rangle \\ + |0\rangle\langle 1|[(j+m)(j-m+1)]^{\frac{1}{2}}\,\langle m|\pm\theta,\phi\rangle\,\langle\pm\theta,\phi|m-1\rangle \\ + |1\rangle\langle 0|[(j-m)(j+m+1)]^{\frac{1}{2}}\,\langle m|\pm\theta,\phi\rangle\,\langle\pm\theta,\phi|m+1\rangle\,\big\}\Big\}.\end{aligned} \tag{3.18}$$

We have very similar internal products involving Dicke states and atomic coherent states. From equation (3.13) in reference [2] and reminding that $(i)\ R_{\theta,\phi}\,|-j\rangle \equiv$

$|\theta,\phi\rangle$,

$$\langle m+n|\pm\theta,\phi\rangle = \binom{2j}{j+m+n}^{\frac{1}{2}} \sin^{j+m+n}(\frac{\pm\theta}{2})\cos^{j-m-n}(\frac{\pm\theta}{2})e^{-i(j+m+n)\phi}, \quad (3.19)$$

with $n = \{-1,0,1\}$. All the internal products in equation 3.18 can be evaluated via relation 3.19. Considering $\hbar = 1$, case (i) yields

$$\begin{aligned}\Lambda_{CG}(|\pm\theta,\phi\rangle\langle\pm\theta,\phi|) = \frac{1}{2}\Big\{ &|0\rangle\langle 0|\Big(1+\frac{1}{j}\sum_m m\binom{2j}{j+m}\sin^{2(j+m)}(\frac{\pm\theta}{2})\cos^{2(j-m)}(\frac{\pm\theta}{2})\Big)\\ &+|1\rangle\langle 1|\Big(1-\frac{1}{j}\sum_m m\binom{2j}{j+m}\sin^{2(j+m)}(\frac{\pm\theta}{2})\cos^{2(j-m)}(\frac{\pm\theta}{2})\Big)\\ &+|0\rangle\langle 1|\frac{1}{j}\sum_m \frac{2j!}{(j-m)!(j+m-1)!}\sin^{2(j+m)-1}(\frac{\pm\theta}{2})\cos^{2(j-m)+1}(\frac{\pm\theta}{2})\,e^{-i\phi}\\ &+|1\rangle\langle 0|\frac{1}{j}\sum_m \frac{2j!}{(j+m)!(j-m-1)!}\sin^{2(j+m)+1}(\frac{\pm\theta}{2})\cos^{2(j-m)-1}(\frac{\pm\theta}{2})\,e^{i\phi}\Big\}.\end{aligned} \quad (3.20)$$

For the coherences $\Lambda_{CG}(|\pm\theta,\phi\rangle\langle\mp\theta,\phi|)$ the procedure is slightly different. Experimentally, the output state $\Lambda_{CG}(|\pm\theta,\phi\rangle\langle\mp\theta,\phi|)$ may be obtained by preparing the input states $|\theta,\phi\rangle$, $|-\theta,\phi\rangle$, $|+\rangle = \frac{1}{\sqrt{2}}(|\pm\theta,\phi\rangle + |\mp\theta,\phi\rangle)$ and $|-\rangle = \frac{1}{\sqrt{2}}(|\pm\theta,\phi\rangle + i\,|\mp\theta,\phi\rangle)$ and forming linear combinations of $\Lambda_{CG}(|+\rangle\langle+|)$, $\Lambda_{CG}(|-\rangle\langle-|)$ and $\Lambda_{CG}(|\pm\theta,\phi\rangle\langle\pm\theta,\phi|)$. To get close to the daily routine in the lab, with the help of equation 8.154 in [84], we have:

$$\begin{aligned}\Lambda_{CG}(|\pm\theta,\phi\rangle\langle\mp\theta,\phi|) = \Lambda_{CG}(|+\rangle\langle+|) + i\Lambda_{CG}(|-\rangle\langle-|)\\ -\frac{1+i}{2}\Lambda_{CG}(|\pm\theta,\phi\rangle\langle\pm\theta,\phi|) - \frac{1+i}{2}\Lambda_{CG}(|\mp\theta,\phi\rangle\langle\mp\theta,\phi|).\end{aligned} \quad (3.21)$$

The terms $\Lambda_{CG}(|\pm\theta,\phi\rangle\langle\pm\theta,\phi|)$ and $\Lambda_{CG}(|\mp\theta,\phi\rangle\langle\mp\theta,\phi|)$ can be computed using equation 3.20, while $\Lambda_{CG}(|+\rangle\langle+|)$ and $\Lambda_{CG}(|-\rangle\langle-|)$ using 3.17 and 3.20.

With the result of expression 3.21 and equation 3.20 we are able to compute the final effective state $\rho_t = \mathbb{1}\otimes\Lambda_{CG}(\Psi_t)$ in equation 3.12. Summations will be simplified making the transformation $j+m \to k$ and also $2j \to n$, then identifying the results with Newton's binomials. We end up with

$$\begin{aligned}\rho_t = |c_0|^2|0\rangle\langle 0|\otimes&\begin{bmatrix}\sin(\frac{\theta}{2})^2 & \frac{\sin(\theta)}{2}e^{-i\phi}\\ \frac{\sin(\theta)}{2}e^{i\phi} & \cos(\frac{\theta}{2})^2\end{bmatrix}\\ +(-1)^{2j}\cos(\theta)^{2j-1}\Big\{&c_0c_1^*|0\rangle\langle 1|\otimes\begin{bmatrix}-\sin(\frac{\theta}{2})^2 & \frac{\sin(\theta)}{2}e^{-i\phi}\\ -\frac{\sin(\theta)}{2}e^{i\phi} & \cos(\frac{\theta}{2})^2\end{bmatrix}\\ &+c_1c_0^*|1\rangle\langle 0|\otimes\begin{bmatrix}-\sin(\frac{\theta}{2})^2 & -\frac{\sin(\theta)}{2}e^{-i\phi}\\ \frac{\sin(\theta)}{2}e^{i\phi} & \cos(\frac{\theta}{2})^2\end{bmatrix}\Big\}\\ &+|c_1|^2|1\rangle\langle 1|\otimes\begin{bmatrix}\sin(\frac{\theta}{2})^2 & -\frac{\sin(\theta)}{2}e^{-i\phi}\\ -\frac{\sin(\theta)}{2}e^{i\phi} & \cos(\frac{\theta}{2})^2\end{bmatrix}.\end{aligned} \quad (3.22)$$

Above is written the total system+apparatus state after an interaction time t, with

the temporal dependence implicit in the rotation angle $\theta \equiv \theta(t) = \omega t$. The coarse-graining channel was applied only in the measuring apparatus, meaning that we already have an effective *quantum* state for the apparatus. The ideal scenario would be, in the case of strong coarse-graining ($j \to \infty$), the disappearance of all quantum correlations and the maintenance and growth of the classical ones.

In order to make a better analysis, the reduced density matrix of the apparatus will be useful. Consider $\rho_A = \mathrm{Tr}_S[\rho_t]$, where we are tracing out the system's degrees of freedom in ρ_t – given by equation 3.22 (case (i)). For convenience, we can choose the axis that defines the rotation plane so as to simplify the calculations. Selecting the rotation plane as x-z, $\phi = 0$ and $e^{-i\phi} = 1$, as depicted in figure 3.1. Therefore,

$$\rho_A = \frac{1}{2}\begin{bmatrix} 1-\cos(\theta) & \sin(\theta)(2|c_0|^2-1) \\ \sin(\theta)(2|c_0|^2-1) & 1+\cos(\theta) \end{bmatrix}. \tag{3.23}$$

Inspecting the apparatus' reduced density matrix ρ_A in 3.23, the first question is whether it is possible to gather information about the target system measuring the populations corresponding to the apparatus' states $|0\rangle\langle 0|$ and $|1\rangle\langle 1|$. In other words, the whole quantum measurement process modeled here is given as follows: the qubit, initially in a superposition, is placed to interact with a spin coherent state, our measuring device; after a certain interaction time, we measure σ_z in the apparatus' effective state ρ_A.

The probabilities of obtaining the two possible outcomes 1 and -1 in the measuring device, associated with the states $|0\rangle\langle 0|$ and $|1\rangle\langle 1|$, respectively, would allow us to recover the values of the coefficients $|c_0|$ and $|c_1|$ in the initial state of the system (3.7). This is what we expected. However, there is no dependence on $|c_0|^2$ in the diagonal of 3.23. Thus, it is not possible to gather information about the system measuring the populations of the apparatus' reduced density matrix.

That was our motivation to analyze the case (ii). We need to find the corresponding reduced density matrix ρ_A. We can start by tracing out system's degrees of freedom in an equation analogous to 3.12 but for case (ii). The only difference is the transformation $|\theta,\phi\rangle \to \left|\theta+\frac{\pi}{2},\phi\right\rangle$. So,

$$\begin{aligned}\rho_A &= \mathrm{Tr}_S(\mathbb{1}\otimes\Lambda_{CG}(\Psi_t)) \\ &= |c_0|^2\Lambda_{CG}(|\theta+\frac{\pi}{2},\phi\rangle\langle\theta+\frac{\pi}{2},\phi|) + |c_1|^2\Lambda_{CG}(|-\theta+\frac{\pi}{2},\phi\rangle\langle-\theta+\frac{\pi}{2},\phi|).\end{aligned} \tag{3.24}$$

Using that the coarse-graining channel Λ_{CG} preserves rotation symmetry,

$$\begin{aligned}\rho_A &= |c_0|^2\Lambda_{CG}(|\theta+\frac{\pi}{2},\phi\rangle\langle\theta+\frac{\pi}{2},\phi|) + |c_1|^2\Lambda_{CG}(|-\theta+\frac{\pi}{2},\phi\rangle\langle-\theta+\frac{\pi}{2},\phi|) \\ &= |c_0|^2\Lambda_{CG}(R_{\theta,\phi}|\frac{\pi}{2},\phi\rangle\langle\frac{\pi}{2},\phi|R^\dagger_{\theta,\phi}) + |c_1|^2\Lambda_{CG}(R_{-\theta,\phi}|\frac{\pi}{2},\phi\rangle\langle\frac{\pi}{2},\phi|R^\dagger_{-\theta,\phi}) \\ &= |c_0|^2\Lambda_{CG}(R_{\theta,\phi}R_{\frac{\pi}{2},\phi}|-j\rangle\langle-j|R^\dagger_{\frac{\pi}{2},\phi}R^\dagger_{\theta,\phi}) + |c_1|^2\Lambda_{CG}(R_{-\theta,\phi}R_{\frac{\pi}{2},\phi}|-j\rangle\langle-j|R^\dagger_{\frac{\pi}{2},\phi}R^\dagger_{-\theta,\phi}) \\ &= |c_0|^2R_{\frac{\pi}{2},\phi}\Lambda_{CG}(R_{\theta,\phi}|-j\rangle\langle-j|R^\dagger_{\theta,\phi})R^\dagger_{\frac{\pi}{2},\phi} + |c_1|^2R_{\frac{\pi}{2},\phi}\Lambda_{CG}(R_{-\theta,\phi}|-j\rangle\langle-j|R^\dagger_{-\theta,\phi})R^\dagger_{\frac{\pi}{2},\phi} \\ &= |c_0|^2R_{\frac{\pi}{2},\phi}\Lambda_{CG}(|\theta,\phi\rangle\langle\theta,\phi|)R^\dagger_{\frac{\pi}{2},\phi} + |c_1|^2R_{\frac{\pi}{2},\phi}\Lambda_{CG}(|-\theta,\phi\rangle\langle-\theta,\phi|)R^\dagger_{\frac{\pi}{2},\phi}.\end{aligned} \tag{3.25}$$

Notice that we already know the quantities $\Lambda_{CG}(|\pm\theta,\phi\rangle\langle\pm\theta,\phi|)$, they are given in matrix form in 3.22. Considering $\phi = 0$ as in case (i), we reach the final result. The

reduced state ρ_A for case (ii) is given by

$$\rho_A = \frac{1}{2}\begin{bmatrix} 1+\sin(\theta)(1-2|c_0|^2) & -\cos(\theta) \\ -\cos(\theta) & 1+\sin(\theta)(2|c_0|^2-1) \end{bmatrix}. \tag{3.26}$$

Remembering the movement in the generalized sphere (figure 3.2), in (i) the two possible configurations of the apparatus, as time passes, will always be in the same latitude (notice the black circle connecting the red areas on the left-hand side sphere). We credit this fact for the non-observance of the effect of the coefficients c_0 and c_1. Measuring on the z basis on the effective apparatus' state is like projecting on the z-axis, and thus we don't see any correlation. In (ii), instead, one possible configuration will take direction to the north pole and the other to the south pole, and the presence of c_0 and c_1 becomes visible – phenomenon shown in figure 3.3.

It is convenient to plot one population – or the probability of obtaining a specific outcome after a series of measurements – as function of θ (or time) and the coefficient c_0. The graph depicted in figure 3.3 is for the population regarding outcome 1. Notice that it is possible to gain information about c_0 and c_1 no matter the apparatus' initial dimension (3.26). On the vertical axis we have the absolute value of the populations (it cannot exceed 1) and on the horizontal axes we have the rotation angle θ and the coefficient c_0.

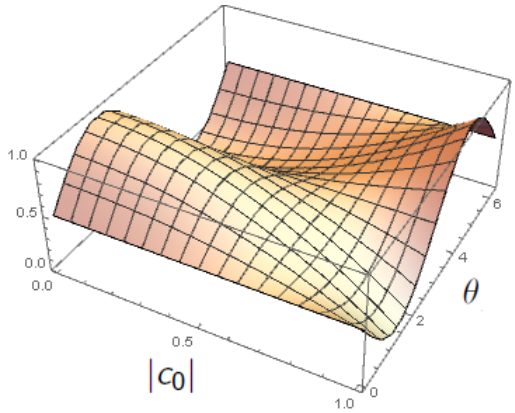

FIGURE 3.3: **Apparatus' reduced density matrix population for outcome** 1 **in the** (ii) **case.** The angle θ is in radians and $j = 100$ – the apparatus' initial dimension $d = 2j+1$.

We have then an effective bi-dimensional state for the measurement apparatus with two possible measurement outcomes, which we will call 1 and -1, or *up* and *down*, making a direct connection with the states $|0\rangle\langle 0|$ and $|1\rangle\langle 1|$, respectively. These two possibilities motivate us to name the quantum measurement process here modeled as *a digital measurement scenario*. Nevertheless, as can be seen inspecting matrices 3.23 and 3.26, the coherences of the apparatus' effective state don't vanish, not even in the limit $j \to \infty$.

Remember that without external influence, system and apparatus interact indefinitely. As expressed in equation 3.9, before the coarse-graining action we have for most of the time a system-apparatus entangled state with a superposition of two directions of rotations associated each with one possible state for the system. In figure 3.3 in order to localize the angular position of the coherent states with respect to the south pole in the $3D$ sphere, one should add $\frac{\pi}{2}$ to the θ value given in the axis for one contribution, and subtract $\frac{\pi}{2}$ for the other.

For an experimentalist, there are certain interaction times, or angles of rotation, which are better to acquire information about the system. Revisiting the discussion about the overlap between two coherent states, $|\langle\theta,\phi|\theta',\phi\rangle|^2 = \cos(\frac{\Theta}{2})^{4j}$, it is minimal – 0 – when the coherent states are in diametrically opposite positions. This is, the best rotation angles to recover c_0 and c_1 are such that the two contributions of the spin coherent state are positioned close to the poles of the sphere – they are initially positioned in equator.

Effectively, in the Bloch sphere, this means close to the orthogonal eigenstates of σ_z, $|0\rangle$ and $|1\rangle$. From the point of view of the purity of the effective state 3.26, given by $\mathrm{Tr}[\rho_A^2]$ and shown in the graph 3.4 as a function of c_0 and θ, in fact, for θ a multiple integer of π we have maximum information about ρ_A – it is a pure state.

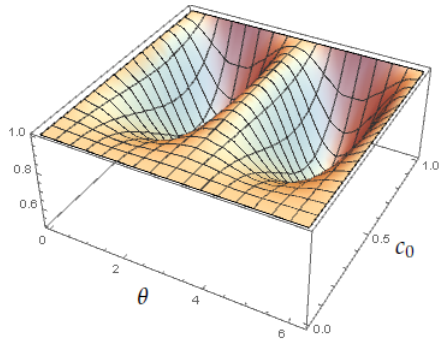

FIGURE 3.4: **Purity of ρ_A (3.26) as a function of c_0 and θ.** It oscillates in time, reaching their maximum value for θ a multiple integer of π.

Our next step is to analyze quantum correlations, in particular entanglement. For such, we calculate for the (i) case the concurrence, analytically and numerically, and the mutual information, just numerically, considering the total system+apparatus state after the coarse graining action as a function of θ and for increasing values of j. We also investigate the situation $j \to \infty$ (apparatus' initial dimension $d \to \infty$).

In figure 3.5 are depicted four graphs with two plots each: concurrence (orange lines) and mutual information (blue lines). The j values grow from left to right and top to bottom and the θ angle grows positively from the south pole in the counter-clockwise direction. The concurrence is defined as $\mathcal{C}(\rho) \equiv \max(0, \lambda_1 - \lambda_2 - \lambda_3 - \lambda_4)$, in which the λ_i's are the eigenvalues, in decreasing order, of the Hermitian matrix $R = \sqrt{\sqrt{\rho}\rho'\sqrt{\rho}}$, $\rho \in \mathcal{D}(\mathcal{H}_4)$, and $\rho' = (\sigma_y \otimes \sigma_y)\rho^*(\sigma_y \otimes \sigma_y)$ [104, 105].

As can be seen from the graphs, the interaction creates entanglement. For θ values close to π, the red areas on the left-hand side of figure 3.2 meet at the north pole, overlap, and entanglement goes to zero. Then begins to grow again, going to zero when the red areas reach the south pole, restarting the cycle. As our inability to resolve the apparatus in all its details increases, meaning here an increase in the apparatus' initial dimension, the entanglement starts to drop considerably (figure 3.5). This event reinforces our idea of the death of quantum features due to a crude view of the studied system.

For the mutual information, which quantifies the presence of quantum or classical correlations, we use the definition $I(S:A) = S(\rho_S) + S(\rho_A) - S(\rho_{SA})$, with $S(\cdot)$ the Von Neumann entropy. The states ρ_S and ρ_A are the reduced states for system and apparatus, and ρ_{SA} the total state. Notice that for small values of j the mutual information reaches its highest value – 2 – (figure 3.5), indicating the presence of classical and quantum correlations. With the increase of the coarse graining

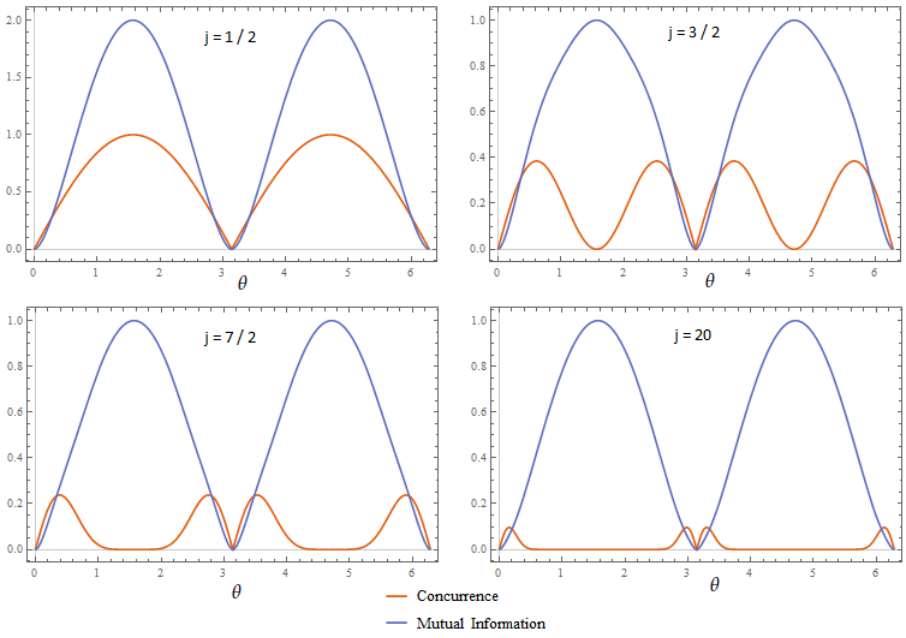

FIGURE 3.5: **Concurrence and mutual information graphs on the total system-apparatus state for increasing values of** j. The larger the j, the larger the apparatus' initial dimension d and, consequently, the stronger the coarse-graining action. The angle θ is in radians and $c_0 = c_1 = \frac{1}{\sqrt{2}}$.

strength, their values decline considerably and then stabilize, meaning the death of quantum correlations and the creation of classical ones.

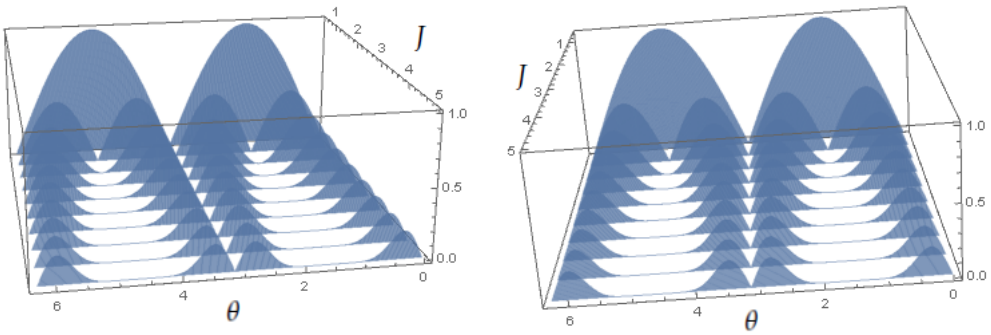

FIGURE 3.6: **Concurrence** $3D$ **graph as a function of the rotation angle** θ **and** j**.** Decay of quantum correlations by increasing the strength of the coarse-graining channel. It is shown the global behaviour of the orange lines in figure 3.5. The angle θ is in radians and $c_0 = c_1 = \frac{1}{\sqrt{2}}$. In the right-hand side the analytical plot and in the left-hand side the numerical plot.

Entanglement's behaviour becomes clearer if we look to figure 3.6, which is a $3D$ concurrence graph as a function of θ and j. Notice the decay of quantum correlations already for not so large values of j. Evaluating the eigenvalues $\lambda_i's$ used to calculate $\mathcal{C}(\rho)$, it is not difficult to find an expression in the form $\mathcal{C}(j,\theta)$. Using the total state 3.22 to find analytically the eigenvalues, there are two of them different from zero.

Following the calculations,

$$\begin{aligned}\lambda_1 - \lambda_2 - \lambda_3 - \lambda_4 &= \left\{|c_0|^2|c_1|^2\tan^2(\theta)(\cos(\theta) + (-1)^{2j+1}\cos^{2j}(\theta))^2\right\}^{\frac{1}{2}} \\ &- \left\{|c_0|^2|c_1|^2\tan^2(\theta)(\cos(\theta) + (-1)^{2j}\cos^{2j}(\theta))^2\right\}^{\frac{1}{2}} \\ &= |c_0c_1\sin(\theta)(1 + (-1)^{2j+1}\cos^{2j-1}(\theta))| - |c_0c_1\sin(\theta)(1 + (-1)^{2j}\cos^{2j-1}(\theta))| \\ &= |c_0c_1\sin(\theta)(1 + (-1)^{2j+1}\cos^{2j-1}(\theta) - 1 + (-1)^{2j+1}\cos^{2j-1}(\theta))| \\ &= |2c_0c_1\sin(\theta)\cos^{2j-1}(\theta)(-1)^{2j+1}|. \\ \\ &\Rightarrow \mathcal{C}(j,\theta) = 2|c_0c_1\sin(\theta)\cos^{2j-1}(\theta)|.\end{aligned} \tag{3.27}$$

This is the plot in the right-hand side of figure 3.6. Notice that j can not assume any value, but $j \in \{0, 0.5, 1, 1.5..\}$. In the limit of a strong coarse-graining,

$$\lim_{j\to\infty} 2|c_0c_1\sin(\theta)\cos^{2j-1}(\theta)| = 0, \tag{3.28}$$

which can be seen writing $\cos^{2j-1}(\theta)$ as $(e^{-i\theta} + e^{i\theta})^{2j-1}\,2^{1-2j}$.

The physical situation becomes even more interesting if we consider another viewpoint in the Schrodinger's cat scenario. Let's imagine the cat as an apparatus with the objective of measuring the atom that is about to decay. Note that we have a digital measurement scenario with two possibilities: 1, dead cat, for instance, the atom has decayed; -1, alive cat, the atom has not decayed. As shown above, due to the action of the coarse graining channel it is possible to observe the decay of quantum correlations. Also, one of the motivations for using the channel was exactly to model a situation in which we do not have access to the system (here, the atom) and only partial information about the apparatus, an effective state (the cat).

Thus, after opening the box and actually measuring, we are not looking at the cat (apparatus) in his fully quantum version, but via an effective description with just two possibilities, dead or alive. This is a possible way to address the Schrodinger's cat paradox without evoking any interference from the surrounding environment or the leakage of information by the box.

Despite of the beautiful results obtained using the coarse-graining channel 3.6, it is difficult to extract a good physical intuition regarding the meaning of the channel itself. In search for a more physically intuitive coarse-graining channel Λ_{CG} able to show us the death of coherences in the apparatus' effective state in the limit of a strong coarse-graining, we set out for the second and third attempts, presented in the next section and in appendix B (for not having obtained conclusive results), respectively.

3.4 Model 2: a magnetization measurement

At this point of our discussions, looking for to improve our model of a quantum measurement process and with the feeling given by the modelling 1, we have decided to imagine the measuring apparatus consisting of N qubits. Instead of looking at the apparatus as a coherent state, it is as if we look at each of its parts. This change of focus along with the design of a new coarse-graining map allowed us to obtain new results, that were not reached before.

The global situation is similar to what we had in model 1: a system to be measured consisting of a qubit initially in a superposition and an apparatus consisting of N qubits ($N >> 1$) interact. The corresponding interaction Hamiltonian is such that it induces a *conditioned rotation*. Depending on the state of the qubit-system the apparatus will rotate in one direction on the other. Thus, information about c_0 and c_1 will be imprinted in the measuring device. Again, the observable that will be measured is magnetization. With a subtle difference from model 1: now, the apparatus' effective state $\rho \in \mathcal{L}(\mathcal{H}_3)$. We will have then three possible outcomes in our *digital measurement scenario*: $-1, 0$ and 1.

Let's start writing the total system+apparatus initial state. The target qubit $|\psi_0\rangle = c_0|0\rangle + c_1|1\rangle$ and $|\Psi\rangle = \sqrt{p}|0\rangle + \sqrt{1-p}e^{i\phi}|1\rangle$ is the state of each one of the N apparatus' constituents – $e^{i\phi}$ a phase and $p \in [0,1]$. The total initial state is then given by

$$\begin{aligned}|\chi_0\rangle &= |\psi_0\rangle_S \otimes \left|\Psi^N\right\rangle_A = |\psi_0\rangle_S \otimes \{\, |\Psi\rangle \otimes |\Psi\rangle \otimes |\Psi\rangle \otimes ... \otimes |\Psi\rangle \,\}_A \\ &= (c_0|0\rangle + c_1|1\rangle) \otimes \Big\{ (\sqrt{p}|0\rangle + \sqrt{1-p}e^{i\phi}|1\rangle) \otimes (\sqrt{p}|0\rangle + \sqrt{1-p}e^{i\phi}|1\rangle) \otimes \\ &\cdots \otimes (\sqrt{p}|0\rangle + \sqrt{1-p}e^{i\phi}|1\rangle) \Big\}.\end{aligned} \tag{3.29}$$

The measuring device is initially in a product state, meaning that neither classical nor quantum correlations are present. In fact, neither between the apparatus' constituents nor between system to be measured and apparatus. The main motivation for such configuration came from systems of nuclear magnetic resonance (NMR), where the nuclear atomic spins play the role of qubits. Measures of magnetization and magnetic fields are important in such systems [106].

As in section 3.3, the main tool used by us to extract information about the quantum measurement process is the density matrix. The initial total system+apparatus density matrix, before any interaction, is given by the separable state

$$|\chi_0\rangle\langle\chi_0| = \{|c_0|^2|0\rangle\langle 0| + c_0c_1^*|0\rangle\langle 1| + c_1c_0^*|1\rangle\langle 0| + |c_1|^2|1\rangle\langle 1|\} \otimes |\Psi^N\rangle\langle\Psi^N|. \tag{3.30}$$

System and apparatus interaction is the responsible for generating entanglement between the parts.

The interaction Hamiltonian is chosen by $H = \hbar\frac{\omega}{N}\sigma_z \otimes \vec{J}_x$, where $\vec{J}_x$ is the vector sum of each individual angular momentum operator in the x-direction $\vec{J_{xi}}$, namely $\vec{J}_x = \vec{J_{x1}} + \vec{J_{x2}} + ... + \vec{J_{xN}}$, and ω the coupling constant, the angular frequency of the rotation induced by the angular momentum operator around the x-axis. It is important to divide the Hamiltonian by N to ensure that it is bounded even for increasing values of N.

The evolution will induce rotations in each apparatus' constituent, clockwise ($-\theta$) and counterclockwise ($+\theta$) directions, conditioned to the system's qubit states $|0\rangle$ and $|1\rangle$ – here, $\sigma_z|0\rangle = +1|0\rangle$ and $\sigma_z|1\rangle = -1|1\rangle$. The evolved total state is then given by

$$\begin{aligned}|\chi_t\rangle\langle\chi_t| &= U_{t,0}|\chi_0\rangle\langle\chi_0|U_{t,0}^\dagger = e^{-i\frac{\omega t}{N}\sigma_z\otimes\vec{J}_x}|\chi_0\rangle\langle\chi_0|e^{+i\frac{\omega t}{N}\sigma_z\otimes\vec{J}_x} \\ &= |c_0|^2|0\rangle\langle 0| \otimes R_{\theta,x}|\Psi^N\rangle\langle\Psi^N|R_{\theta,x}^\dagger + c_0c_1^*|0\rangle\langle 1| \otimes R_{\theta,x}|\Psi^N\rangle\langle\Psi^N|R_{-\theta,x}^\dagger \\ &+ c_1c_0^*|1\rangle\langle 0| \otimes R_{-\theta,x}|\Psi^N\rangle\langle\Psi^N|R_{\theta,x}^\dagger + |c_1|^2|1\rangle\langle 1| \otimes R_{-\theta,x}|\Psi^N\rangle\langle\Psi^N|R_{-\theta,x}^\dagger,\end{aligned} \tag{3.31}$$

with $R_{\theta,x} = e^{-i\frac{\omega t}{N}\vec{J}_x}$ and $\theta \equiv \frac{\omega t}{N}$. In equation 3.31 we have a system+apparatus entangled state representing a rotation of θ or $-\theta$ (around the x-axis) in the apparatus' constituents conditioned to the eigenvalue $+1$ or -1 of the operator σ_z acting in the system's state.

Our first objective here is to recover c_0 and $c_1 \in [0,1]$; to gain information about the system looking at the measuring apparatus. Just as we are considering in our modeling the system inaccessible, we also do not have access to the measuring device in all its details, but via an effective description. Mathematically, this effective description will be provided by a coarse graining channel Λ_{CG}, which we will define soon. Differently from the model 1, here $\Lambda_{\text{CG}} : \mathcal{L}(\mathcal{H}_{2^N}) \to \mathcal{L}(\mathcal{H}_3)$, with $\mathcal{L}(\mathcal{H}_i)$ the space of linear operators acting on the Hilbert space $\mathcal{H}_i$. Once again, however, the output dimension is fixed.

Notice that the output dimension of the coarse graining channel is 3, and no longer 2. Which means that when measuring magnetization of the effective state of the apparatus in the z-direction, three outcomes will be possible: -1, 0 and 1. Therefore, our digital measurement scenario now has three possibilities. There will be some probability of finding $1, 0$ or -1 in the apparatus' display, after a time t of interaction, which will be related to the absolute values of c_0 and c_1. Let's start by analyzing such probabilities in order to gain intuition and construct Λ_{CG}.

Let's define the total magnetization of the apparatus by the sum of σ_z:

$$M_z = \sum_{i=1}^{N} \sigma_{z\,i}, \tag{3.32}$$

where we are summing on all the N constituents. This would be the case if we had access to each one of the N qubits. Unfortunately, we don't have such resolution. Inspired by the work done by David Poulin when studying macroscopic observables – defined by the author as the total value of a physical quantity over a collection of quantum systems [107] –, we decided to model this lack of resolution through a division in bins.

Our coarse description will be such that: if more than $\frac{2}{3}$ of the N apparatus' constituents are in the state $|0\rangle$ ($\sigma_z |0\rangle = +1 |0\rangle$), the measuring device will show in the display *magnetization 1*; if less than $\frac{N}{3}$ are in the state $|0\rangle$, it will show *magnetization -1*; if in the interval $(\frac{N}{3}, \frac{2N}{3})$, the apparatus will show *magnetization 0*. With this division in three bins, or regions $[0,\frac{N}{3}]$, $(\frac{N}{3},\frac{2N}{3})$ and $[\frac{2N}{3},N]$, projectors on different magnetization subspaces are being grouped and perceived as an effective one depending on the region that contains it. In other words, rather than perceiving changes in total magnetization with the resolution of one qubit, only changes involving $\frac{N}{3}$ qubits are perceptible.

In this context, the probabilities will be represented by $\Pr(Z_i^N|\Psi_t^N)$, with $\Psi_t^N = \text{Tr}_S(|\chi_t\rangle\langle\chi_t|) \in \mathcal{L}(\mathcal{H}_{2^N})$ the evolved reduced density matrix of the apparatus and Z_i^N we define as the sum of projectors on subspaces of the same total magnetization (expressions 3.33), representing sums of the POVM elements of the total magnetization on the z-direction.

Now the expressions for Z_i^N:

$$\begin{aligned} Z_1^N &= \sum_{l=\frac{2N}{3}}^{N} \sum_{\sigma} \Pi_\sigma |0_1 0_2 .. 0_l 1_1 .. 1_{N-l}\rangle\langle 0_1 0_2 .. 0_l 1_1 .. 1_{N-l}| \Pi_\sigma^\dagger; \\ Z_0^N &= \sum_{l>\frac{N}{3}}^{<\frac{2N}{3}} \sum_{\sigma} \Pi_\sigma |0_1 0_2 .. 0_l 1_1 .. 1_{N-l}\rangle\langle 0_1 0_2 .. 0_l 1_1 .. 1_{N-l}| \Pi_\sigma^\dagger; \\ Z_{-1}^N &= \sum_{l=0}^{N/3} \sum_{\sigma} \Pi_\sigma |0_1 0_2 .. 0_l 1_1 .. 1_{N-l}\rangle\langle 0_1 0_2 .. 0_l 1_1 .. 1_{N-l}| \Pi_\sigma^\dagger, \end{aligned} \tag{3.33}$$

where each sum also includes all possible states represented by permutations of 0's and 1's. To give an intuition, consider the following example with $N = 3$:

$$\begin{aligned} Z_1^3 &= |001\rangle\langle 001| + |010\rangle\langle 010| + |100\rangle\langle 100| + |000\rangle\langle 000|; \\ Z_{-1}^3 &= |110\rangle\langle 110| + |101\rangle\langle 101| + |011\rangle\langle 011| + |111\rangle\langle 111|. \end{aligned} \tag{3.34}$$

It is an emblematic example, no projector makes up Z_0^N. Nevertheless, there is no contradiction or counter-intuitive fact here. As suggested by the projectors in equation 3.33, the application of the new coarse-graining map in the computational basis elements of a state of N qubits, with Π_σ the permutation operator, will be given by:

$$\begin{aligned} &\Lambda_{\mathrm{CG}}(\Pi_\sigma |0_1 0_2 .. 0_l 1_1 .. 1_{N-l}\rangle\langle 0_1 0_2 .. 0_l 1_1 .. 1_{N-l}| \Pi_\sigma^\dagger) = \begin{cases} |-1\rangle\langle -1|, & \text{if } l \leq \frac{N}{3} \ \forall \sigma; \\ |1\rangle\langle 1|, & \text{if } l \geq \frac{2N}{3} \ \forall \sigma; \\ |0\rangle\langle 0|, & \text{if } \frac{N}{3} < l < \frac{2N}{3} \ \forall \sigma; \end{cases} \\ &\Lambda_{\mathrm{CG}}(\Pi_\sigma |0_1 0_2 .. 0_l 1_1 .. 1_{N-l}\rangle\langle 0_1 0_2 .. 0_l 1_1 .. 1_{N-l}| \Pi_{\sigma'}^\dagger) = 0, \ \forall \ \sigma \neq \sigma'; \end{aligned} \tag{3.35}$$

The states $|1\rangle\langle 1|$, $|0\rangle\langle 0|$ and $|-1\rangle\langle -1|$ represent the diagonal terms, from top to bottom, in that order, in our effective description $\in \mathcal{L}(\mathcal{H}_3)$. They are directly related with the magnetization outcomes 1, 0 and -1, respectively.

The action of the map on the elements $\Pi_\sigma |0_1 0_2 .. 0_l 1_1 .. 1_{N-l}\rangle\langle 0_1 0_2 .. 0_l 1_1 .. 1_{N-l}| \Pi_{\sigma'}^\dagger$ is 0 by the fact that our description does not distinguish between $\Pi_\sigma |0_1 0_2 .. 0_l 1_1 .. 1_{N-l}\rangle$ and $\Pi'_\sigma |0_1 0_2 .. 0_l 1_1 .. 1_{N-l}\rangle$, two elements with the same number of 0's and 1's exchanged in a different way. Therefore, there can be no coherence between them. In the example 3.34 the projectors which make up Z_1^3 will be mapped in $|1\rangle\langle 1|$ and the projectors which make up Z_{-1}^3 in $|-1\rangle\langle -1|$.

It is time to think about the probabilities $\Pr(Z_i^N | \Psi_t^N)$. The quantities Z_i^N have already been defined. Let's now focus on Ψ_t^N, the evolved reduced density matrix of the apparatus. For such, let's look at equation 3.31. Not all terms will survive the operation of tracing out the system, necessary since we do not have access to it. We will have left with

$$\begin{aligned} \Psi_t^N &= \mathrm{Tr}_S(|\chi_t\rangle\langle\chi_t|) \\ &= |c_0|^2 R_{\theta,x} \, |\Psi^N\rangle\langle\Psi^N| R_{\theta,x}^\dagger + |c_1|^2 R_{-\theta,x} \, |\Psi^N\rangle\langle\Psi^N| R_{-\theta,x}^\dagger. \end{aligned} \tag{3.36}$$

We need to calculate $R_{\theta,x} = e^{-i\frac{\omega t}{N}\vec{J}_x}$ and $R_{-\theta,x} = e^{+i\frac{\omega t}{N}\vec{J}_x}$, where θ is given by $\omega t/N$, with the time dependence implicit. Remembering that the total angular momentum

operator $\vec{J}_x = (\vec{J}_{x1} + \vec{J}_{x2} + ... + \vec{J}_{xN})$, it is possible to write

$$R_{\theta,x}\,|\Psi^N\rangle\langle\Psi^N|R^\dagger_{\theta,x} = R_{\theta,x,1}\,|\Psi\rangle\langle\Psi|_1 R^\dagger_{\theta,x,1} \otimes R_{\theta,x,2}\,|\Psi\rangle\langle\Psi|_2 R^\dagger_{\theta,x,2} ... \otimes R_{\theta,x,N}\,|\Psi\rangle\langle\Psi|_N R^\dagger_{\theta,x,N}. \tag{3.37}$$

Rotations by the same angle θ will be induced in each constituent of the apparatus. This is what the above equation is showing us.

Noticing that $|\Psi\rangle\langle\Psi| \in \mathcal{L}(\mathcal{H}_2)$, for each constituent we have $J_x = \frac{\sigma_x}{2}$, considering $\hbar = 1$. Using that $e^{-i\frac{\theta}{2}\sigma_x} = \mathbb{1}\cos(\frac{\theta}{2}) - i\,\sigma_x \sin(\frac{\theta}{2})$,

$$\begin{aligned} R_{\theta,x}\,|\Psi\rangle\langle\Psi|\,R^\dagger_{\theta,x} = &\begin{bmatrix} \cos\theta/2 & -i\,\sin\theta/2 \\ -i\,\sin\theta/2 & \cos\theta/2 \end{bmatrix} \cdot \\ &\begin{bmatrix} p & \sqrt{p(1-p)}e^{-i\phi} \\ \sqrt{p(1-p)}e^{i\phi} & 1-p \end{bmatrix} \cdot \begin{bmatrix} \cos\theta/2 & i\,\sin\theta/2 \\ i\,\sin\theta/2 & \cos\theta/2 \end{bmatrix}. \end{aligned} \tag{3.38}$$

Which gives

$$\begin{aligned} R_{\theta,x}\,|\Psi\rangle\langle\Psi|\,R^\dagger_{\theta,x} = \frac{1}{2}\Big\{ &|0\rangle\langle 0|\big\{1 + (-1+2p)\cos\theta + 2\sqrt{p(1-p)}\sin\theta\sin\phi\big\} \\ &+ |0\rangle\langle 1|\big\{i(-1+2p)\sin\theta + 2\sqrt{p(1-p)}(\cos\phi - i\cos\theta\sin\phi)\big\} \\ &+ |1\rangle\langle 0|\big\{i(1-2p)\sin\theta + 2\sqrt{p(1-p)}(\cos\phi + i\cos\theta\sin\phi)\big\} \\ &+ |1\rangle\langle 1|\big\{1 + \cos\theta - 2p\cos\theta - 2\sqrt{p-p^2}\sin\theta\sin\phi\big\}\Big\}. \end{aligned} \tag{3.39}$$

Making the tensor product $(..) \otimes (..) \otimes .. \otimes (..)$ of 3.39 N times, we will finally have $R_{\theta,x}\,|\Psi^N\rangle\langle\Psi^N|\,R^\dagger_{\theta,x}$. It is a complicated calculation. However, our first objective is to find the probabilities, which requires only the knowledge of the diagonal elements. Writing $x \equiv \big\{\frac{1}{2} + (-\frac{1}{2}+p)\cos\theta + \sqrt{p(1-p)}\sin\theta\sin\phi\big\}$, $1-x \equiv \frac{1}{2}\big\{1 + \cos\theta - 2p\cos\theta - 2\sqrt{p-p^2}\sin\theta\sin\phi\big\}$ and forgetting for now the off-diagonals elements – Z^N_1, Z^N_0 and Z^N_{-1} will only select the diagonal ones –, we should calculate

$$\begin{bmatrix} x & \\ & 1-x \end{bmatrix}_1 \otimes \begin{bmatrix} x & \\ & 1-x \end{bmatrix}_2 \otimes .. \otimes \begin{bmatrix} x & \\ & 1-x \end{bmatrix}_N = \begin{bmatrix} x^N & & \\ & x^{N-1}(1-x)^1 & \\ \vdots & & \ddots \end{bmatrix}. \tag{3.40}$$

The subscripts are identifying the constituents. For N constituents there are 2^N diagonal elements in the resulting matrix. Each x represents an entry associated with the projector $|0\rangle\langle 0|$ and each $1-x$ represents an entry associated with the projector $|1\rangle\langle 1|$.

Therefore,

$$\begin{aligned} \Pr(Z^N_1|\,\Psi^N_t) &= \Pr(Z^N_1|\,|c_0|^2 R_{\theta,x}\,|\Psi^N\rangle\langle\Psi^N|R^\dagger_{\theta,x} + |c_1|^2 R_{-\theta,x}\,|\Psi^N\rangle\langle\Psi^N|R^\dagger_{-\theta,x}) \\ &= |c_0|^2 \sum_{k=\frac{2N}{3}}^{N} \binom{N}{k} x^k (1-x)^{N-k} + |c_1|^2 \sum_{k=\frac{2N}{3}}^{N} \binom{N}{k} y^k (1-y)^{N-k}, \end{aligned} \tag{3.41}$$

where we get y from x doing $\theta \to -\theta$. We can also rewrite $|c_1|^2 = 1 - |c_0|^2$. The binomial term accounts for the permutations of 0's and 1's once fixed the number k of 0's. At the point of equation 3.41 the probability depends on p, θ, ϕ, N and c_0. In

other words, on the initial states of system and apparatus and the time ($\theta = \omega t/N$). Notice that $\Pr(Z_1^N|\,\Psi_t^N)$ is exactly the first diagonal element of the effective state of the apparatus, after the coarse-graining. Proceeding, for magnetization outcome 0 and 1, respectively,

$$\begin{aligned}\Pr(Z_0^N|\,\Psi_t^N) &= \Pr(Z_0^N|\,|c_0|^2 R_{\theta,x}\,|\Psi^N\rangle\langle\Psi^N|R_{\theta,x}^\dagger + |c_1|^2 R_{-\theta,x}\,|\Psi^N\rangle\langle\Psi^N|R_{-\theta,x}^\dagger)\\ &= |c_0|^2 \sum_{k>\frac{N}{3}}^{<\frac{2N}{3}} \binom{N}{k} x^k(1-x)^{N-k} + (1-|c_0|^2) \sum_{k>\frac{N}{3}}^{<\frac{2N}{3}} \binom{N}{k} y^k(1-y)^{N-k};\end{aligned} \tag{3.42}$$

$$\begin{aligned}\Pr(Z_{-1}^N|\,\Psi_t^N) &= \Pr(Z_{-1}^N|\,|c_0|^2 R_{\theta,x}\,|\Psi^N\rangle\langle\Psi^N|R_{\theta,x}^\dagger + |c_1|^2 R_{-\theta,x}\,|\Psi^N\rangle\langle\Psi^N|R_{-\theta,x}^\dagger)\\ &= |c_0|^2 \sum_{k=0}^{\frac{N}{3}} \binom{N}{k} x^k(1-x)^{N-k} + (1-|c_0|^2) \sum_{k=0}^{\frac{N}{3}} \binom{N}{k} y^k(1-y)^{N-k}.\end{aligned} \tag{3.43}$$

The expressions 3.41, 3.42 and 3.43 are the probabilities of outcomes $1, 0$ and -1 in the measuring device after system+apparatus interaction – remember that x and $1-x$ have implicit temporal dependence. The calculation of the probabilities using Z_i^N gives us exactly the same result as if we had applied the coarse-graining map and then evaluated the probabilities in the effective description, as expected.

Before the interaction, or in other words, immediately after switching on the apparatus, $\theta = 0$, x and $y \to p$ and $(1-x)$ and $(1-y) \to (1-p)$. The dependence on c_0 disappears, as expected. They are given by

$$\begin{aligned}&\Pr(Z_1^N|\,|c_0|^2\,|\Psi^N\rangle\langle\Psi^N| + |c_1|^2\,|\Psi^N\rangle\langle\Psi^N|)\\ &\quad= |c_0|^2 \sum_{k=\frac{2N}{3}}^{N} \binom{N}{k} p^k(1-p)^{N-k} + (1-|c_0|^2) \sum_{k=\frac{2N}{3}}^{N} \binom{N}{k} p^k(1-p)^{N-k}\\ &\quad= \sum_{k=\frac{2N}{3}}^{N} \binom{N}{k} p^k(1-p)^{N-k}.\end{aligned} \tag{3.44}$$

Similarly,

$$\Pr(Z_0^N|\,|c_0|^2\,|\Psi^N\rangle\langle\Psi^N| + |c_1|^2\,|\Psi^N\rangle\langle\Psi^N|) = \sum_{k>\frac{N}{3}}^{<\frac{2N}{3}} \binom{N}{k} p^k(1-p)^{N-k}; \tag{3.45}$$

$$\Pr(Z_{-1}^N|\,|c_0|^2\,|\Psi^N\rangle\langle\Psi^N| + |c_1|^2\,|\Psi^N\rangle\langle\Psi^N|) = \sum_{k=0}^{\frac{N}{3}} \binom{N}{k} p^k(1-p)^{N-k}. \tag{3.46}$$

Below follow 3D plots for the above probabilities as functions of the superposition coefficient p for the initial states of the apparatus' constituents and the number of constituents N (figures 3.7 to 3.9). Notice that, for large values of N, with the purpose of measuring magnetization in the z-axis, if we choose $p = 0.5$ the apparatus will always show 0 on the display. The probabilities of showing 1 or -1 are zero. In fact, before coupling the measurement apparatus to the system, and when turning it on, it is expected to show magnetization 0. It is a really interesting result, which approaches our model to the real daily in the lab. The condition of a huge number of constituents is important to give a feeling of the situation with an apparatus with

size that we are familiar with in daily-life.

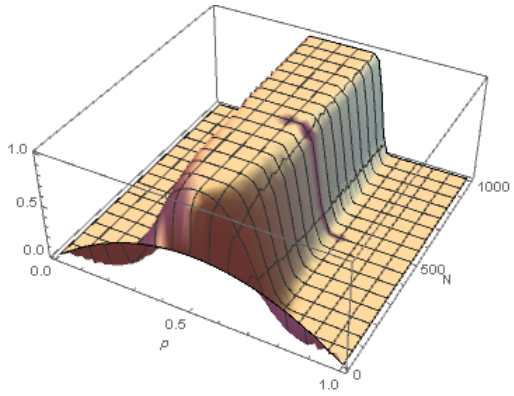

FIGURE 3.7: **Probability of measuring magnetization 0 before the interaction.** For large N and p close to 0.5, it is one. On the graph, N starts from 2.

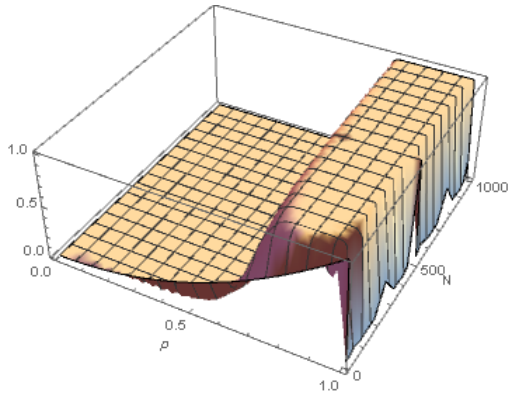

FIGURE 3.8: **Probability of measuring magnetization +1 before the interaction.** For large N and p close to 0.5, it is zero. On the graph, N starts from 2.

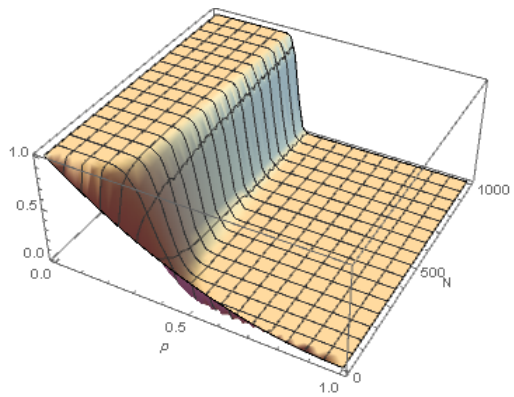

FIGURE 3.9: **Probability of measuring magnetization -1 before the interaction.** For large N and p close to 0.5, it is zero. On the graph, N starts from 2.

For times greater than zero, the probabilities oscillate over time periodically, reaching local maxima whose values depends on the coefficient c_0. Note that the oscillatory nature of the probabilities was expected, since the rotations to which the

apparatus' constituents are subjected occur continuously. The graphs shown in figures 3.7 to 3.9 suggest the choice of $p = 0.5$. For simplicity, we have also chosen $\phi = \frac{\pi}{2}$. Below follow 3D plots for the probabilities as function of a parametrization of time $\theta = \frac{\omega t}{N}$ and the number of constituents N (figures 3.10 to 3.12). For each outcome 1, 0 and -1 we construct two graphs, corresponding to $c_0 = \frac{1}{\sqrt{2}}$ (on the left) and $c_0 = \frac{1}{\sqrt{3}}$ (on the right).

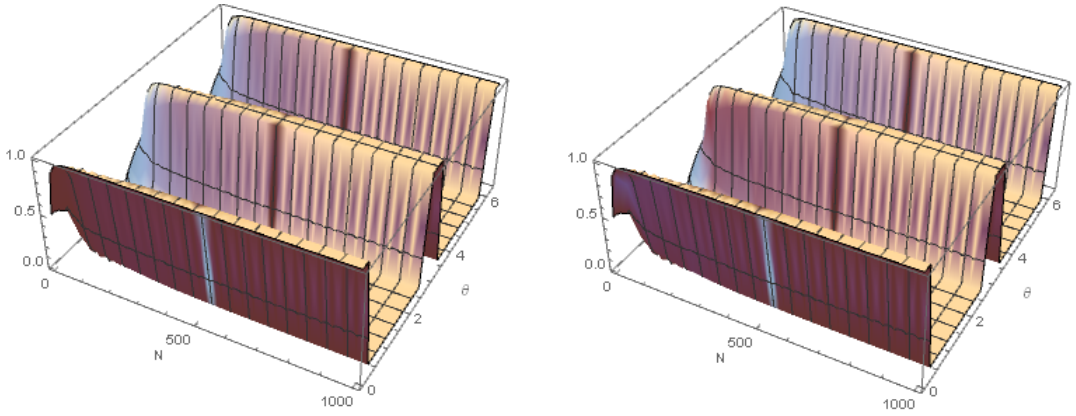

FIGURE 3.10: **Probability of measuring magnetization 0 as a function of a parametrization of time $\theta = \frac{\omega t}{N}$ and N.** On the left, $c_0 = \frac{1}{\sqrt{2}}$; on the right, $c_0 = \frac{1}{\sqrt{3}}$. In both, N starts from 2.

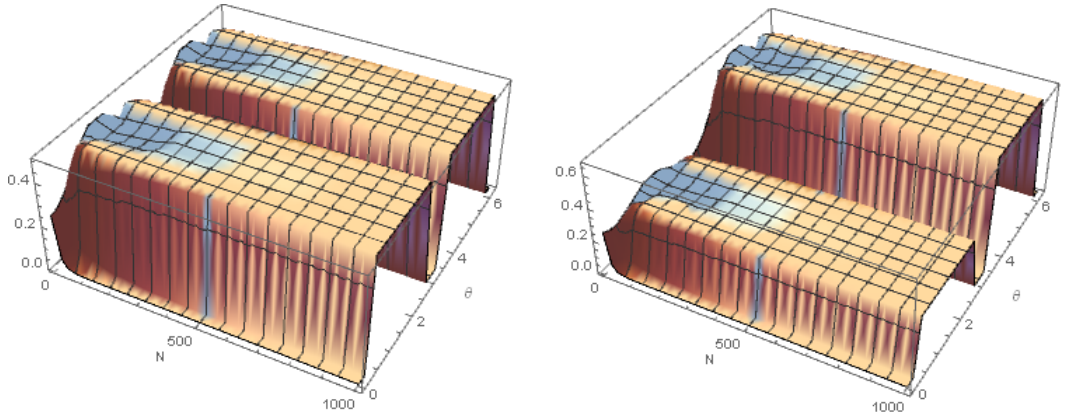

FIGURE 3.11: **Probability of measuring magnetization 1 as a function of a parametrization of time $\theta = \frac{\omega t}{N}$ and N.** On the left, $c_0 = \frac{1}{\sqrt{2}}$; on the right, $c_0 = \frac{1}{\sqrt{3}}$. In both, N starts from 2.

Recapitulating, we are measuring magnetization of the apparatus' effective state with respect to the z-axis, with each of its N constituents rotating over the x-axis from the initial state $|\Psi\rangle = \frac{1}{\sqrt{2}}|0\rangle + \frac{i}{\sqrt{2}}|1\rangle$, and the θ angle growing positively in the counterclockwise direction. That is, considering the Bloch sphere for each constituent, it is initially aligned with the equator. This is the reason for the apparatus to measure 0. In fact, the probability of measuring 0 is maximum when the constituents are close to the equator's plane in the Bloch sphere – θ a multiple integer of π (figure 3.10. As the interaction occurs, the apparatus remains in a superposition of rotating in two directions. The best moments to acquire information about the system being close to the poles, aligned with the z-axis (figures 3.11 and 3.12).

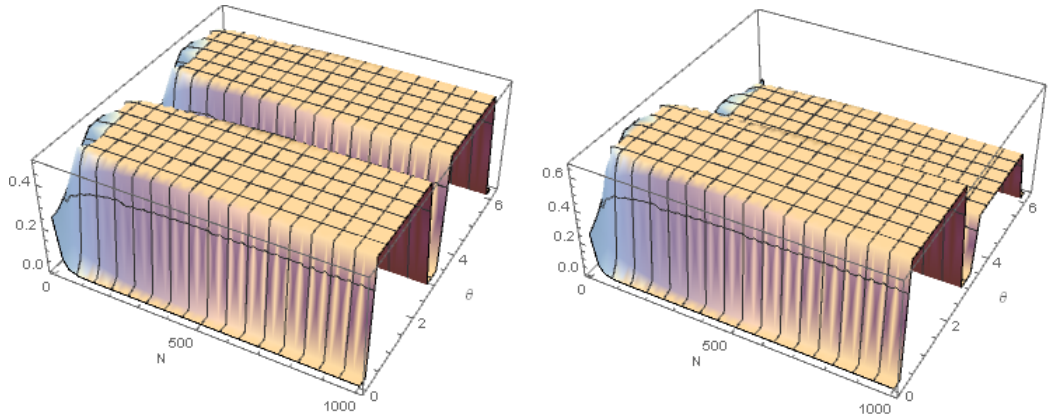

FIGURE 3.12: **Probability of measuring magnetization -1 as a function of a parametrization of time $\theta = \frac{\omega t}{N}$ and N.** On the left, $c_0 = \frac{1}{\sqrt{2}}$; on the right, $c_0 = \frac{1}{\sqrt{3}}$. In both, N starts from 2.

In the case of large values of N, interesting processes occur. First, the plateaus that are seen in the graphs increase, meaning that for more and more time we have a well defined resulting outcome. I.e., the temporal region in which we can best acquire information about the system increase. Second, for large values of N ($N >> 1$), the time required to go through a period will be infinite, since $\theta = \frac{\omega t}{N}$. In practise, in the limit $N \to \infty$ there will be no more oscillation. Thus, having waited for the time necessary to reach the plateau, the observer can look at the display in any time, being able to gain information about the system's initial state via c_0 and c_1. Again, our model approaches the daily-life situation.

Having analyzed the probabilities of each outcome $-1, 1$ and 0, and in order to study the behavior of quantum coherences, we need to define the coarse-graining map action in the rest of the computational basis elements. Using the same arguments as before, we define $\Lambda_{CG}(\Pi_\sigma|0_1 0_2..0_l 1_1 1_2..1_{N-l}\rangle\langle 0_1 0_2..0_{l'} 1_1 1_2..1_{N-l'}|\Pi^\dagger_{\sigma'})$ equal to:

$$
\begin{aligned}
&n_1(N)\,|-1\rangle\langle 1|, \text{ if } l \leq \frac{N}{3} \text{ and } l' \geq \frac{2N}{3};\\
&n_2(N)\,|-1\rangle\langle 0|, \text{ if } l \leq \frac{N}{3} \text{ and } \frac{N}{3} < l' < \frac{2N}{3};\\
&n_3(N)\,|1\rangle\langle 0|, \text{ if } l \geq \frac{2N}{3} \text{ and } \frac{N}{3} < l' < \frac{2N}{3};\\
&0 \text{ if } l \geq \frac{2N}{3} \text{ and } l' \geq \frac{2N}{3},\ l \neq l';\\
&0 \text{ if } l \leq \frac{N}{3} \text{ and } l' \leq \frac{N}{3},\ l \neq l'.
\end{aligned}
\tag{3.47}
$$

Above,

$$
\begin{aligned}
n_1(N) &= \left\{ \sum_{k=0}^{\frac{N}{3}} \sum_{n=\frac{2N}{3}-k}^{N-k} \sum_{m=\frac{2N}{3}-n}^{N-n-k} \frac{N!}{k!n!m!(N-n-k-m)!} \right\}^{\frac{-1}{2}}; \\
n_2(N) &= \left\{ \sum_{k>\frac{N}{3}}^{<\frac{2N}{3}} \sum_{n=\frac{2N}{3}-k}^{N-k} \sum_{m>\frac{N}{3}-k}^{<\frac{2N}{3}-k} \frac{N!}{k!n!m!(N-n-k-m)!} \right\}^{\frac{-1}{2}}; \\
n_3(N) &= \left\{ \sum_{k>\frac{N}{3}}^{<\frac{2N}{3}} \sum_{n>\frac{N}{3}-k}^{<\frac{2N}{3}-k} \sum_{m=0}^{\frac{N}{3}-n} \frac{N!}{k!n!m!(N-n-k-m)!} \right\}^{\frac{-1}{2}}.
\end{aligned}
\tag{3.48}
$$

It will be clear in a while where the normalization factors $n_1(N)$, $n_2(N)$ and $n_3(N)$ came from. Now we are able to write the full effective state $\rho_t^N = \Lambda_{\mathrm{CG}}(\Psi_t^N) \in \mathcal{L}(\mathcal{H}_3)$ for the apparatus after the coarse-graining channel in equations 3.35 and 3.47. Namely,

$$
\rho_t^N = |c_0|^2 \, \Lambda_{\mathrm{CG}}(R_{\theta,x} \, |\Psi^N\rangle\langle\Psi^N| R_{\theta,x}^\dagger) + |c_1|^2 \, \Lambda_{\mathrm{CG}}(R_{-\theta,x} \, |\Psi^N\rangle\langle\Psi^N| R_{-\theta,x}^\dagger). \tag{3.49}
$$

Writing the evolved total state $R_{\theta,x} \, |\Psi^N\rangle\langle\Psi^N| R_{\theta,x}^\dagger$ as (similar to equation 3.40):

$$
\begin{bmatrix} x & x_c^* \\ x_c & 1-x \end{bmatrix}_1 \otimes \begin{bmatrix} x & x_c^* \\ x_c & 1-x \end{bmatrix}_2 \otimes .. \otimes \begin{bmatrix} x & x_c^* \\ x_c & 1-x \end{bmatrix}_N, \tag{3.50}
$$

with subscript c meaning coherence,

$$
x \equiv \{ \frac{1}{2} + (-\frac{1}{2} + p) \cos\theta + \sqrt{p(1-p)} \sin\theta \sin\phi \} \tag{3.51}
$$

and

$$
x_c \equiv \frac{1}{2} \{ i(1-2p) \sin\theta + 2\sqrt{p-p^2} (\cos\phi + i \cos\theta \sin\phi) \}. \tag{3.52}
$$

We need to find the general $2^N \times 2^N$ matrix resulting from 3.50, apply the coarse-graining map in its elements and insert the result in 3.49, not forgetting the contribution coming from $|c_1|^2 \, \Lambda_{\mathrm{CG}}(R_{-\theta,x} \, |\Psi^N\rangle\langle\Psi^N| R_{-\theta,x}^\dagger)$. But how is it possible to get the coarse-graining effective state of the general $2^N \times 2^N$ matrix? Counting! For instance, consider the generic element

$$
\Pi_\sigma |0_1 0_2 .. 0_l 1_1 .. 1_{N-l}\rangle\langle 0_1 0_2 .. 0_l 1_1 .. 1_{N-l}| \Pi_{\sigma'}^\dagger. \tag{3.53}
$$

The permutation operators are placed as a way to represent not only this element, but all that result from permutations of 0's and 1's in the ket (Π_σ) and in the bra ($\Pi_{\sigma'}^\dagger$).

However, the permutations are related, because each element as above comes from the composition of N elements of dimension 2. For example, the element $|011\rangle\langle 110| = |0\rangle\langle 1| \otimes |1\rangle\langle 1| \otimes |1\rangle\langle 0|$ (in case $N = 3$) is associated with the combination $x_c^*(1-x)x_c$ in the tensor product 3.50. It is the permutations of the latter combination, which means to exchange the order of $|0\rangle\langle 1|$, $|1\rangle\langle 1|$ and $|1\rangle\langle 0|$ in the example above, that we should count. This is the origin of the factors $\frac{N!}{k!n!m!(N-n-k-m)!}$, $n_1(N)$, $n_2(N)$ and $n_3(N)$. With this counting in mind and equations 3.35 and 3.47 it is possible to construct the effective state ρ_t^N.

Finished this procedure, the total evolved effective state for the apparatus ρ_t^N is given by:

$$
\begin{aligned}
\rho_t^N &= |c_0|^2\,\Lambda_{\mathrm{CG}}(R_{\theta,x}\,|\Psi^N\rangle\langle\Psi^N|R_{\theta,x}^\dagger) + |c_1|^2\,\Lambda_{\mathrm{CG}}(R_{-\theta,x}\,|\Psi^N\rangle\langle\Psi^N|R_{-\theta,x}^\dagger)\\
&= |1\rangle\langle 1|\Big(|c_0|^2\sum_{k=\frac{2N}{3}}^{N}\binom{N}{k}x^k(1-x)^{N-k} + |c_1|^2\sum_{k=\frac{2N}{3}}^{N}\binom{N}{k}y^k(1-y)^{N-k}\Big)\\
&+ |0\rangle\langle 0|\Big(|c_0|^2\sum_{k>\frac{N}{3}}^{<\frac{2N}{3}}\binom{N}{k}x^k(1-x)^{N-k} + (1-|c_0|^2)\sum_{k>\frac{N}{3}}^{<\frac{2N}{3}}\binom{N}{k}y^k(1-y)^{N-k}\Big)\\
&+ |-1\rangle\langle -1|\Big(|c_0|^2\sum_{k=0}^{\frac{N}{3}}\binom{N}{k}x^k(1-x)^{N-k} + (1-|c_0|^2)\sum_{k=0}^{\frac{N}{3}}\binom{N}{k}y^k(1-y)^{N-k}\Big)\\
&+ |1\rangle\langle 0|\,n_3(N)\,\Big(|c_0|^2\sum_{k>\frac{N}{3}}^{<\frac{2N}{3}}x^k\sum_{n>\frac{N}{3}-k}^{<\frac{2N}{3}-k}x_c^n\sum_{m=0}^{\frac{N}{3}-n}(1-x)^m(x_c^*)^{N-k-n-m}\frac{N!}{k!n!m!(N-n-k-m)!}\\
&+ |c_1|^2\sum_{k>\frac{N}{3}}^{<\frac{2N}{3}}y^k\sum_{n>\frac{N}{3}-k}^{<\frac{2N}{3}-k}y_c^n\sum_{m=0}^{\frac{N}{3}-n}(1-y)^m(y_c^*)^{N-k-n-m}\frac{N!}{k!n!m!(N-n-k-m)!}\Big)\\
&+ |1\rangle\langle -1|\,n_1(N)\,\Big(|c_0|^2\sum_{k=0}^{\frac{N}{3}}x^k\sum_{n=\frac{2N}{3}-k}^{N-k}x_c^n\sum_{m=\frac{2N}{3}-n}^{N-n-k}(1-x)^m(x_c^*)^{N-k-n-m}\frac{N!}{k!n!m!(N-n-k-m)!}\\
&+ |c_1|^2\sum_{k=0}^{\frac{N}{3}}y^k\sum_{n=\frac{2N}{3}-k}^{N-k}y_c^n\sum_{m=\frac{2N}{3}-n}^{N-n-k}(1-y)^m(y_c^*)^{N-k-n-m}\frac{N!}{k!n!m!(N-n-k-m)!}\Big)\\
&+ |-1\rangle\langle 0|\,n_2(N)\,\Big(|c_0|^2\sum_{k>\frac{N}{3}}^{<\frac{2N}{3}}x_c^k\sum_{n=\frac{2N}{3}-k}^{N-k}(1-x)^n\sum_{m>\frac{N}{3}-k}^{<\frac{2N}{3}-k}x^m(x_c^*)^{N-k-n-m}\frac{N!}{k!n!m!(N-n-k-m)!}\\
&+ |c_1|^2\sum_{k>\frac{N}{3}}^{<\frac{2N}{3}}y_c^k\sum_{n=\frac{2N}{3}-k}^{N-k}(1-y)^n\sum_{m>\frac{N}{3}-k}^{<\frac{2N}{3}-k}y^m(y_c^*)^{N-k-n-m}\frac{N!}{k!n!m!(N-n-k-m)!}\Big)\\
&+ |0\rangle\langle -1|\,n_2(N)\,\Big(|c_0|^2\sum_{k>\frac{N}{3}}^{<\frac{2N}{3}}(x_c^*)^k\sum_{n=\frac{2N}{3}-k}^{N-k}(1-x)^n\sum_{m>\frac{N}{3}-k}^{<\frac{2N}{3}-k}x^m x_c^{N-k-n-m}\frac{N!}{k!n!m!(N-n-k-m)!}\\
&+ |c_1|^2\sum_{k>\frac{N}{3}}^{<\frac{2N}{3}}(y_c^*)^k\sum_{n=\frac{2N}{3}-k}^{N-k}(1-y)^n\sum_{m>\frac{N}{3}-k}^{<\frac{2N}{3}-k}y^m y_c^{N-k-n-m}\frac{N!}{k!n!m!(N-n-k-m)!}\Big)\\
&+ |-1\rangle\langle 1|\,n_1(N)\,\Big(|c_0|^2\sum_{k=0}^{\frac{N}{3}}x^k\sum_{n=\frac{2N}{3}-k}^{N-k}(x_c^*)^n\sum_{m=\frac{2N}{3}-n}^{N-n-k}(1-x)^m x_c^{N-k-n-m}\frac{N!}{k!n!m!(N-n-k-m)!}\\
&+ |c_1|^2\sum_{k=0}^{\frac{N}{3}}y^k\sum_{n=\frac{2N}{3}-k}^{N-k}(y_c^*)^n\sum_{m=\frac{2N}{3}-n}^{N-n-k}(1-y)^m y_c^{N-k-n-m}\frac{N!}{k!n!m!(N-n-k-m)!}\Big)\\
&+ |0\rangle\langle 1|\,n_3(N)\,\Big(|c_0|^2\sum_{k>\frac{N}{3}}^{<\frac{2N}{3}}x^k\sum_{n>\frac{N}{3}-k}^{<\frac{2N}{3}-k}(x_c^*)^n\sum_{m=0}^{\frac{N}{3}-n}(1-x)^m x_c^{N-k-n-m}\frac{N!}{k!n!m!(N-n-k-m)!}\\
&+ |c_1|^2\sum_{k>\frac{N}{3}}^{<\frac{2N}{3}}y^k\sum_{n>\frac{N}{3}-k}^{<\frac{2N}{3}-k}(y_c^*)^n\sum_{m=0}^{\frac{N}{3}-n}(1-y)^m y_c^{N-k-n-m}\frac{N!}{k!n!m!(N-n-k-m)!}\Big).
\end{aligned}
\tag{3.54}
$$

In the expression 3.54 for the total effective state of the apparatus, it is important to remember that we get y from x and y_c from x_c doing $\theta \to -\theta$ in expressions 3.51 and 3.52. Notice that all the coefficients x, y, x_c and y_c have implicit temporal dependence. Looking at the populations of states $|1\rangle\langle 1|$, $|0\rangle\langle 0|$ and $|-1\rangle\langle -1|$, which in turn are associated with apparatus' outcomes $1, 0$ and -1, respectively, we have the probabilities of system's magnetization $1, 0$ and -1 as a function of time, obtained in expressions 3.41, 3.42 and 3.43.

With the help of all the figures from 3.7 up to 3.12, we have already studied the behaviour of the probabilities and how to recover the superposition coefficients c_0 and c_1 of the target system. Now it is time to look at the behaviour of the coherences in the effective reduced state of the apparatus ρ_t^N.

Each coherence term involves, in its numerator and denominator, equal sums containing the factor $\frac{N!}{k!n!m!(N-n-k-m)!}$, all sums growing with N. However, in numerator are present quantities in absolute values smaller than 1 – they are x, x_c, y, $(1-x)$, $(1-y)$ and y_c – to powers which, summed up, are of the order of N. This ensures that for large values of N, i. e. in the limit of a huge measuring apparatus, for instance consisting of moles of atoms, the coherences vanishes exponentially – see graphs in figure 3.13. Not only by the size of the apparatus, but mainly by our inability to access it in all its degrees of freedom, our coarser description.

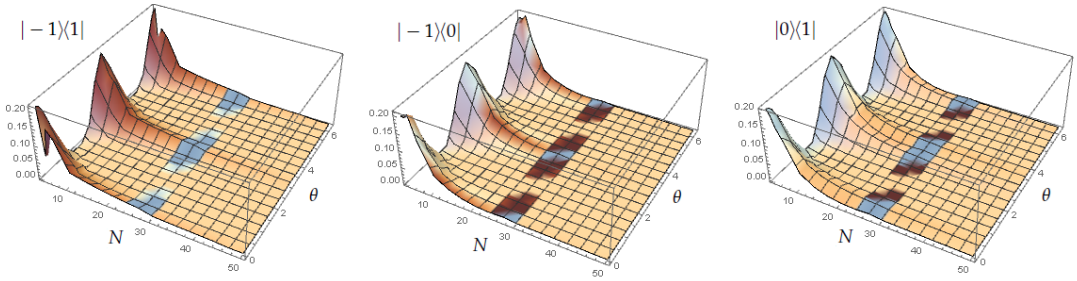

FIGURE 3.13: **Death of coherences for the total evolved effective state of the apparatus.** The θ angle in radians, $p = 0.5$, $\phi = \frac{\pi}{2}$ and $c_0 = \frac{1}{\sqrt{2}}$.

I close this chapter after these interesting results first making it clear that we managed to see death of quantum coherences without evoking any interaction with the environment and the formalism of decoherence. This makes us very motivated: the work continues! In order to give continuity to the proposal in section 3.2, our next immediate step is to formalize the coarse-graining map in equations 3.35 and 3.47.

Chapter 4

Conclusions and Perspectives

Emphasizing the main aspects of the work developed, in this last chapter we summarize the leading results of the thesis and its possibilities of application. We also list perspectives for the continuity of our work and make final comments about the most important message we want to convey.

4.1 Emerging dynamics

In chapter 2 we developed a general framework to investigate what kinds of dynamics emerge when one does not have full access to the degrees of freedom of a given system, for example in the case of a practical limitation or even a choice. Generally, we believe that our formalism is useful in the study of quantum many-body systems, where a complete description of such a systems and their dynamics becomes highly unpractical as the number of constituents increase, since the systems degrees of freedom grows exponentially with that number. That's why effective descriptions are so important, and essential in the study of macroscopic (with a huge number of micro-constituents) systems.

Notice that in developing the formalism in chapter 2 we did not distinguish between closed or open quantum systems, so that it can be applied in both cases. Regarding the theory of open quantum systems [108], in this case the usual split is made between system and environment degrees of freedom, while in our formalism the split that takes place is between accessible and non-accessible degrees of freedom. Notice that this is also the case of decoherence. Here, however, precisely in chapter 3, we take into account practical aspects of the measuring process, not only locality but also imprecision.

Remember that our general effective evolution channel Γ_t is not in Kraus form. The reason is due to the fact that we have the possibility of correlations between the accessible and non-accessible degrees of freedom, represented by the term $\zeta(\alpha)$ in equation (2.14). This possibility of correlations allowed for the distance between two effective states to increase under the action of the same effective channel, differently from what occurs in the underlying level (section 2.2.2).

Other interesting aspect to point out is the fact that the Kraus operators in the effective evolution (first term in equation (2.14)) may depend on the input state. Then, if we look at the system only in time intervals in which the correlation term $\zeta(\alpha)$ might vanish (in other words, for a coarse grained time [109]), the non-linearity of the Kraus-term might become apparent. This possibility, together with the possibility of an increase of the distinguishability between states may contribute to explain how non-linear dynamics may emerge and how chaotic systems may arise from the underlying quantum linear description.

One important tool we are learning about and that we believe will be very important in the application of the formalism of chapter 2 in quantum thermodynamics, more specifically in an attempt to explain the thermalization of closed quantum systems [110, 111], and also in the study of a quantum measurement process is the framework of [101] *quantum master equations*. Let's give a sense of what it is about and our perspectives on this path.

4.1.1 Quantum master equations

In section 2.1 we have discussed key properties of quantum channels, the most general transformations that can be applied over quantum states. For instance an unitary transformation evolving a quantum system from time t_1 to time t_2. Generally, if we want to describe the time evolution of open quantum systems, we need a one-parameter family of quantum channels $\{\Lambda_t, t \geq 0\}$. A large class of interesting physical phenomena may be described by evolution which satisfies the expression $\Lambda_{t+s} = \Lambda_t \Lambda_s$, usually called the *semi-group condition* or *Markov property* [108].

The latter named in honour of the Russian mathematician Andrey Markov (1856-1922). In probability theory and statistics, a stochastic process has the Markov property if the conditional probability distribution of future states of the process depends only upon the present state, not on the sequence of events that preceded it. A dynamical map is called Markovian if it does not carry any memory effects, the evolution does not depends on the systems history.

Mathematically speaking, a dynamical map Λ is Markovian if it is completely positive, trace-preserving, and satisfies the semi-group property $\Lambda_{t+s,0} = \Lambda_{t,0}\Lambda_{s,0}$. Then, $\Lambda(t) = e^{\mathcal{L}t}$ and it leads to a Markovian equation in Lindblad form [112, 113], namely

$$\frac{d\rho_t}{dt} = \mathcal{L}\rho_t, \tag{4.1}$$

where $\rho_t = \Lambda_t(\rho)$, $\rho \in \{\text{domain of } \mathcal{L}\}$, and the linear map $\mathcal{L}$ the semi-group generator, usually called Lindbladian. Notice that $\mathcal{L}$ is an operator acting on a vector space of linear operators. Therefore, a super-operator. Equation (4.1) is also called *quantum master equation*, Lindblad equation, or quantum Markovian master equation.

In reference [114], the authors propose a less restrictive definition, where a map is defined as Markovian when it is a trace preserving and divisible CP map. In that case, $\Lambda_{t_1+t_2,0} = \Lambda_{t_1+t_2,t_1}\Lambda_{t_1,0}$, where $\Lambda_{t_1+t_2,0}$ is completely positive for any $t_1, t_2 > 0$. The generators $\mathcal{L}$ then can also be time dependent. This will be the case if we had the situation depicted in figure 2.8. When dealing with such a situation, we have to be sure that for all time steps t_i, the underlying corresponding states ψ_i generates the same effective quantum channel.

Regarding an arbitrary channel Λ, it is possible to find a general form for $\mathcal{L}$, the step by step procedure is found in references [115, 108, 116]. A quantum system will undergo a Markovian dynamics provided that its evolution satisfies a master equation of the Lindblad form:

$$\mathcal{L}\rho = -i[H,\rho] + \sum_{k=0}^{d^2-1} \gamma_k (V_k \rho V_k^\dagger - \frac{1}{2}\{V_k^\dagger V_k, \rho\}). \tag{4.2}$$

The Hermitian operator H is the effective Hamiltonian of the system, $\gamma_k \geq 0, \forall k$, and the operators V_k are usually called Lindblad operators. The γ_k's play the role of relaxation rates for the different decay modes of the open quantum system, and the

second term of equation (4.2) accounts for dissipative and dephasing effects. If the dissipative term is equal to zero, we end up with a quantum analogue of the classical Liouville equation, where the first term represents the unitary dynamics generated by the effective Hamiltonian H. In the case of time-dependent generators, $\mathcal{L}(t)$ can be written in the standard form (4.2) with $H(t)$, $\gamma_k(t) \geq 0$ and $V_k(t)$ potentially time dependent [114]. If one have a Markovian dynamics, $\gamma_k \geq 0$; if non-Markovian, γ_k's are negative [112].

We have the prospect of deriving a quantum master equation for the effective, emerging, dynamics (upper level of diagrams in figures 2.1 and 2.3). Notice that Λ, as a quantum channel, has the Kraus form 1. However, our general dynamics (2.14) cannot be written in such a way. The second term, which is not in Kraus form, makes calculations more complicated.

Finding such a master equation will allow us to study in more detail and depth the Markovianity properties of the emerging dynamics. We can also study the states ρ_t that make the left hand side of equation (4.1) equal to zero, the *stationary states*. Besides that, the fact that our effective dynamics Γ_t can increase the distance (or distinguishability) between states (section 2.2.2) makes us wonder if we are dealing with the emergence of non-linear effects from linear. This implication can also be investigated.

4.1.2 Thermalization

A possible application of the emerging dynamics approach is to understand how the well known properties of the microscopic world can be modelled by a statistical theory in which quantum thermodynamic laws emerge. This is one of the focus of quantum thermodynamics, a research field that has grown considerably in the last decades, supported by great advances in technology and experimental physics [117, 118]. Quantum thermodynamics tries to extend standard thermodynamics in order to include quantum effects and ensembles with ever smaller sizes. The understanding of how quantum fluctuations compete with thermal fluctuations is essential to adapt technologies to be valid in decreasing scales, and to develop new ones [117].

One of the perspectives that has emerged in quantum thermodynamics is the study of thermalization. In the quantum information theory approach of thermalization, arguments of entanglement play an important role [119, 117]. But what does it mean to thermalize? One can use the term thermalization to refer to equilibration towards a state that is close to being indistinguishable from a thermal state proportional to $e^{-\beta H}$, for some inverse temperature $\beta > 0$ [110].

When thermalization occurs for a given system, it is expected that for almost all initial states of the system it will end up in a thermal state, and the expectation values of many macroscopic observables will saturate to values predicted from thermal states. In generic isolated systems, non-equilibrium dynamics is expected to result in thermalization: a relaxation to states in which the values of macroscopic quantities are stationary, universal with respect to widely differing initial conditions, and predictable using statistical mechanics.

With our formalism and a quantum master equation in hands, we have the prospect of going in the discussion of thermalization of closed quantum many-body systems focusing on the dynamical approach of it [120].

4.2 Modeling a measurement process

At the end of the work described in this thesis, we managed to model a quantum measurement process in two similar but different ways which we judge interesting and that have brought us beautiful results. In general, we model a process in which the system is a two level system (a qubit) and the measuring device composed by a spin coherent state (section 3.3) and N qubits (section 3.4). One of the goals achieved was to recover the coefficients c_0 and c_1 and gain information about the system. For such, the system+apparatus dynamics corresponded to a rotation in the apparatus conditioned to the system's state $|0\rangle$ and $|1\rangle$.

Using the first coarse-graining channel, motivated by reference [102], we were able to model a digital measurement scenario with two outcomes. We visualize the death of quantum correlations between system and the apparatus' effective state and the creation of classical correlations when the strength of the coarse graining channel is increased. We also find an analytical expression for the concurrence as a function of θ (or time) and j. Though, the channel Λ_{CG} still lacked a stronger physical motivation.

Using the channel in model 2, which we still need further to formalize, allowed us to model a digital measurement scenario with three outcomes, representing magnetization positive, negative and zero. More interesting is the fact that the outcome zero in the limit of a large apparatus only appears when we turn on the measuring device. This is a situation closer to everyday life in the lab. We also visualize the death of coherences in the apparatus' reduced effective state the coarser the description. A situation akin to decoherence, although it was not necessary to evoke any interaction with the surrounding environment. In particular, in section 3.4, for large N the effective state 3.54 can be seen as a statistical mixture of possibilities.

At this point, what I consider the most difficult part is the modelling of the coarse graining map. It is imperative the map to have a clear physical motivation, it must be a quantum channel and with general input-output dimensions.

Also because of this fact, in the short term, as an immediate continuation of our work, we will continue to analyze different coarse-graining descriptions. Although we have achieved beautiful results in sections 3.3 and 3.4 confirming our intuition of the death of quantum correlations due to the lack of access to all system's degrees of freedom, we still believe we can go further. To do so, we believe it is necessary to find a coarse-graining channel with a very clear and strong physical description. So that we can find the corresponding effective dynamics and analyze different levels of coarse graining, as was our initial proposal.

As a final comment, I would like to highlight again some papers in the field that caught our attention [66, 101, 121]. In [66], the authors present a new theoretical approach to macroscopic realism and emergence of classical physics within quantum theory. They focus on the limits of observability of quantum effects of macroscopic objects, which is closely related to our idea of coarse-graining (chapter 2). The authors demonstrate that for unrestricted measurement accuracy, no classical description is possible for arbitrarily large systems. However, for a certain time evolution they show that under coarse-grained measurements macrorealism emerges out of the Schrödinger equation and the projection postulate.

In [101], the authors reaffirms his point of view: "The classical world arises from within quantum theory when neighboring outcomes are not distinguished but bunched together into slots in the measurements of limited precision" [101]. Note that according to the authors the classical world seems to arise via a coarse-graining

procedure, which is the key idea of this thesis. In particular, a very similar procedure was made in section 3.4. I believe that we can contribute more to this discussion when developing future works.

Appendix A

Emerging dynamics arising from coarse-grained quantum systems

Emerging dynamics arising from coarse-grained quantum systems

Cristhiano Duarte,[1,*] Gabriel Dias Carvalho,[2,†] Nadja K. Bernardes,[3,4,‡] and Fernando de Melo[2,§]
[1]*Departamento de Matemática, Instituto de Ciências Exatas, Universidade Federal de Minas Gerais, Caixa Postal 702, CEP 30123-970, Belo Horizonte, Minas Gerais, Brazil*
[2]*Centro Brasileiro de Pesquisas Físicas, Rio de Janeiro, Rio de Janeiro, CEP 22290-180, Brazil*
[3]*Departamento de Física, Instituto de Ciências Exatas, Universidade Federal de Minas Gerais, Caixa Postal 702, CEP 30123-970, Belo Horizonte, Minas Gerais, Brazil*
[4]*Departamento de Física, Universidade Federal de Pernambuco, 50670-901 Recife, Pernambuco, Brazil*
(Received 11 May 2017; published 18 September 2017)

The purpose of physics is to describe nature from elementary particles all the way up to cosmological objects like cluster of galaxies and black holes. Although a unified description for all this spectrum of events is desirable, this would be highly impractical. To not get lost in unnecessary details, effective descriptions are mandatory. Here we analyze the dynamics that may emerge from a full quantum description when one does not have access to all the degrees of freedom of a system. More concretely, we describe the properties of the dynamics that arise from quantum mechanics if one has access only to a coarse-grained description of the system. We obtain that the effective maps are not necessarily of Kraus form, due to correlations between accessible and nonaccessible degrees of freedom, and that the distance between two effective states may increase under the action of the effective map. We expect our framework to be useful for addressing questions such as the thermalization of closed quantum systems, as well as the description of measurements in quantum mechanics.

DOI: 10.1103/PhysRevA.96.032113

I. INTRODUCTION

It is widely accepted that quantum mechanics provides currently the best description we have of the physical world. However, the description of systems in our daily lives does not require the whole framework arising from quantum mechanics. In fact, our everyday life experiences heavily rely on effective (macroscopic) descriptions which are far less complex than their underlying intricate quantum characterization. For example, to describe the behavior of a macroscopic object, like the thermal expansions or compressions of a rail line, we do not need to specify the quantum states of all atoms composing such an object. In this situation, we resort to the theory of thermodynamics [1], which is probably the clearest example of effective theories. Although the systems treated within this theory are composed of many quantum interacting particles, macroscopic variables—such as temperature, volume, and pressure—describe the systems well enough, allowing, for instance, for the design of thermal machines.

The idea of different scales is central in physics. But how does the description in one scale emerge from the description in a deeper scale? Different ways of *coarse graining* the description of a system are often employed [2–6] in order to "zoom out" from one level and obtain an effective description. Coarse grainings frequently appear in statistical physics [6] and are arguably the central tool in the renormalization method developed by Kadanoff and Wilson [7,8]. Nevertheless, some of these early methods are sometimes based on not-so-well-controlled approximations or on projections, leading thus to ill-defined and/or probabilistic effective dynamics when applied to quantum systems.

In recent decades, with the birth of the quantum information field, various tools were developed to deal with many-body quantum systems [9]. In particular, the theory of completely positive linear maps [10–12], which aims at describing the most general transformations that can be applied to a system (including the most general time evolution), became well established. This has been accompanied and supported by the formalization and development of a theory for quantum correlations [13] and by efficient descriptions of many-body quantum states [14,15]. The goal of the present contribution is to employ some of these tools in order to obtain effective descriptions of quantum systems and their dynamics. More concretely (see Fig. 1), given a system in the state represented by a density operator ψ_0 evolving by the unitary map $\mathfrak{U}_t$, what is the dynamics Γ_t induced by a coarse graining Λ_{CG}? What types of dynamics might emerge when we departure from a full quantum description of the systems?

In what follows, we present a framework to address these questions. Its construction is closely related to that of open quantum systems [16–19]. In fact, concepts like the correlation between system and environment, and map divisibility will play an important role here as well. Nevertheless, our framework encompasses and generalizes this previous formalism, as ours can be used in many other situations. It can, for instance, be used to describe closed systems from which just partial information is available, which might play a significant role in the thermalization of closed quantum systems [20,21]. Our work is also related to recent articles by Kofler and Brukner [22,23]. In these articles, the authors analyze the effect of coarse-grained measurements in order to explain the emergence of the classical word. Their approach, however, is not dynamical, and that is exactly the gap we want to fill out.

Our article is organized as follows: In Sec. II, we introduce two different characterizations of completely positive and trace preserving (CPTP) linear maps, which will allow us to describe

*cristhiano@mat.ufmg.br
†gabrieldc@cbpf.br
‡nadjakb@df.ufpe.br
§fmelo@cbpf.br

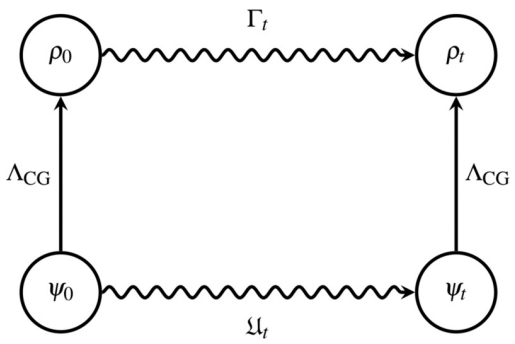

FIG. 1. Coarse-graining-induced dynamics. Schematic diagram representing the different levels of description connected by a coarse graining. Given an initial state of the system, with density operator ψ_0, its evolution, $\mathfrak{U}_t$, and a coarse-graining map Λ_{CG}, we want to determine the induced dynamics Γ_t and its properties, such that $\Gamma_t \circ \Lambda_{CG}(\psi_0) = \Lambda_{CG} \circ \mathfrak{U}_t(\psi_0)$.

generalized quantum dynamics and the coarse-graining maps. In this contribution, a coarse-graining map will simply be a CPTP linear map that reduces the dimension of the system. Such maps were recently used to obtain a sufficient criteria for the entanglement of high-dimensional bipartite states [24]. After that, in Sec. III, we obtain the effective dynamics Γ_t induced by the coarse-graining Λ_{CG}, underlying evolution $\mathfrak{U}_t$, and initial state ψ_0. The properties of the effective map Γ_t are discussed in Sec. IV. In Sec. V, we show that the distance between two effective states may increase under the action of the same effective map Γ_t. This is in contrast with the usual contractive property of CPTP linear maps [9]. Finally, in Sec. VI, we draw some final conclusions and hint at some possible applications of the developed formalism.

II. CPTP LINEAR MAPS: GENERAL DYNAMICS AND COARSE GRAINING

In order to define the coarse-graining operations, which are the ones we are interested here, we will first briefly review some properties of CPTP linear maps. Comprehensive expositions can be found, for example, in Refs. [9–12].

Let $\mathscr{H}_D \simeq \mathbb{C}^D$ be the Hilbert space assigned to a D-dimensional quantum system. We define $\mathscr{L}(\mathscr{H}_D)$ as the set of all linear operators acting on $\mathscr{H}_D$, and $\mathscr{D}(\mathscr{H}_D) = \{\psi \in \mathscr{L}(\mathscr{H}_D) | \ \psi \geqslant 0, \mathrm{Tr}(\psi) = 1\}$ as the convex set containing all the possible states of the system. Let $\Lambda : \mathscr{L}(\mathscr{H}_D) \to \mathscr{L}(\mathscr{H}_d)$ be a linear map which abides by two constraints: (i) it is trace preserving, meaning that $\forall \psi \in \mathscr{L}(\mathscr{H}_D)$ we have $\mathrm{Tr}(\psi) = \mathrm{Tr}(\Lambda(\psi))$; and (ii) it is completely positive, i.e., for all positive operators $\psi \in \mathscr{L}(\mathscr{H}_D \otimes \mathscr{H}_Z)$, with $\mathscr{H}_Z$ an arbitrary finite-dimensional Hilbert space, the linear map $\Lambda \otimes \mathbb{1} : \mathscr{L}(\mathscr{H}_D \otimes \mathscr{H}_Z) \to \mathscr{L}(\mathscr{H}_d \otimes \mathscr{H}_Z)$ is such that $\Lambda \otimes \mathbb{1}(\psi) \geqslant 0$ [12]. The first imposition guarantees that probabilities are conserved through the map action, while the completely positivity condition ensures that states are mapped into states even if the map acts only on a subsystem of the whole system. The following well-known theorem gives a very useful characterization of CPTP linear maps.

Theorem 1 ([9,12]). A linear map $\Lambda : \mathscr{L}(\mathscr{H}_D) \to \mathscr{L}(\mathscr{H}_d)$ is completely positive and trace preserving if and only if there exists a finite set of linear operators $\{K_i\}_{i=1}^N$, with each $K_i : \mathscr{H}_D \to \mathscr{H}_d$ known as a Kraus operator, such that $\forall \psi \in \mathscr{L}(\mathscr{H}_D)$:

$$\Lambda(\psi) = \sum_{i=1}^{N} K_i \psi K_i^\dagger \text{ with } \sum_{i=1}^{N} K_i^\dagger K_i = \mathbb{1}_D.$$

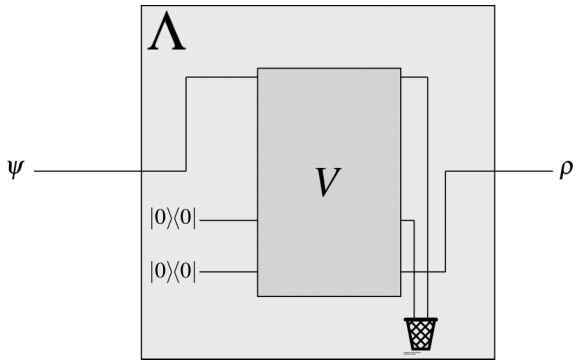

FIG. 2. Operational interpretation of a CPTP linear map Λ.

It is worth noticing that CPTP linear maps generalize the evolution of a quantum system, with the unitary evolution being a particular linear map $\mathfrak{U}_t : \mathscr{L}(\mathscr{H}_D) \to \mathscr{L}(\mathscr{H}_D)$ with a single Kraus operator, namely the unitary U_t itself. In general, the number of Kraus operators is unlimited, but it is always possible to characterize a CPTP linear map $\Lambda : \mathscr{L}(\mathscr{H}_D) \to \mathscr{L}(\mathscr{H}_d)$ with a set of Kraus operators with at most Dd elements [9], as this is the number of generators for the map. Moreover, the set of Kraus operators describing a given CPTP linear map is not unique. Given the two sets $\{K_i\}_{i=1}^N$ and $\{K_i'\}_{i=1}^M$, with $N \geqslant M$, they represent the same CPTP linear map if, and only if, there exists a unitary $U \in \mathrm{SU}(N)$ such that $K_i = \sum_j U_{ij} K_j'$ (where, if necessary, we pad the smallest set with zeros) [9,12].

This more general type of evolution allows for describing processes where there is a loss of information about the system, with pure states evolving to mixed ones. That is the case, for instance, when one is dealing with open quantum systems [16].

For the coarse-graining operations we are going to employ below, the following (see Fig. 2) operational way to describe CPTP linear maps will be handy.

Theorem 2 ([12]). Let $\Lambda : \mathscr{L}(\mathscr{H}_D) \to \mathscr{L}(\mathscr{H}_d)$ be a CPTP linear map. Then there exists an auxiliary Hilbert space $\mathscr{H}_r$, with dimension $r \leqslant d$, and a unitary V acting on $\mathscr{H}_D \otimes \mathscr{H}_r \otimes \mathscr{H}_d$ such that $\forall \psi \in \mathscr{L}(\mathscr{H}_D)$

$$\Lambda(\psi) = \mathrm{Tr}_{Dr}[V(\psi \otimes |0\rangle\langle 0| \otimes |0\rangle\langle 0|)V^\dagger].$$

Operationally, this theorem means that we can interpret CPTP linear maps Λ as a unitary interaction among three systems and further discard the first two parties. See Fig. 2. This interpretation is reminiscent of open quantum systems, where the system interacts unitarily with the environment, with the latter being discarded as we have no control over or interest in it. Here, however, the roles of system and environment are not so well delineated. As we want to allow for maps with different input-output dimensions, the partial trace is taken over the auxiliary system and also over the factor encoding the initial system state.

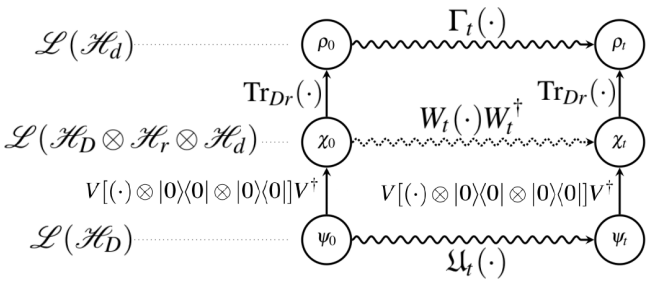

FIG. 3. The distinct levels and dynamics induced by the coarse-graining Λ_{CG}.

The theorems above provide equivalent characterization of CPTP linear maps, and hence we will use them interchangeably. In fact, it is easy to relate them by setting $\forall\,|\psi\rangle \in \mathscr{H}_D$, $V(|\psi\rangle\otimes|0\rangle\otimes|0\rangle) = \sum_{i=1}^{D}\sum_{j=1}^{r}|i\rangle\otimes|j\rangle\otimes K_{ij}(|\psi\rangle)$. This connection shows that the auxiliary system is necessary as to accommodate CPTP linear maps which require a number of Kraus operators bigger than D. We should stress that for a CPTP linear map with a set of Kraus operators $\{K_i\}_{i=1}^{N}$, we take the dimension of $\mathscr{H}_r$ as $r = \lceil N/D\rceil$, and must find an equivalent set of Kraus operators with Dr elements, $\{K_i'\}_{i=1}^{Dr}$. Hence, whenever $N > D$ the auxiliary dimension r will be greater than one.

We are finally in position to establish the coarse-graining operations. Roughly speaking, descriptions are named *coarse grained* when some fine details of the underlying model are smoothed out or replaced by average behaviors. In order to get valid descriptions of states after the coarse graining, we define it as a CPTP linear map that reduces the dimension of the system:

$$\Lambda_{\mathrm{CG}} : \mathscr{L}(\mathscr{H}_D) \to \mathscr{L}(\mathscr{H}_d) \text{ with } D > d.$$

When one is not able to resolve the system in full detail, the coarse-graining map gives an effective state for the system.

Resorting to the characterization of CPTP linear maps in Theorem 2, we know that there exists an auxiliary space $\mathscr{H}_r$ and a unitary $V : \mathscr{H}_D\otimes\mathscr{H}_r\otimes\mathscr{H}_d \to \mathscr{H}_D\otimes\mathscr{H}_r\otimes\mathscr{H}_d$, such that

$$\Lambda_{\mathrm{CG}}(\psi) = \mathrm{Tr}_{Dr}[V(\psi\otimes|0\rangle\langle 0|\otimes|0\rangle\langle 0|)V^\dagger].$$

Operationally, what the unitary V accomplishes is to "write" the accessible degrees of freedom into the party in $\mathscr{H}_d$, while the unaccessible degrees of freedom are left in $\mathscr{H}_D\otimes\mathscr{H}_r$ to be later discarded. See Fig. 3. The intermediate states $\chi_0 = V(\psi_0\otimes|0\rangle\langle 0|\otimes|0\rangle\langle 0|)V^\dagger$ and $\chi_t = V(\psi_t\otimes|0\rangle\langle 0|\otimes|0\rangle\langle 0|)V^\dagger$, which live in $\mathscr{H}_D\otimes\mathscr{H}_r\otimes\mathscr{H}_d$, are virtual states, in the sense that they are mathematical abstractions. In this level, the two contributions of degrees of freedom, accessible and nonaccessible, are split but may be correlated.

A. Example: A blurred and saturated detector

In order to give a concrete example, let us consider a typical optical lattice experiment [25–27]. In these experiments, a periodic oscillating potential is constructed by counterpropagating light beams, and individual atoms are trapped in each potential minimum. In the deep Mott insulator regime, two hyperfine levels of each atom act as a qubit, and neighboring qubits interact with each other via a Heisenberg-like Hamiltonian. The measurement of each atom is made via a fluorescence technique: The atoms are illuminated with a laser in way that if an atom is in the state, say, $|1\rangle$, light is scattered by the atom, whereas if its state is $|0\rangle$, no light is scattered. To resolve the light coming from each atom, a powerful lens is necessary, and only recently a single-atom resolution was accomplished [28].

TABLE I. Coarse graining for a blurred and saturated detector. If a detector does not distinguish between the two systems and does not differ between one or two excitations, this coarse graining gives the effective description of the system.

$\Lambda_{\mathrm{CG}}(\|00\rangle\langle 00\|) = \|0\rangle\langle 0\|$	$\Lambda_{\mathrm{CG}}(\|01\rangle\langle 00\|) = \frac{\|1\rangle\langle 0\|}{\sqrt{3}}$
$\Lambda_{\mathrm{CG}}(\|00\rangle\langle 01\|) = \frac{\|0\rangle\langle 1\|}{\sqrt{3}}$	$\Lambda_{\mathrm{CG}}(\|01\rangle\langle 01\|) = \|1\rangle\langle 1\|$
$\Lambda_{\mathrm{CG}}(\|00\rangle\langle 10\|) = \frac{\|0\rangle\langle 1\|}{\sqrt{3}}$	$\Lambda_{\mathrm{CG}}(\|01\rangle\langle 10\|) = 0$
$\Lambda_{\mathrm{CG}}(\|00\rangle\langle 11\|) = \frac{\|0\rangle\langle 1\|}{\sqrt{3}}$	$\Lambda_{\mathrm{CG}}(\|01\rangle\langle 11\|) = 0$
$\Lambda_{\mathrm{CG}}(\|10\rangle\langle 00\|) = \frac{\|1\rangle\langle 0\|}{\sqrt{3}}$	$\Lambda_{\mathrm{CG}}(\|11\rangle\langle 00\|) = \frac{\|1\rangle\langle 0\|}{\sqrt{3}}$
$\Lambda_{\mathrm{CG}}(\|10\rangle\langle 01\|) = 0$	$\Lambda_{\mathrm{CG}}(\|11\rangle\langle 01\|) = 0$
$\Lambda_{\mathrm{CG}}(\|10\rangle\langle 10\|) = \|1\rangle\langle 1\|$	$\Lambda_{\mathrm{CG}}(\|11\rangle\langle 10\|) = 0$
$\Lambda_{\mathrm{CG}}(\|10\rangle\langle 11\|) = 0$	$\Lambda_{\mathrm{CG}}(\|11\rangle\langle 11\|) = \|1\rangle\langle 1\|$

To simplify, consider the case with only two atoms. Suppose that the lens available is not good enough to resolve the light coming from each individual atom. In this situation, the states $|01\rangle$ and $|10\rangle$ cannot be distinguished. Moreover, imagine that the amount of light coming from a single atom is already sufficient to saturate the detector. Then, having two excitations, $|11\rangle$, or one excitation, $|01\rangle$ or $|10\rangle$, leads to the same signal. In such conditions, describing the experiment with two atoms is superfluous, and an effective description becomes handy. These experimental conditions suggest the coarse graining presented in Table I.

Note that as the detector does not distinguish among the states $|01\rangle$, $|10\rangle$, and $|11\rangle$, there can be no coherence in this subspace. Furthermore, the $1/\sqrt{3}$ factors are necessary to make Λ_{CG} a CPTP linear map. This signals that coherences in the effective description might decrease, but they do not necessarily vanish [21]. This can be readily seen by evaluating the action of Λ_{CG} over a general two-qubit pure state $|\psi\rangle = \sum_{i,j=0}^{1} c_{ij}\,|ij\rangle$, with $c_{ij}\in\mathbb{C}$, which gives

$$\Lambda_{\mathrm{CG}}(|\psi\rangle\langle\psi|) = \begin{pmatrix} |c_{00}|^2 & c_{00}\frac{c_{01}^*+c_{10}^*+c_{11}^*}{\sqrt{3}} \\ c_{00}^*\frac{c_{01}+c_{10}+c_{11}}{\sqrt{3}} & |c_{01}|^2+|c_{10}|^2+|c_{11}|^2 \end{pmatrix}.$$

This effective state accounts for the statistics of all possible measurements that can be carried out by the detector here modeled. It is thus the description that really matters for this experimental condition, not carrying unaccessible information.

The Kraus operators for this map can be easily obtained by a quantum process tomography [9], and are given by

$$K_1 = \begin{pmatrix} 1 & 0 & 0 & 0 \\ 0 & 1/\sqrt{3} & 1/\sqrt{3} & 1/\sqrt{3} \end{pmatrix};$$

$$K_2 = \begin{pmatrix} 0 & 0 & 0 & 0 \\ 0 & 1/\sqrt{3} & 0 & -1/\sqrt{3} \end{pmatrix};$$

$$K_3 = \begin{pmatrix} 0 & 0 & 0 & 0 \\ 0 & 1/\sqrt{3} & -1/\sqrt{3} & 0 \end{pmatrix};$$

$$K_4 = \begin{pmatrix} 0 & 0 & 0 & 0 \\ 0 & 0 & 1/\sqrt{3} & -1/\sqrt{3} \end{pmatrix}.$$

As we have four Kraus operators, $N = 4$, and the dimension of the underlying system is also four, $D = 4$, then the auxiliary system in $\mathscr{H}_r$ can be taken as one dimensional and as such can be ignored. With the above Kraus operators, and neglecting the system in $\mathscr{H}_r$, one can immediately obtain the corresponding unitary V for this example:

$$V = \begin{pmatrix} 1 & 0 & 0 & 0 & 0 & 0 & 0 & 0 \\ 0 & 0 & 1/\sqrt{3} & 0 & 1/\sqrt{3} & 0 & 1/\sqrt{3} & 0 \\ 0 & 1 & 0 & 0 & 0 & 0 & 0 & 0 \\ 0 & 0 & 1/\sqrt{3} & -1/\sqrt{3} & 0 & 0 & -1/\sqrt{3} & 0 \\ 0 & 0 & 0 & 0 & 0 & 1 & 0 & 0 \\ 0 & 0 & 1/\sqrt{3} & 1/\sqrt{3} & -1/\sqrt{3} & 0 & 0 & 0 \\ 0 & 0 & 0 & 0 & 0 & 0 & 0 & 1 \\ 0 & 0 & 0 & 1/\sqrt{3} & 1/\sqrt{3} & 0 & -1/\sqrt{3} & 0 \end{pmatrix}.$$

III. COARSE-GRAINING-INDUCED DYNAMICS

Now we address the central question of this contribution: What are the dynamics that might emerge from a fully quantum description if we are not able to resolve the system in all its details? More concretely, we look for an effective map Γ_t which makes the diagram in Fig. 1 consistent, i.e, in a way that $\rho_t \equiv \Gamma_t(\rho_0) = \Lambda_{\mathrm{CG}} \circ \mathfrak{U}_t(\psi_0)$, with $\rho_0 = \Lambda_{\mathrm{CG}}(\psi_0)$. The induced dynamics then emerges from a coarse-grained description of the underlying dynamics.

To obtain the induced dynamics Γ_t acting on the effective state ρ_0, we generalize the procedure suggested by Štelmachovič and Bužek in Ref. [18]. There they proposed to write the state of the system and environment as the tensor product of its local parts plus a correlation term. Despite the fact that here we do not have such a splitting between system and environment, the action of the unitary V, see Fig. 3, suggests the following decomposition:

$$\chi_0 = (\omega_0 \otimes \rho_0) + (\chi_0 - \omega_0 \otimes \rho_0), \tag{1}$$

where $\chi_0 = V(\psi_0 \otimes |0\rangle\langle 0| \otimes |0\rangle\langle 0|)V^\dagger$, $\rho_0 = \Lambda_{\mathrm{CG}}(\psi_0) = \mathrm{Tr}_{Dr}(\chi_0)$, $\omega_0 = \mathrm{Tr}_d(\chi_0)$. Note that ω_0 is a state in $\mathscr{D}(\mathscr{H}_D \otimes \mathscr{H}_r)$. Equation (1) is equivalent to Štelmachovič and Bužek decomposition in the abstract level $\mathscr{H}_D \otimes \mathscr{H}_r \otimes \mathscr{H}_d$, with the last term now representing the correlation between the degrees of freedom which can be accessed and those that cannot. As V is unitary, we can equivalently write

$$\psi_0 \otimes |0\rangle\langle 0| \otimes |0\rangle\langle 0| = V^\dagger(\omega_0 \otimes \rho_0)V + V^\dagger(\chi_0 - \omega_0 \otimes \rho_0)V. \tag{2}$$

From the left-hand side of Eq. (2), we get the evolved effective state by applying the underlying evolution map $\mathfrak{U}_t$ onto the first tensor factor, followed by the application of V and further partial trace of the two first tensor factors:

$$\begin{aligned} \rho_t &= \Lambda_{\mathrm{CG}} \circ \mathfrak{U}_t(\psi_0) \\ &= \mathrm{Tr}_{Dr}[V(\mathfrak{U}_t(\psi_0) \otimes |0\rangle\langle 0| \otimes |0\rangle\langle 0|)V^\dagger] = \Gamma_t(\rho_0). \end{aligned}$$

The last equality comes from demanding consistence of the diagram in Fig. 1. Accordingly, assuming the underlying evolution map of the form $\mathfrak{U}_t(\cdot) = U_t(\cdot)U_t^\dagger$, from the right-hand side of Eq. (1) we get the effective evolution:

$$\begin{aligned} \Gamma_t(\rho_0) = &\mathrm{Tr}_{Dr}(W_t(\omega_0 \otimes \rho_0)W_t^\dagger) \\ &+ \mathrm{Tr}_{Dr}(W_t(\chi_0 - \omega_0 \otimes \rho_0)W_t^\dagger), \end{aligned} \tag{3}$$

where $W_t = V(U_t \otimes \mathbb{1} \otimes \mathbb{1})V^\dagger$ is the unitary evolution operator in the level $\mathscr{H}_D \otimes \mathscr{H}_r \otimes \mathscr{H}_d$, i.e., $\chi_t = W_t\chi_0 W_t^\dagger$. See Fig 3.

The above evolution equation can be rewritten in a more meaningful way as

$$\Gamma_t(\rho_0) = \sum_{i,j} M_{ij}\rho_0 M_{ij}^\dagger + \mathrm{Tr}_{Dr}[W_t(\chi_0 - \omega_0 \otimes \rho_0)W_t^\dagger], \tag{4}$$

with $M_{ij} = \sqrt{p_j}(\langle\phi_i| \otimes \mathbb{1})W_t(|\phi_j\rangle \otimes \mathbb{1})$, where we employed the spectral decomposition $\omega_0 = \sum_j p_j|\phi_j\rangle\langle\phi_j|$. This is the dynamics that emerges if one is not able, or does not wish, to resolve all the details of the underlying system.

The expression in Eq. (4) is composed by two contributions: The first one displays a Kraus form (see Theorem 1), with $\{M_{ij}\}$ being the corresponding set of effective Kraus operators; the second one represents the evolution of the correlations between accessible and nonaccessible degrees of freedom. This second term can be more clearly appreciated by evoking the Bloch representation of χ_0:

$$\begin{aligned} \chi_0 = \frac{1}{Drd}\Bigg(&\mathbb{1}_{Dr} \otimes \mathbb{1}_d + \mathbb{1}_{Dr} \otimes \vec{\alpha}.\vec{\sigma}_d \\ &+ \vec{\beta}\vec{\sigma}_{Dr} \otimes \mathbb{1}_d + \sum_{i,j} \theta_{ij}\sigma_{Dr}^{(i)} \otimes \sigma_d^{(j)}\Bigg), \end{aligned} \tag{5}$$

where $\vec{\sigma}_q = (\sigma_q^{(1)}, \sigma_q^{(2)}, \ldots, \sigma_q^{(q^2-1)})^T$ is a vector whose components are the $q \times q$ generalized Pauli matrices, $\vec{\alpha} \in \mathbb{R}^{d^2-1}$ is the Bloch vector of ρ_0, $\vec{\beta} \in \mathbb{R}^{(Dr)^2-1}$ is the Bloch vector of ω_0, and the $[(Dr)^2 - 1](d^2 - 1)$ coefficients $\theta_{ij} \in \mathbb{R}$ fix the correlation between accessible and nonaccessible degrees of freedom. Defining the correlation matrix $[\Theta]_{ij} = (\theta_{ij} - \beta_i\alpha_j)/Drd$, the evolution of the coarse-grained state can be written as

$$\Gamma_t(\rho_0) = \sum_{i,j} M_{ij}\rho_0 M_{ij}^\dagger + \sum_{i,j} \Theta_{ij}\mathrm{Tr}_{Dr}\left(W_t\sigma_{Dr}^{(i)} \otimes \sigma_d^{(j)}W_t^\dagger\right). \tag{6}$$

It can be easily verified that $\sum_{i,j} M_{ij}^\dagger M_{ij} = \mathbb{1}_d$, and that $\mathrm{Tr}_d(\mathrm{Tr}_{Dr}(W_t\sigma_{Dr}^{(i)} \otimes \sigma_d^{(j)}W_t^\dagger)) = 0$ as W_t is unitary and the (generalized) Pauli matrices are traceless. These conditions guarantee that $\mathrm{Tr}_d(\Gamma_t(\rho_0)) = 1$ for all times. The structure of this type of evolution is very similar to the one describing open quantum systems when system and environment are initially correlated [17,18].

A. Example: Effective dynamics as seen by a blurred and saturated detector

Consider again the situation described in Subsec. II A: two atoms in neighboring wells of an optical lattice being observed by a blurred and saturated detector. Suppose now that the atoms

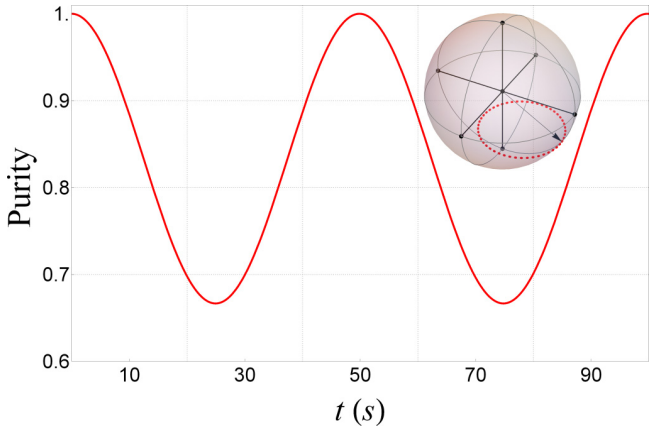

FIG. 4. Effective evolution as seen by a blurred-saturated detector. The plot shows an oscillatory behavior for the purity of the effective state. The inset shows the effective state trajectory in the Bloch sphere. The underlying dynamics is determined by the Hamiltonian $H = \hbar J \sigma_z \otimes \sigma_z$, and we set $J = 1$ rad/s.

interact as specified by the Hamiltonian $H = \hbar J \sigma_z \otimes \sigma_z$, with J a coupling constant in units of frequency. In such situation, an initial two-qubit pure state $|\psi_0\rangle = \sum_{i,j=0}^{1} c_{ij} |ij\rangle$ evolves to

$$|\psi_t\rangle = (c_{00}|00\rangle + c_{11}|11\rangle)e^{-iJt} + (c_{01}|01\rangle + c_{10}|10\rangle)e^{iJt}.$$

The evolution of the effective state can then be easily evaluated via $\rho_t = \Lambda_{CG}(\psi_t)$ to give

$$\rho_t = \begin{pmatrix} |c_{00}|^2 & c_{00}\frac{e^{-2iJt}(c_{01}^*+c_{10}^*)+c_{11}^*}{\sqrt{3}} \\ c_{00}^*\frac{e^{2iJt}(c_{01}+c_{10})+c_{11}}{\sqrt{3}} & |c_{01}|^2+|c_{10}|^2+|c_{11}|^2 \end{pmatrix}.$$

As a concrete example, the effective evolution of a state ψ_0 with all coefficients c_{ij} equal, $c_{ij} = 1/2$ for $i,j \in \{0,1\}$, is shown in the inset of Fig. 4. Figure 4 also shows how the purity, $\mathrm{Tr}(\rho_t^2)$, oscillates with time, exhibiting the alternation between pure and mixed state in the effective level. This is in clear contrast with the complete description of the system, where the system is pure for all times.

It is interesting to notice that the coefficients of ψ_0 define the state ρ_0 but also enter in the definition of the effective map Γ_t. In the above example, this can be verified by evaluating $\omega_0 = \mathrm{Tr}_{Dr}\chi_0$, which will also depend on the coefficients c_{ij}. That in turn, means that the effective Kraus operators M_{ij} will also change with the c_{ij}—thus by changing ρ_0 the map may change. The same is true for the correlation matrix Θ_{ij}. This interdependence of the parameters is treated in the next section, where the properties of Γ_t are analyzed.

IV. PROPERTIES OF Γ_t

The effective map Γ_t is generated by the underlying evolution $\mathfrak{U}_t$, the coarse-graining map Λ_{CG}, and the state ψ_0. Equation (6), however, does not make explicit how the map depends on the elemental state ψ_0. For instance, how do we change the effective map Γ_t for a fixed input state ρ_0? Or, how to change the effective input state keeping Γ_t fixed? In what follows, we address these and other questions, making use of the Bloch representation for ψ_0:

$$\psi_0 = \frac{1}{D}(\mathbb{1}_D + \vec{\gamma}_0.\vec{\sigma}_D), \tag{7}$$

where $\vec{\gamma}_0 \in \mathbb{R}^{D^2-1}$ is the Bloch vector of ψ_0.

A. Fix ρ_0, change Γ_t

Fixed the coarse-graining map, the Bloch vector $\vec{\alpha}$ of ρ_0 is obtained from $\vec{\gamma}_0$ by the linear relations:

$$\begin{cases} \alpha_1 &= \mathrm{Tr}\big[\Lambda_{CG}(\psi_0(\vec{\gamma}_0))\sigma_d^{(1)}\big]; \\ \alpha_2 &= \mathrm{Tr}\big[\Lambda_{CG}(\psi_0(\vec{\gamma}_0))\sigma_d^{(2)}\big]; \\ \vdots & \vdots \quad\quad \vdots \\ \alpha_{d^2-2} &= \mathrm{Tr}\big[\Lambda_{CG}(\psi_0(\vec{\gamma}_0))\sigma_d^{(d^2-2)}\big]; \\ \alpha_{d^2-1} &= \mathrm{Tr}\big[\Lambda_{CG}(\psi_0(\vec{\gamma}_0))\sigma_d^{(d^2-1)}\big]. \end{cases} \tag{8}$$

In the (D^2-1)-dimensional space of Bloch vectors $\vec{\gamma}_0$ of ψ_0, these constraints represent hyperplanes whose intersection depicts the effective state ρ_0. It is important to notice that since $D > d$, the set of linear equations for the coefficients α_j is underdetermined, meaning that various states ψ_0 lead to the same effective state ρ_0. Geometrically, in the γ space, this many-to-one mapping is visualized as an hypersurface of possible solutions.

Now, with this geometric perspective in mind, a fixed coarse graining and a fixed underlying evolution, it can be seem that changes in ψ_0 that move $\vec{\gamma}_0$ parallel to the hyperplanes within the solution hypersurface will not affect the effective state ρ_0. Nevertheless, such change can induce modifications in ω_0 or in Θ, and as such Γ_t will change. A simple example is presented in Fig. 5, and an abstract representation of the γ space and the change in Γ_t can be seen in Fig. 6.

B. Fix Γ_t, change ρ_0: The domain of Γ_t

To change the effective state ρ_0 we must change the value of the α_i's. Geometrically this is represented by moving the hyperplanes, defined in Eq. (8), in the γ space. After the hyperplanes' displacement, a new intersection is obtained representing now another effective state, say, ρ_1. As moving $\vec{\gamma}_0$ parallel to the hyperplanes changes the map, this time we must move $\vec{\gamma}_0$ perpendicular to the hyperplanes. This guarantees that only the effective state is changing. See Fig. 6(a).

It is important to notice that this change might in fact modify ω_0 or Θ. This, however, comes only because of the change in the effective input state, as these quantities might be functions of $\vec{\alpha}$. Putting it differently, the effective Kraus operators might change, but this is only due to the change in the input of the effective map Γ_t. The dynamical equation (6) can be rewritten as to make this dependence explicit:

$$\Gamma_t[\rho_0(\alpha)] = \sum_{i,j} M_{ij}(\alpha)\rho_0(\alpha)M_{ij}^\dagger(\alpha) + \zeta(\alpha), \tag{9}$$

where $\zeta(\alpha) = \sum_{i,j}\Theta_{ij}(\alpha)\mathrm{Tr}_{Dr}(W_t\sigma_{Dr}^{(i)} \otimes \sigma_d^{(j)}W_t^\dagger)$.

We can now determine the domain of a given Γ_t. An effective map Γ_t is generated by an elemental state ψ_0, an underlying evolution map $\mathfrak{U}_t$, and a coarse-graining map Λ_{CG}. This information already gives the first element in the domain

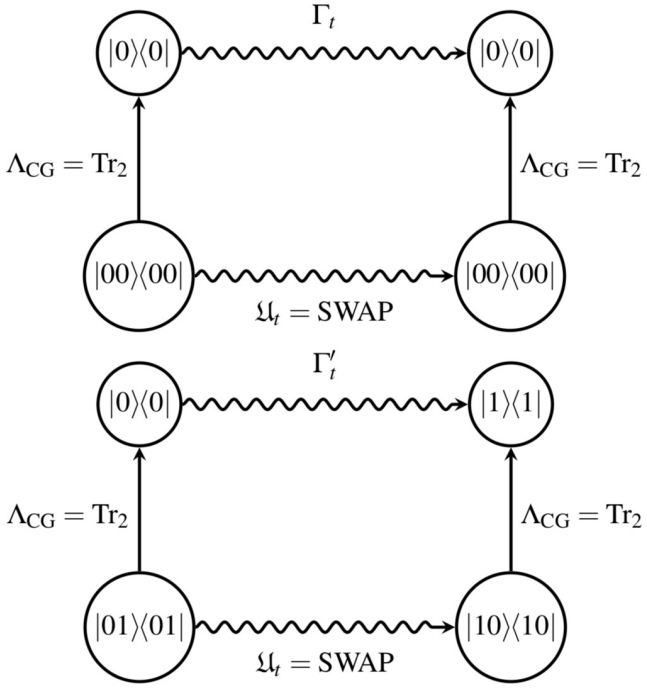

FIG. 5. Simple example of fixing ρ_0 and changing the effective map. For the case where we fix the unitary mapping as the $SWAP$, i.e., $U_t\,|ij\rangle = SWAP\,|ij\rangle = |ji\rangle$, and the coarse graining as the usual partial trace on the second component, we see that different underlying states generate different effective maps. The fact that the emergent maps cannot be the same is clear because if that was the case the same input would lead to two different outputs.

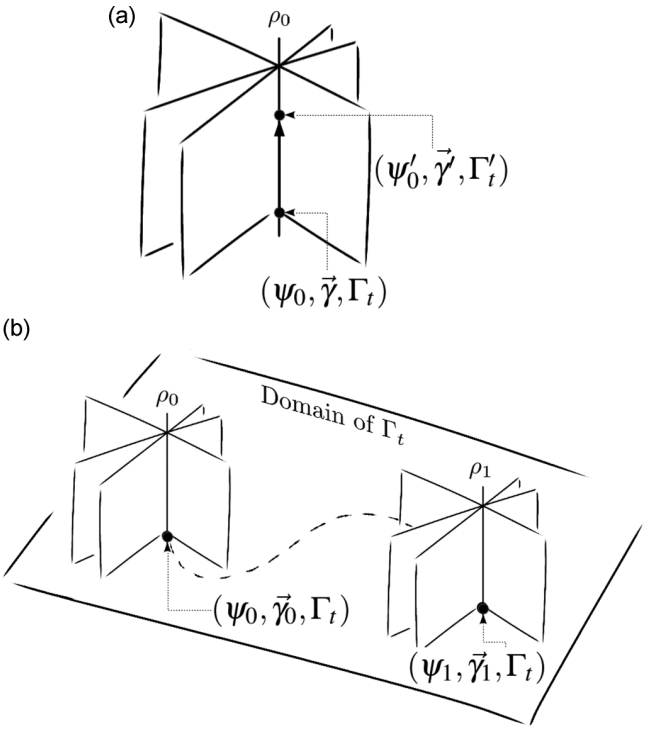

FIG. 6. The γ space, and the effects of changing the underlying state. The intersection between the hyperplanes defines the effective state. A non-point-like region reflects the fact that many underlying states lead to the same effective state. (a) The top panel shows a change in the underlying state that does not change the effective state ρ_0. This change may, nevertheless, have impact on the effective map. (b) Changing the underlying state such that its Bloch vector $\vec{\gamma}$ moves normally to the hyperplanes changes only the effective state preserving the effective map. The region obtained by such normal displacement of the Bloch vector defines the domain of an effective map.

of Γ_t, namely, $\rho_0 = \Lambda_{CG}(\psi_0)$. The coarse graining Λ_{CG} fixes the hyperplanes in the γ space through Eq. (8). Let $\vec{v}_i$ be the normal vector for the ith hyperplane, and $\vec{\gamma}_0$ be the Bloch vector of ψ_0. The domain of Γ_t is then given by all $\rho = \Lambda_{CG}(\psi)$ generated from ψ with Bloch vector $\vec{\gamma}$ for which there exists coefficients $c_i \in \mathbb{R}$ such that $\vec{\gamma} = \vec{\gamma}_0 + \sum_i c_i \vec{v}_i$. The latter condition guarantees that the Bloch vector of all states in the domain of Γ_t can be reached from $\vec{\gamma}_0$ by moving it perpendicular to the hyperplanes in Eq. (8), and as such not changing the effective map.

This immediately implies that the domain of Γ_t is convex: Let $\rho_a = \Lambda_{CG}(\psi_a)$ and $\rho_b = \Lambda_{CG}(\psi_b)$ be in the domain of Γ_t. This means that there exists coefficients $\{a_i\} \subset \mathbb{R}$ and $\{b_i\} \subset \mathbb{R}$ such that the Bloch vectors of ψ_a and ψ_b can be written as $\vec{\gamma}_a = \vec{\gamma}_0 + \sum_i a_i \vec{v}_i$ and $\vec{\gamma}_b = \vec{\gamma}_0 + \sum_i b_i \vec{v}_i$, respectively. There are many states in $\mathscr{L}(\mathscr{H}_D)$ which after the coarse graining lead to the convex combination $\rho = p\rho_a + (1-p)\rho_b$, with $p \in [0,1]$. In particular, the state $\psi = p\psi_a + (1-p)\psi_b$ is such that $\Lambda_{CG}(\psi) = \rho$ and it has Bloch vector $\vec{\gamma}_0 + \sum_i [pa_i + (1-p)b_i]\vec{v}_i$. Therefore the convex combination ρ is also in the domain of Γ_t.

C. Effective positivity and complete-positivity of Γ_t

Equation (9) clearly shows that in general Γ_t is not of Kraus form, like shown in Theorem 1. This means that if Γ_t is taken as a map between states from $\mathscr{D}(\mathscr{H}_d)$ to itself, then Γ_t is not completely positive, possibly not even positive.

However, as we have just seen, the domain of a given Γ_t is not necessarily all the states in $\mathscr{D}(\mathscr{H}_d)$. Restricting the action of Γ_t to its domain guarantees the positivity of the map. This can be immediately verified by the simple consistence of the diagram in Fig. 3, which demands

$$\Gamma_t(\rho_0) = \Gamma_t \circ \Lambda_{CG}(\psi_0) = \Lambda_{CG} \circ \mathfrak{U}_t(\psi_0).$$

As the rightmost part of this equation is a composition of positive maps, then the positivity of the first term is also guaranteed.

The same line of thought can be used to argue for the complete positivity of Γ_t. Indeed, as we are constructing our framework upon quantum mechanics, no contradiction with it can be obtained. However, this argument should not go through without a caveat: Not all extensions of effective states ρ in the domain of a given Γ_t into $\omega \in \mathscr{D}(\mathscr{H}_A \otimes \mathscr{H}_d)$, with $\mathscr{H}_A$ the Hilbert space of an auxiliary system, are possible. The possible extensions for $\rho = \Lambda_{CG}(\psi)$ are those that can be obtained from states $\Psi \in \mathscr{D}(\mathscr{H}_A \otimes \mathscr{H}_D)$ such that $\mathrm{Tr}_A(\Psi) = \psi$, which guarantees that $\mathrm{Tr}_A[\mathbb{1}_A \otimes \Lambda_{CG}(\Psi)] = \rho$, and that ψ generates the map Γ_t (together with the underlying evolution $\mathfrak{U}_t$). We call such a family of states Ψ as the *set of effective complete positivity* for Γ_t. Physically this constraint comes from the

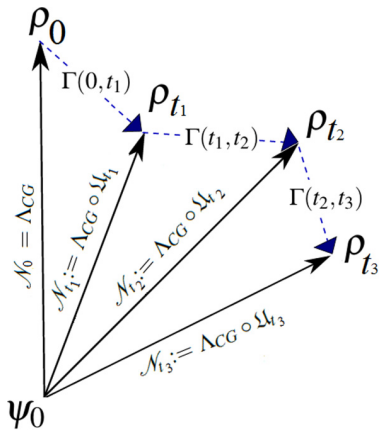

FIG. 7. Recovering strict complete positivity for the effective map. One way to obtain a family of CP effective maps is to require the map $\mathcal{N}_{t_k} = \Lambda_{CG} \circ \mathfrak{U}_{t_k}$ to be CP divisible.

fact that if one does not have control of all the degrees of freedom of a system, then not all the states can be generated. In another perspective, the entanglement that can be created in the fundamental level $\mathscr{H}_A \otimes \mathscr{H}_D$ is, in general, decreased by the action of the coarse-graining map [24].

Strict complete positivity can be reobtained if we demand that the composite map $\mathcal{N}_t := \Lambda_{CG} \circ \mathfrak{U}_t$ to be CP divisible [29]. If that is the case, the definition of CP-divisible maps requires $\mathcal{N}_{t_k} = \Gamma_{(t_k,t_j)} \circ \mathcal{N}_{t_j}$ for all $t_k \geqslant t_j$, with $\Gamma_{(t_k,t_j)}$, the effective evolution map for the time interval $[t_j, t_k]$, completely positive (see Fig. 7). This shows a connection between the theory of coarse-grained maps and the theory of non-Markovian maps [19,29].

V. CONSEQUENCE: EFFECTIVE DISTANCE INCREASE BY Γ_t

A common property of CPTP linear maps (1) is that the distance between two input states cannot increase. Mathematically, let $\Lambda : \mathscr{L}(\mathscr{H}_D) \to \mathscr{L}(\mathscr{H}_d)$ be a CPTP linear map and ψ and ψ' be states in $\mathscr{L}(\mathscr{H}_D)$. Then $||\Lambda(\psi) - \Lambda(\psi')||_1 \leqslant ||\psi - \psi'||_1$, where the 1-norm is defined as $||A||_1 := \mathrm{Tr}(\sqrt{A^\dagger A})$. Physically, this means, for instance, that the discrimination between two unknown quantum states cannot be improved by any further processing of the states [9].

The effective map Γ_t, as discussed in the previous section, is not in general of Kraus form. Can then the distance between two effective states increase? As argued before, no contradiction with quantum mechanics can arise. In fact, it is simple to check that the distance between two effective states is upper bounded, for all times, by the distance between the underlying initial states. Let $\rho_0 = \Lambda_{CG}(\psi_0)$ and $\rho_0' = \Lambda_{CG}(\psi_0')$ be effective states in $\mathscr{L}(\mathscr{H}_d)$ with respective evolved states $\rho_t = \Gamma_t(\rho_0)$ and $\rho_t' = \Gamma_t(\rho_0')$. Then

$$\begin{aligned} ||\rho_t - \rho_t'||_1 &= ||\Lambda_{CG}(\psi_t) - \Lambda_{CG}(\psi_t')||_1; \\ &\leqslant ||\psi_t - \psi_t'||_1; \qquad (10) \\ &= ||\mathfrak{U}_t(\psi_0) - \mathfrak{U}_t(\psi_0')||_1; \\ &\leqslant ||\psi_0 - \psi_0'||_1. \qquad (11) \end{aligned}$$

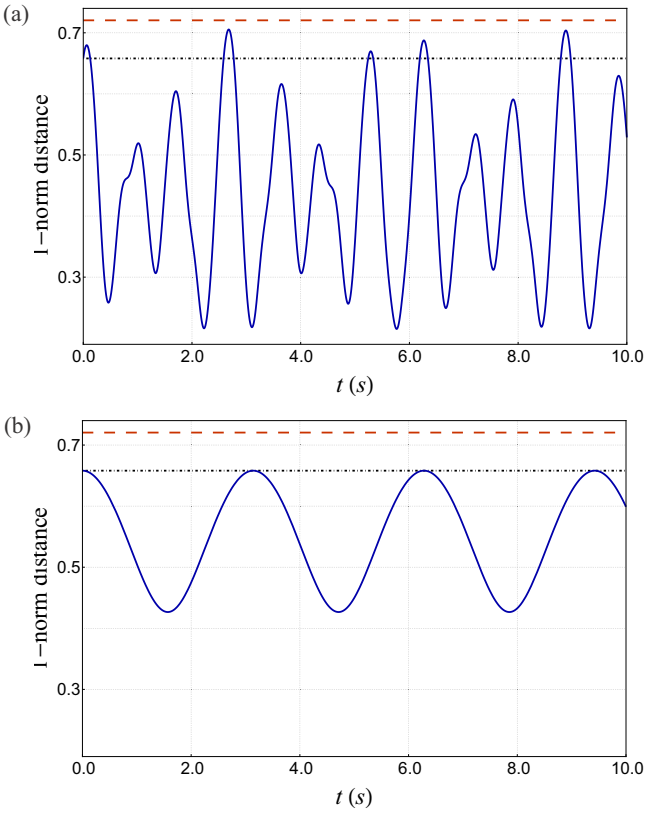

FIG. 8. Distance increase for the effective dynamics. In the above plots, $||\rho_t - \rho_t'||_1$, $||\psi_0 - \psi_0'||_1$, and $||\rho_0 - \rho_0'||_1$ are represented, respectively by the blue continuous line, red dashed line, and the black dot-dashed line. Contrary to the usual contractive property of CPTP linear maps, on the effective level, the distance between two states undergoing the same process may increase. This increase is, however, upper bounded by the distance between the underlying states (red dashed line). (a) The underlying interaction is dictated by the Hamiltonian $H = \hbar J \sigma_z \otimes \sigma_z$. We see that the distance oscillates, increasing for some time intervals. Nevertheless, in this case, we always have $||\rho_0 - \rho_0'||_1 \geqslant ||\rho_t - \rho_t'||_1$. (b) The underlying evolution is dictated by the Hamiltonian $H = \hbar J \sigma_z \otimes \sigma_z + \hbar\Omega(\sigma_x \otimes \mathbb{1} + \mathbb{1} \otimes \sigma_x)$, and we set $J = 1$ rad/s and $\Omega = 3$ rad/s. In this case, we see that $||\rho_t - \rho_t'||_1$ can even go beyond $||\rho_0 - \rho_0'||_1$.

The last inequality turns into an equality in the case of a unitary mapping $\mathfrak{U}_t$, i.e., $\mathfrak{U}_t(.) = U_t(.)U_t^\dagger$ for some unitary U_t.

This, however, does not imply that a distance increasing between effective states is not allowed. In fact, it is possible to have an increase in distance between the effective states undergoing the same effective map. Take, for example, the coarse graining describing the blurred-saturated detector (Sec. II A), the underlying dynamics given by the Hamiltonian $H = \hbar J \sigma_z \otimes \sigma_z$ (Sec. III A), and select two states ψ_0 and ψ_0' which generate the same effective map as in Sec. IV B. Figure 8(a) shows the distance evolution between the two effective states $\rho_t = \Lambda_{\mathrm{CG}}(\psi_t)$ and $\rho_t' = \Lambda_{\mathrm{CG}}(\psi_t')$. A clear oscillation of the distance is observed. In this example, nevertheless, we have that $||\rho_0 - \rho_0'||_1 \geqslant ||\rho_t - \rho_t'||_1$ for all times.

Now, switch on a transversal field, turning the Hamiltonian into $H = \hbar J \sigma_z \otimes \sigma_z + \hbar\Omega(\sigma_x \otimes \mathbb{1} + \mathbb{1} \otimes \sigma_x)$, with Ω the field frequency, and take initial states ψ_0 and ψ_0' in a way to have the same effective map. The evolution of the distance between the effective states is shown in Fig. 8(b). In this case, we see that the distance $||\rho_t - \rho_t'||_1$ can go beyond $||\rho_0 - \rho_0'||_1$ for some specific times.

VI. CONCLUSION

When dealing with complex many-body quantum systems, the full description of the system and of its dynamics is prohibitive. Even in principle, it assumes that one has access to all the system's exponentially (in the number of constituents) many degrees of freedom. A simple system composed of 60 qubits would require in general the measurement of about $(2^{60})^2 \approxeq .1.33 \times 10^{36}$ observables to be fully characterized—even if each measurement is performed in one femtosecond, this would take more than 3000 times the age of the universe to be accomplished. This is only for the state; the characterization of the dynamics is far more complex. Effective descriptions are thus mandatory in order to perceive macroscopic systems.

Pursuing the direction of effective descriptions, here we investigated what types of dynamics may emerge from a full quantum description when one does not have access to, or is not interested in, all the degrees of freedom of a given system. The presented formalism generalizes the theory of open quantum systems, as it works also for closed systems. Here the split between system and environment is substituted by the split between accessible and nonaccessible degrees of freedom. The possibility of correlations between these two types of degrees of freedom may generate effective dynamics that are not of Kraus form—without violating any principle of quantum mechanics. This, in turn, allowed for the distance between two effective states to increase under the action of a fixed effective—in contrast to what is achievable in the underlying quantum description.

Other aspects of this effective dynamics can be further explored: most notably, the fact that the Kraus operators may depend on the state the map is acting on. This suggests a possible way to explain how nonlinear dynamics may emerge from the quantum linear description: If one looks at the system only at time intervals for which the term quantifying correlations between accessible and nonaccessible degrees of freedom, $\zeta(\alpha)$ in Eq. (9), vanishes; i.e., for a coarse-grained time [30], then the nonlinearity of the first term may become apparent. This (possible) nonlinearity together with the distance increase between effective states undergoing the same effective map may be the key to explain how chaotic systems arise from the underlying quantum mechanical description.

Lastly, we hope that the formalism here presented can shed some light on the quantum-to-classical transition: the higher the "zoom out" (stronger coarse graining, in the sense of larger difference between D and d), the more simplified the description of the system and its dynamics becomes, with quantum features fading away. We believe that these ideas can be of interest for areas as quantum thermodynamics—which tries to explain the thermalization of closed quantum systems [20,21]—and even to address the measurement problem in quantum mechanics [31].

ACKNOWLEDGMENTS

Special thanks goes to F. Brito for countless discussions and careful reading of the manuscript. We also thank R. C. Drumond, D. Jonathan, and R. L. de Matos Filho for stimulating discussions. This work is supported by the Brazilian funding agencies CNPq and CAPES, and it is part of the INCT-IQ from CNPq.

[1] H. B. Callen, *Thermodynamics and an Introduction to Thermostatistics*, 2nd ed. (Wiley, New York, 1985).
[2] R. Zwanzig, Phys. Rev. **124**, 983 (1961).
[3] H. Mori, Prog. Theor. Phys. **33**, 423 (1965).
[4] P. Castiglione, M. Falcioni, A. Lesne, and A. Vulpiani, *Chaos and Coarse Grainings in Statistical Mechanics* (Cambridge University Press, Cambridge, UK, 2008).
[5] M. Gell-Mann and J. B. Hartle, Phys. Rev. A **89**, 052125 (2014).
[6] H. Grabert, *Projection Operator Techniques in Nonequilibrium Statistical Mechanics* (Springer Verlag, Berlin, 1982).
[7] L. P. Kadanoff, Physics **2**, 263 (1966).
[8] K. G. Wilson, Rev. Mod. Phys. **47**, 773 (1975).
[9] M. A. Nielsen and I. L. Chuang, *Quantum Computation and Quantum Information* (Cambridge University Press, Cambridge, UK, 2000).
[10] J. Watrous, Theory of quantum information, lecture notes, 2006 [https://cs.uwaterloo.ca/∼watrous/LectureNotes.html].
[11] M. M. Wilde, *Quantum Information Theory* (Cambridge University Press, Cambridge, UK, 2017).
[12] M. M. Wolf, Quantum channels and operations, 2012 [available at https://www-m5.ma.tum.de/foswiki/pub/M5/Allgemeines/MichaelWolf/].
[13] R. Horodecki, P. Horodecki, M. Horodecki, and K. Horodecki, Rev. Mod. Phys. **81**, 865 (2009).
[14] D. Perez-Garcia, F. Verstraete, M. Wolf, and J. Cirac, Quantum Inf. Comput. **7**, 401 (2007).
[15] R. Orús, Ann. Phys. **349**, 117 (2014).
[16] H. P. Breuer and F. Petruccione, *The Theory of Open Quantum Systems* (Oxford University Press, Oxford, UK, 2002).
[17] H. A. Carteret, D. R. Terno, and K. Zyczkowski, Phys. Rev. A **77**, 042113 (2008).
[18] P. Štelmachovič and V. Bužek, Phys. Rev. A **64**, 062106 (2001).
[19] Á. Rivas, S. F. Huelga, and M. B. Plenio, Rep. Prog. Phys. **77**, 094001 (2014).
[20] J. Eisert, M. Friesdorf, and C. Gogolin, Nat. Phys. **11**, 124 (2015).
[21] P. Faist, Quantum coarse-graining: An information-theoretic approach to thermodynamics, Ph.D. thesis, ETH Zurich, Switzerland, 2016.
[22] J. Kofler and C. Brukner, Phys. Rev. Lett. **99**, 180403 (2007).
[23] J. Kofler and C. Brukner, Phys. Rev. Lett. **101**, 090403 (2008).
[24] I. Saideh, S. Felicetti, T. Coudreau, P. Milman, and A. Keller, Phys. Rev. A **94**, 032312 (2016).

[25] J. F. Sherson, C. Weitenberg, M. Endres, M. Cheneau, I. Bloch, and S. Kuhr, Nature (London) **467**, 68 (2010).
[26] T. Fukuhara, S. Hild, J. Zeiher, P. Schauß, I. Bloch, M. Endres, and C. Gross, Phys. Rev. Lett. **115**, 035302 (2015).
[27] P. M. Preiss, R. Ma, M. E. Tai, A. Lukin, M. Rispoli, P. Zupancic, Y. Lahini, R. Islam, and M. Greiner, Science **347**, 1229 (2015).
[28] S. Kuhr, Natl. Sci. Rev. **3**, 170 (2016).
[29] F. Buscemi and N. Datta, Phys. Rev. A **93**, 012101 (2016).
[30] N. K. Bernardes, A. R. R. Carvalho, C. H. Monken, and M. F. Santos, Phys. Rev. A **95**, 032117 (2017).
[31] C. Brukner, in *Quantum [Un]Speakables II: Half a Century of Bell's Theorem*, edited by R. Bertlmann and A. Zeilinger (Springer, Cham, 2017).

Appendix B

Model 3: Λ_{CG} involving averages in the coherent states space

The physical system is the same as before: a system and an apparatus initially in states $|\chi_0\rangle = c_0\,|0\rangle + c_1\,|1\rangle$ and $|x_0\rangle = |-j\rangle$ interact via the Hamiltonian $H = \hbar\omega\,\sigma_z \otimes \vec{n}\cdot\vec{J}$. After a time t, the total entangled state is

$$|\psi_t\rangle = c_0\,e^{-it\omega\,\mathbb{1}\otimes\vec{n}\cdot\vec{J}}\,|0\rangle\,|-j\rangle + c_1\,e^{+it\omega\,\mathbb{1}\otimes\vec{n}\cdot\vec{J}}\,|1\rangle\,|-j\rangle = c_0\,|0\rangle\,|\theta,\phi\rangle + c_1\,|1\rangle\,|-\theta,\phi\rangle\,,$$

representing a superposition of two possible states: an atomic coherent state rotating in clockwise and counterclockwise directions, determined by the states of the target system.

Our objective is to model a quantum measurement process in which the measurement of the apparatus allows the experimentalist to acquire information about the system. And more, due to the inability to access all the apparatus' degrees of freedom, we obtain an effective state for such. We believe that this aspect must be taken into account in the search for understanding why we experience a classical reality in our daily lives.

Inspired by a suggestion of Prof. Časlav Brukner, here we construct a coarse-graining map using the expectation values of the input state ρ on the atomic coherent states $|\Omega_j\rangle \equiv |\theta,\phi\rangle_j$, each of them a point in a generalized sphere which represents the space of angular momentum with dimension $d = 2j+1$. We work with the three different constructions shown below:

$$\begin{aligned}
(i)\,\Lambda_{\mathrm{CG}}(\rho) &= \int d\Omega_j\,\mathcal{N}\,|\Omega_{\frac{1}{2}}\rangle\langle\Omega_j|\rho|\Omega_j\rangle\langle\Omega_{\frac{1}{2}}|;\\
(ii)\,\Lambda_{\mathrm{CG}}(\rho) &= \int d\Omega_j \int d\Omega_j^{'}\,\mathcal{N}_n\,f_n(\Omega_j)\,|\Omega_{\frac{1}{2}}\rangle\langle\Omega_j|\rho|\Omega_j^{'}\rangle\langle\Omega_{\frac{1}{2}}^{'}|\,f_n(\Omega_j^{'})\\
&\quad + \int d\Omega_j \int d\Omega_j^{'}\,\mathcal{N}_s\,f_s(\Omega_j)\,|\Omega_{\frac{1}{2}}\rangle\langle\Omega_j|\rho|\Omega_j^{'}\rangle\langle\Omega_{\frac{1}{2}}^{'}|\,f_s(\Omega_j^{'});
\end{aligned} \tag{B.1}$$

And the (iii),

$$\Lambda_{\mathrm{CG}}(\rho) = \sum_{m,m'}\int d\Omega_j\,\{f_n(\Omega_j) + f_s(\Omega_j)\}g(m,\Omega,\kappa,j)g^*(m',\Omega,\kappa,j)|\Omega_{\frac{1}{2}}\rangle\langle m|\rho|m'\rangle\langle\Omega_{\frac{1}{2}}|, \tag{B.2}$$

with

$$\begin{aligned}
g(m,\Omega,\kappa,j) &= \sqrt{\mathcal{N}(m,\kappa,j)}\,c(\Omega,m,j)\\
&= \sqrt{\mathcal{N}(m,\kappa,j)}\binom{2j}{j+m}^{\frac{1}{2}}\sin^{j+m}(\frac{\theta}{2})\cos^{j-m}(\frac{\theta}{2})e^{i(j+m)\phi}.
\end{aligned} \tag{B.3}$$

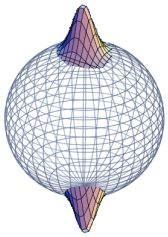

FIGURE B.1: **Fisher-Bingham distribution representing Gaussian functions on the poles of a sphere.** If $\kappa \to 0$ we have an uniform distribution over the sphere. As κ grows, the spread of the distribution increases. In the limit $\kappa \to \infty$ we have delta functions at the poles.

In all cases, $\Lambda_{\text{CG}} : \mathcal{L}(\mathcal{H}_d) \to \mathcal{L}(\mathcal{H}_2)$. We are averaging the d-dimensional state ρ and, after the application of the coarse-graining channel, we end up with an effective description for the apparatus' state in the bi-dimensional angular momentum space. The $\mathcal{N}$'s are normalization constants, and must be determined so that the channels in B.1-B.3 are trace-preserving maps.

The factors $f_n(\Omega_j)$ and $f_s(\Omega_j)$ are Gaussian functions on the surface of a generalized sphere, which represents the d-dimensional angular momentum space, centred in the north (subscript n) and south poles (subscript s) (figure B.1). The role of the Gaussian functions is to introduce a weight in the contributions of the expectation values, favouring those closest to the poles. Its analytical expression is given by the Fisher-Bingham distribution [122], and here takes the form

$$f_n(\Omega) = f_n(\theta) = \frac{\kappa}{4\pi \sinh(\kappa)} e^{-\kappa \cos(\theta)\, j^2}, \tag{B.4}$$

with the parameter $\kappa \geq 0$ controlling the spread of the distribution. For the south pole the exponential argument has opposite sign.

The reader should be warned that we still don't have conclusive results regarding correlations, like those in section 3.3, for the channels listed in B.1. Before proceeding with the calculations, it is important to determine the normalization constants $\mathcal{N}$'s. For simplicity, let's start by the (i) map. Identifying the Kraus operators as $K_\Omega = \sqrt{\mathcal{N}} |\Omega_{\frac{1}{2}}\rangle\langle\Omega_j|$ we must have

$$\int d\Omega\, K_\Omega^\dagger K_\Omega = \mathbb{1} \;\Rightarrow\; \int d\Omega_j \mathcal{N}\, |\Omega_j\rangle\langle\Omega_{\frac{1}{2}}|\Omega_{\frac{1}{2}}\rangle\langle\Omega_j| = \int d\Omega_j \mathcal{N}\, |\Omega_j\rangle\langle\Omega_j| = \mathbb{1}. \tag{B.5}$$

From reference [2] it is known that

$$\int d\Omega_j |\Omega_j\rangle\langle\Omega_j| = \int d\theta d\phi \sin(\theta)\, |\theta,\phi\rangle\langle\theta,\phi| = \frac{4\pi}{2j+1}. \tag{B.6}$$

Then, in the (i) case $\mathcal{N} = \frac{2j+1}{4\pi}$. For the (ii) case we can identify the Kraus operators as

$$K_n = \int d\Omega_j \sqrt{\mathcal{N}_n}\, f_n(\Omega_j)\, |\Omega_{\frac{1}{2}}\rangle\langle\Omega_j| \text{ and } K_s = \int d\Omega_j \sqrt{\mathcal{N}_s}\, f_s(\Omega_j)\, |\Omega_{\frac{1}{2}}\rangle\langle\Omega_j|. \tag{B.7}$$

In order to have a trace-preserving channel, it must be true that $K_n^\dagger K_n + K_s^\dagger K_s = \mathbb{1}$.

$$\begin{aligned}&\int d\Omega_j \int d\Omega_j^{'} \mathcal{N}_n \, f_n(\Omega_j) \, |\Omega_j\rangle\langle\Omega_{\frac{1}{2}}|\Omega_{\frac{1}{2}}^{'}\rangle\langle\Omega_j^{'}| \, f_n(\Omega_j^{'}) \\ + &\int d\Omega_j \int d\Omega_j^{'} \mathcal{N}_s \, f_s(\Omega_j) \, |\Omega_j\rangle\langle\Omega_{\frac{1}{2}}|\Omega_{\frac{1}{2}}^{'}\rangle\langle\Omega_j^{'}| \, f_s(\Omega_j^{'}) = \mathbb{1}.\end{aligned} \tag{B.8}$$

As the two terms above are quite similar, let's work with one of them. Inserting the completeness relation for Dicke states and omitting one of the integration symbols,

$$\int d\Omega_j \, d\Omega_j^{'} \mathcal{N}_n \, f_n(\Omega_j) \, f_n(\Omega_j^{'}) \sum_{m,m',m''} |m\rangle\langle m|\Omega_j\rangle\langle\Omega_{\frac{1}{2}}|m''\rangle\langle m''|\Omega_{\frac{1}{2}}^{'}\rangle\langle\Omega_j^{'}|m'\rangle\langle m'|. \tag{B.9}$$

Notice that the m'' can only assume the values $\{-\frac{1}{2}, \frac{1}{2}\}$ and that in the internal products involving m'', $j = \frac{1}{2}$. Using the relation 3.19,

$$\begin{aligned}&\sum_{m,m',m''} |m\rangle\langle m'| \binom{2j}{m+j}^{\frac{1}{2}} \binom{2j}{m'+j}^{\frac{1}{2}} \int d\theta d\theta' d\phi d\phi' \sin(\theta)\sin(\theta') \, \mathcal{N}_n \, (\frac{\kappa}{4\pi\sinh(\kappa)})^2 \\ &e^{-\kappa j^2(\cos(\theta)+\cos(\theta'))} \sin^{j+m+m''+\frac{1}{2}}(\frac{\theta}{2}) \cos^{j-m-m''+\frac{1}{2}}(\frac{\theta}{2}) e^{-i(j+m-m''-\frac{1}{2})\phi} \\ &\sin^{j+m'+m''+\frac{1}{2}}(\frac{\theta'}{2}) \cos^{j-m'-m''+\frac{1}{2}}(\frac{\theta'}{2}) e^{-i(-j-m'+m''+\frac{1}{2})\phi'}.\end{aligned} \tag{B.10}$$

Discriminating each integral,

$$\begin{aligned}&\sum_{m,m',m''} |m\rangle\langle m'| \binom{2j}{m+j}^{\frac{1}{2}} \binom{2j}{m'+j}^{\frac{1}{2}} \mathcal{N}_n \, (\frac{\kappa}{4\pi\sinh(\kappa)})^2 \\ &\int_0^\pi d\theta \, \sin(\theta) \, \sin^{j+m+m''+\frac{1}{2}}(\frac{\theta}{2}) \, \cos^{j-m-m''+\frac{1}{2}}(\frac{\theta}{2}) \, e^{-\kappa j^2\cos(\theta)} \\ &\int_0^\pi d\theta' \, \sin(\theta') \, \sin^{j+m'+m''+\frac{1}{2}}(\frac{\theta'}{2}) \, \cos^{j-m'-m''+\frac{1}{2}}(\frac{\theta'}{2}) \, e^{-\kappa j^2\cos(\theta')} \\ &\int_0^{2\pi} d\phi \, e^{-i(j+m-m''-\frac{1}{2})\phi} \int_0^{2\pi} d\phi' \, e^{-i(-j-m'+m''+\frac{1}{2})\phi'}.\end{aligned} \tag{B.11}$$

In order to evaluate the integrals in θ, we should make the transformation of variables $\cos(\theta) = u$. Then, evaluating all the integrals; the sum in m''; incorporating the term with the function $f_s(\Omega_j)$ of equation B.8; and finally simplifying, we end

up with

$$\sum_{m,m'} |m\rangle\langle m'| \binom{2j}{m+j}^{\frac{1}{2}} \binom{2j}{m'+j}^{\frac{1}{2}} (\frac{\kappa}{4\pi \sinh(\kappa)})^2 e^{-2\kappa j^2}$$
$$\Big\{ \frac{-4e^{-2i\pi(j+m-\frac{1}{2})}(1+e^{2i\pi(j-\frac{1}{2}+m)})(-1+e^{2i\pi(j+m'-1)})}{(j+m-1)(-1+j+m')}$$
$$\Gamma[\frac{1}{2}(2-m+j)]\Gamma[\frac{1}{2}(3+m+j)]\,\Gamma[\frac{1}{2}(2-m'+j)]\,\Gamma[\frac{1}{2}(3+m'+j)]$$
$$\Big\{ e^{4\kappa j^2}\mathcal{N}_n\,\mathrm{H1F1R}[\frac{1}{2}(2-m+j),\frac{5}{2}+j,-2\kappa j^2]\,\mathrm{H1F1R}[\frac{1}{2}(2-m'+j),\frac{5}{2}+j,-2\kappa j^2]$$
$$+\mathcal{N}_s\,\mathrm{H1F1R}[\frac{1}{2}(2-m+j),\frac{5}{2}+j,+2\kappa j^2]\,\mathrm{H1F1R}[\frac{1}{2}(2-m'+j),\frac{5}{2}+j,+2\kappa j^2]\Big\}$$
$$-e^{-2i\pi(j+m+\frac{1}{2})}(1+e^{2i\pi(j+m+\frac{1}{2})})(-1+e^{2i\pi(j+m')})$$
$$\Gamma[\frac{1}{2}(3-m+j)]\,\Gamma[\frac{1}{2}(m+j)]\,\Gamma[\frac{1}{2}(3-m'+j)]\,\Gamma[\frac{1}{2}(m'+j)]$$
$$\Big\{ e^{4\kappa j^2}\mathcal{N}_n\,\mathrm{H1F1R}[\frac{1}{2}(3-m+j),\frac{5}{2}+j,-2\kappa j^2]\,\mathrm{H1F1R}[\frac{1}{2}(3-m'+j),\frac{5}{2}+j,-2\kappa j^2]$$
$$+\mathcal{N}_s\,\mathrm{H1F1R}[\frac{1}{2}(3-m+j),\frac{5}{2}+j,+2\kappa j^2]\,\mathrm{H1F1R}[\frac{1}{2}(3-m'+j),\frac{5}{2}+j,+2\kappa j^2]\Big\}\Big\} = \mathbb{1}_d, \tag{B.12}$$

where $\Gamma(\cdot)$ is the usual gamma function and H1F1R[a,b,z] is our notation to the regularized confluent hypergeometric function $\frac{{}_1F_1(a,b,z)}{\Gamma(b)}$.

Inspecting equation B.12, it is not simple to find $\mathcal{N}_n$ and $\mathcal{N}_s$ so that the (ii) channel is trace-preserving for any input dimension $d = 2j+1$. To gain some intuition, consider the case $j = \frac{1}{2}$. Back to the ϕ-integrals in sum B.11, they result in $2\pi\,\delta_{m,m''}\,2\pi\,\delta_{m',m''}$.

$$\Rightarrow \sum_{m=-1/2}^{1/2} |m\rangle\langle m| (\frac{\kappa}{\sinh(\kappa)})^2 \frac{1}{4}\{\mathcal{N}_n \int_0^\pi d\theta \sin(\theta)\sin^{1+2m}(\frac{\theta}{2})\cos^{1-2m}(\frac{\theta}{2})\,e^{-\kappa\cos(\theta)/4}$$
$$\int_0^\pi d\theta' \sin(\theta')\sin^{1+2m}(\frac{\theta'}{2})\cos^{1-2m}(\frac{\theta'}{2})\,e^{-\kappa\cos(\theta')/4} + \mathcal{N}_s \int_0^\pi d\theta \sin(\theta)$$
$$\sin^{1+2m}(\frac{\theta}{2})\cos^{1-2m}(\frac{\theta}{2})\,e^{+\kappa\cos(\theta)/4} \int_0^\pi d\theta' \sin(\theta')\sin^{1+2m}(\frac{\theta'}{2})\cos^{1-2m}(\frac{\theta'}{2})\,e^{+\kappa\cos(\theta')/4}\}. \tag{B.13}$$

$$\Rightarrow \sum_{m=-1/2}^{1/2} |m\rangle\langle m| (\frac{\kappa}{\sinh(\kappa)})^2 \frac{1}{4}\Big\{\mathcal{N}_n\{\int_0^\pi d\theta \sin(\theta)\sin^{1+2m}(\frac{\theta}{2})\cos^{1-2m}(\frac{\theta}{2})\,e^{-\kappa\cos(\theta)/4}\}^2$$
$$+\mathcal{N}_s\{\int_0^\pi d\theta \sin(\theta)\sin^{1+2m}(\frac{\theta}{2})\cos^{1-2m}(\frac{\theta}{2})\,e^{+\kappa\cos(\theta)/4}\}^2\Big\}. \tag{B.14}$$

Considering $\mathcal{N}_n = \mathcal{N}_s = \mathcal{N}$,

$$\begin{aligned}
&\Rightarrow |\frac{1}{2}\rangle\langle\frac{1}{2}|\,\mathcal{N}(\frac{\kappa}{\sinh(\kappa)})^2\frac{1}{4}\Big\{\{\int_0^\pi d\theta\,\sin(\theta)\,\sin^2(\frac{\theta}{2})\,e^{-\kappa\cos(\theta)/4}\}^2\\
&+\{\int_0^\pi d\theta\,\sin(\theta)\,\sin^2(\frac{\theta}{2})\,e^{+\kappa\cos(\theta)/4}\}^2\Big\}\\
&+|\frac{-1}{2}\rangle\langle\frac{-1}{2}|\,\mathcal{N}(\frac{\kappa}{\sinh(\kappa)})^2\frac{1}{4}\Big\{\{\int_0^\pi d\theta\,\sin(\theta)\,\cos^2(\frac{\theta}{2})\,e^{-\kappa\cos(\theta)/4}\}^2\\
&+\{\int_0^\pi d\theta\,\sin(\theta)\,\cos^2(\frac{\theta}{2})\,e^{+\kappa\cos(\theta)/4}\}^2\Big\}.
\end{aligned} \tag{B.15}$$

Finally,

$$\begin{aligned}
&\mathcal{N}\,\frac{8[-8+(8+\kappa^2)\cosh(\frac{\kappa}{2})-4\,\kappa\sinh(\frac{\kappa}{2})]}{\sinh^2(\kappa)\,\kappa^2}\;\{|\frac{1}{2}\rangle\langle\frac{1}{2}|+|\frac{-1}{2}\rangle\langle\frac{-1}{2}|\}=\mathbb{1}_2.\\
&\Rightarrow\mathcal{N}(\kappa)=\frac{\sinh^2(\kappa)\,\kappa^2}{8[-8+(8+\kappa^2)\cosh(\frac{\kappa}{2})-4\,\kappa\sinh(\frac{\kappa}{2})]}.
\end{aligned} \tag{B.16}$$

Above we have the normalization constant for the (ii) coarse-graining channel, where we assume that $\mathcal{N}_n = \mathcal{N}_s = \mathcal{N}$ and $j = 1/2$. However, a map $\Lambda_{CG} : \mathcal{L}(\mathcal{H}_2) \to \mathcal{L}(\mathcal{H}_2)$ is not what we consider the ideal case. Motivated by the complexity of the equation B.12, we modified a the coarse-graining channel (ii), obtaining the (iii) map. For such, the Kraus operators can be written as

$$K(\Omega)=\sqrt{f_n(\Omega)+f_s(\Omega)}\sum_{m=-j}^{j}\sqrt{\mathcal{N}(m,\kappa,j)}\,c(\Omega,m,j)|\Omega_{\frac{1}{2}}\rangle\langle m|. \tag{B.17}$$

with $\Lambda_{\mathrm{CG}}(\rho)=\int d\Omega K(\Omega)\rho K^\dagger(\Omega)$. Let's find the normalization $\mathcal{N}(m,\kappa,j)$.

$$\begin{aligned}
\Rightarrow\int d\Omega K^\dagger(\Omega)K(\Omega)&=\int d\Omega\{f_n(\Omega)+f_s(\Omega)\}\\
&\sum_{m,m'}c^*(\Omega,m,j)c(\Omega,m',j)\sqrt{\mathcal{N}(m,\kappa,j)}\sqrt{\mathcal{N}(m',\kappa,j)}|m\rangle\langle m'|.
\end{aligned} \tag{B.18}$$

$$\begin{aligned}
&=\sum_{m,m'}\sqrt{\mathcal{N}(m',\kappa,j)}\sqrt{\mathcal{N}(m,\kappa,j)}\binom{2j}{j+m}^{\frac{1}{2}}\binom{2j}{j+m'}^{\frac{1}{2}}|m\rangle\langle m'|\\
&\int_0^\pi d\theta\,\sin(\theta)\{f_n(\theta)+f_s(\theta)\}\sin^{2j+m+m'}(\frac{\theta}{2})\cos^{2j-m-m'}(\frac{\theta}{2})\int_0^{2\pi}d\phi\,e^{i(m'-m)\phi}.
\end{aligned} \tag{B.19}$$

Since the ϕ-integral give us $2\pi\,\delta_{m,m'}$,

$$\begin{aligned}
&=\sum_m\mathcal{N}(m,\kappa,j)\binom{2j}{j+m}|m\rangle\langle m|\frac{\kappa}{2\sinh(\kappa)}\\
&\Big\{\int_0^\pi d\theta\,\sin(\theta)e^{-\kappa j^2\cos(\theta)}\sin^{2j+2m}(\frac{\theta}{2})\cos^{2j-2m}(\frac{\theta}{2})\\
&+\int_0^\pi d\theta\,\sin(\theta)e^{+\kappa j^2\cos(\theta)}\sin^{2j+2m}(\frac{\theta}{2})\cos^{2j-2m}(\frac{\theta}{2})\Big\}.
\end{aligned} \tag{B.20}$$

Evaluating the θ-integrals,

$$\Rightarrow \int d\Omega K^{\dagger}(\Omega)K(\Omega) = \sum_{m} \mathcal{N}(m,\kappa,j)|m\rangle\langle m| \frac{2j!\,\kappa\, e^{-j^2\kappa}}{\sinh(\kappa)} \big\{ \mathrm{H1F1R}[1+j-m, 2+2j, 2j^2\kappa] + \mathrm{H1F1R}[1+j+m, 2+2j, 2j^2\kappa] \big\}. \tag{B.21}$$

Therefore, the normalization $\mathcal{N}(m,\kappa,j)$ for the (iii) map must be

$$\mathcal{N}(m,\kappa,j) = \frac{e^{j^2\kappa}\sinh(\kappa)}{2j!\,\kappa\,\big\{\mathrm{H1F1R}[1+j-m, 2+2j, 2j^2\kappa] + \mathrm{H1F1R}[1+j+m, 2+2j, 2j^2\kappa]\big\}}. \tag{B.22}$$

In the last few pages we have built three different coarse-graining channels with a better physical intuition than the one of section 3.3, as well as find their respective normalization constants. However, when inspecting the quantum correlations through the concurrence and mutual information, the results are not so interesting as the ones in section 3.3. This motivates us to continue our attempts to model a quantum measurement process, seeking to construct a coarse-graining map as close as possible to the ideal.

Bibliography

[1] Jacob F. Sherson, Christof Weitenberg, Manuel Endres, Marc Cheneau, Immanuel Bloch, and Stefan Kuhr. Single-atom-resolved fluorescence imaging of an atomic mott insulator. *Nature*, 467:68–72, September 2010.

[2] F. T. Arecchi, Eric Courtens, Robert Gilmore, and Harry Thomas. Atomic coherent states in quantum optics. *Phys. Rev. A*, 6:2211–2237, Dec 1972.

[3] Krishan Kumar Zahar. Modernization. *Encyclopedia Britannica*, March 2016.

[4] W. Mulligan and M. Bric. *A Global History of Anti-Slavery Politics in the Nineteenth Century*. Palgrave Macmillan UK, 2013.

[5] J.C. Maxwell. *A treatise on electricity and magnetism*. Number v. 1-2 in A Treatise on Electricity and Magnetism. Dover Publications, 1954.

[6] H.R. Hertz. Ueber sehr schnelle electrische schwingungen. *Annalen der Physik*, 267(7):421–448, may 1887.

[7] H.R. Hertz. Ueber die einwirkung einer geradlinigen electrischen schwingung auf eine benachbarte strombahn. *Annalen der Physik*, 270(5):155–170, march 1888.

[8] H.R. Hertz. Ueber die ausbreitungsgeschwindigkeit der electrodynamischen wirkungen. *Annalen der Physik*, 270(7):551–569, May 1888.

[9] H.R. Hertz. Ueber einen einfluss des ultravioletten lichtes auf die electrische entladung. *Annalen der Physik*, 267(31):983–1000, june 1887.

[10] Pierre-Marie Robitaille. Kirchhoff's law of thermal emission: 150 years. *Progress in Physics*, 4, October 2009.

[11] M. Born. *My life: recollections of a Nobel laureate*. Scribner, 1978.

[12] J J O'Connor and E F Robertson. William thomson (lord kelvin). *MacTutor History of Mathematics archive*, October 2003.

[13] Max Planck. On the law of distribution of energy in the normal spectrum. *Annalen der Physik*, 4:553, 1901.

[14] Ludwig Boltzmann. Über die beziehung zwischen dem zweiten hauptsatze der mechanischen wärmetheorie und der wahrscheinlichkeitsrechnung respektive den sätzen über das wärmegleichgewicht. *Wien. Ber.*, 76:373–435, 1877.

[15] Albert Einstein. On a heuristic point of view about the creation and conversion of light. *Annalen der Physik*, 17:132–148, 1905.

[16] Iwo Bialynicki-Birula and Zofia Bialynicka-Birula. Why photons cannot be sharply localized. *Phys. Rev. A*, 79:032112, Mar 2009.

[17] A. Einstein. Die plancksche theorie der strahlung und die theorie der spezifischen wärme. *Annalen der Physik*, 327(1):180–190, 1907.

[18] N. Bohr. The spectra of helium and hydrogen. *Nature*, 92:231–232, 1913.

[19] W. Gerlach and O. Stern. Der experimentelle nachweis des magnetischen moments des silberatoms. *Zeitschrift für Physik*, 8(1):110–111, Dec 1922.

[20] Walther Gerlach and Otto Stern. Der experimentelle nachweis der richtungsquantelung im magnetfeld. *Zeitschrift für Physik*, 9(1):349–352, Dec 1922.

[21] Walther Gerlach and Otto Stern. Das magnetische moment des silberatoms. *Zeitschrift für Physik*, 9(1):353–355, Dec 1922.

[22] Louis De Broglie. Xxxv. a tentative theory of light quanta. *Philosophical Magazine Letters*, 86(7):446–458, 1924.

[23] M. Born and P. Jordan. Zur quantenmechanik. *Zeitschrift für Physik*, 34(1):858–888, Dec 1925.

[24] M. Born, W. Heisenberg, and P. Jordan. Zur quantenmechanik. ii. *Zeitschrift für Physik*, 35(8):557–615, Aug 1926.

[25] E. Schrödinger. An undulatory theory of the mechanics of atoms and molecules. *Phys. Rev.*, 28:1049–1070, Dec 1926.

[26] Paul Adrien Maurice Dirac. The quantum theory of the electron. *Proceedings of the royal society A*, 117:610–624, Feb 1928.

[27] W. Heisenberg. Über den anschaulichen inhalt der quantentheoretischen kinematik und mechanik. *Zeitschrift für Physik*, 43(3):172–198, Mar 1927.

[28] Nicolas Gisin. *Collapse. What Else?*, page 207–224. Cambridge University Press, 2018.

[29] A. Einstein, B. Podolsky, and N. Rosen. Can quantum-mechanical description of physical reality be considered complete? *Phys. Rev.*, 47:777–780, May 1935.

[30] E. Schrödinger. Die gegenwärtige situation in der quantenmechanik. *Die Naturwissenschaften*, 23:807–812, 1935.

[31] C. Davisson and L. H. Germer. Diffraction of electrons by a crystal of nickel. *Phys. Rev.*, 30:705–740, Dec 1927.

[32] J. von Neumann. *Matematische Grundlagen der Quantenmechanic*. Springer, Berlin, 1932.

[33] Hugh Everett. "relative state" formulation of quantum mechanics. *Rev. Mod. Phys.*, 29:454–462, Jul 1957.

[34] B.S. Dewitt and N. Graham. *The Many Worlds Interpretation of Quantum Mechanics*. Princeton Series in Physics. Princeton University Press, 2015.

[35] David Bohm. A suggested interpretation of the quantum theory in terms of "hidden" variables. i. *Phys. Rev.*, 85:166–179, Jan 1952.

[36] David Bohm. A suggested interpretation of the quantum theory in terms of "hidden" variables. ii. *Phys. Rev.*, 85:180–193, Jan 1952.

[37] H.H. Stroke. *The Physical Review: The First Hundred Years*. Key papers in physics. American Inst. of Physics, 1999.

[38] Valia Allori, Detlef D$uuml$rr, Shelly Goldstein, and Nino Zangh$iacute$. Seven steps towards the classical world. *Journal of Optics B: Quantum and Semiclassical Optics*, 4(4):S482–S488, aug 2002.

[39] M. Schlosshauer. Decoherence, the measurement problem, and interpretations of quantum mechanics. *Rev. Mod. Phys.*, 76(4):1267, 2004.

[40] Harvey R. Brown and David Wallace. Solving the measurement problem: De broglie–bohm loses out to everett. *Foundations of Physics*, 35(4):517–540, Apr 2005.

[41] Peter Markowich, Thierry Paul, and Christof Sparber. Bohmian measures and their classical limit. *Journal of Functional Analysis*, 259(6):1542 – 1576, 2010.

[42] Eugene P. Wigner. Remarks on the mind-body question. In I. J. Good, editor, *The Scientist Speculates*. Heineman, 1961.

[43] Paola Cappellaro. Quantum engineering group mit. http://qeg.mit.edu/, 2019.

[44] Macimilian A. Schlosshauer. *Decoherence and the Quantum-To-Classical Transition*. Springer-Verlag Berlin Heidelberg, 1st edition, 2007.

[45] W. H. Zurek. Pointer basis of quantum apparatus: Into what mixture does the wave packet collapse? *Phys. Rev. D*, 24:1516–1525, Sep 1981.

[46] W. H. Zurek. Environment-induced superselection rules. *Phys. Rev. D*, 26:1862–1880, Oct 1982.

[47] H. D. Zeh. On the interpretation of measurement in quantum theory. *Foundations of Physics*, 1(1):69–76, 1970.

[48] Osvaldo Pessoa. Can the decoherence approach help to solve the measurement problem? *Synthese*, 113(3):323–346, Dec 1997.

[49] A.O Caldeira and A.J Leggett. Quantum tunnelling in a dissipative system. *Annals of Physics*, 149(2):374 – 456, 1983.

[50] Wojciech Hubert Zurek. Decoherence, einselection, and the quantum origins of the classical. *Rev. Mod. Phys.*, 75:715–775, May 2003.

[51] W. H. Zurek. Quantum darwinism. *Nature Physics*, 5, 2009.

[52] C. Jess Riedel and Wojciech H. Zurek. Quantum darwinism in an everyday environment: Huge redundancy in scattered photons. *Phys. Rev. Lett.*, 105:020404, Jul 2010.

[53] F.G.S.L. Brandão, M. Piani, and P. Horodecki. Generic emergence of classical features in quantum darwinism. *Nature Communications*, 6, 2015.

[54] Harold Ollivier, David Poulin, and Wojciech H. Zurek. Objective properties from subjective quantum states: Environment as a witness. *Phys. Rev. Lett.*, 93:220401, Nov 2004.

[55] Robin Blume-Kohout and Wojciech H. Zurek. Quantum darwinism: Entanglement, branches, and the emergent classicality of redundantly stored quantum information. *Phys. Rev. A*, 73:062310, Jun 2006.

[56] W. K. Wootters and W. H. Zurek. A single quantum cannot be cloned. *Nature*, 299:802–803, 1982.

[57] Harold Ollivier, David Poulin, and Wojciech H. Zurek. Environment as a witness: Selective proliferation of information and emergence of objectivity in a quantum universe. *Phys. Rev. A*, 72:042113, Oct 2005.

[58] F. M. Cucchietti, J. P. Paz, and W. H. Zurek. Decoherence from spin environments. *Phys. Rev. A*, 72:052113, Nov 2005.

[59] Juan Pablo Paz and Wojciech Hubert Zurek. Quantum limit of decoherence: Environment induced superselection of energy eigenstates. *Phys. Rev. Lett.*, 82:5181–5185, Jun 1999.

[60] Diego A. R. Dalvit, Jacek Dziarmaga, and Wojciech H. Zurek. Unconditional pointer states from conditional master equations. *Phys. Rev. Lett.*, 86:373–376, Jan 2001.

[61] Michael Zwolak, H. T. Quan, and Wojciech H. Zurek. Quantum darwinism in a mixed environment. *Phys. Rev. Lett.*, 103:110402, Sep 2009.

[62] C. Jess Riedel, Wojciech H. Zurek, and Michael Zwolak. Objective past of a quantum universe: Redundant records of consistent histories. *Phys. Rev. A*, 93:032126, Mar 2016.

[63] Maciej Lewenstein, Anna Sanpera, Veronica Ahufinger, Bogdan Damski, Adit Sen(De), and Ujjwal Sen. Ultracold atomic gases in optical lattices: mimicking condensed matter physics and beyond. *Advances in Physics*, 56(2):243–379, 2007.

[64] Immanuel Bloch, Jean Dalibard, and Sylvain Nascimbene. Quantum simulations with ultracold quantum gases. *Nature Physics*, 8:267–276, april 2012.

[65] C. Foti, T. Heinosaari, S. Maniscalco, and P. Verrucchi. Whenever a quantum environment emerges as a classical system, it behaves like a measuring apparatus. *ArXiv e-prints*, 2018.

[66] Johannes Kofler and Časlav Brukner. Classical world arising out of quantum physics under the restriction of coarse-grained measurements. *Phys. Rev. Lett.*, 99:180403, Nov 2007.

[67] Johannes Kofler and Časlav Brukner. Conditions for quantum violation of macroscopic realism. *Phys. Rev. Lett.*, 101:090403, Aug 2008.

[68] Brian Julsgaard, Alexander Kozhekin, and Eugene S. Polzik. Experimental long-lived entanglement of two macroscopic objects. *Nature*, 413:400, 2001.

[69] K. C. Lee, M. R. Sprague, B. J. Sussman, J. Nunn, N. K. Langford, X.-M. Jin, T. Champion, P. Michelberger, K. F. Reim, D. England, D. Jaksch, and I. A. Walmsley. Entangling macroscopic diamonds at room temperature. *Science*, 334(6060):1253–1256, 2011.

[70] Paul V. Klimov, Abram L. Falk, David J. Christle, Viatcheslav V. Dobrovitski, and David D. Awschalom. Quantum entanglement at ambient conditions in a macroscopic solid-state spin ensemble. *Science Advances*, 1(10), 2015.

[71] C. F. Ockeloen-Korppi, E. Damskägg, J.-M. Pirkkalainen, M. Asjad, A. A. Clerk, F. Massel, M. J. Woolley, and M. A. Sillanpää. Stabilized entanglement of massive mechanical oscillators. *Nature*, 556:478–482, 2018.

[72] Bastian Hacker, Stephan Welte, Severin Daiss, Armin Shaukat, Stephan Ritter, Lin Li, and Gerhard Rempe. Deterministic creation of entangled atom–light schrödinger-cat states. *Nature Photonics*, 13:110–115, January 2019.

[73] Robert Zwanzig. Memory effects in irreversible thermodynamics. *Phys. Rev.*, 124:983, Nov 1961.

[74] Hazime Mori. Transport, collective motion, and brownian motion*). *Progress of Theoretical Physics*, 33(3):423, 1965.

[75] P. Castiglione, M. Falcioni, A. Lesne, and A. Vulpiani. *Chaos and Coarse Grainings in Statistical Mechanics*. Cambridge University Press, 2008.

[76] Murray Gell-Mann and James B. Hartle. Adaptive coarse graining, environment, strong decoherence, and quasiclassical realms. *Phys. Rev. A*, 89:052125, May 2014.

[77] H. Grabert. *Projection Operator Techniques in Nonequilibrium Statistical Mechanics*. Springer Verlag, 1982.

[78] Leo P. Kadanoff, Wolfgang Götze, David Hamblen, Robert Hecht, E. A. S. Lewis, V. V. Palciauskas, Martin Rayl, J. Swift, David Aspnes, and Joseph Kane. Static phenomena near critical points: Theory and experiment. *Rev. Mod. Phys.*, 39:395–431, Apr 1967.

[79] Kenneth G. Wilson. Renormalization group and critical phenomena. i. renormalization group and the kadanoff scaling picture. *Phys. Rev. B*, 4:3174–3183, Nov 1971.

[80] Michael M. Wolf. Quantum channels & operations, 2012. available at https://www-m5.ma.tum.de/foswiki/pub/M5/Allgemeines/MichaelWolf/.

[81] J. Watrous. Theory of quantum information. lecture notes., 2006. available on-line at https://cs.uwaterloo.ca/∼watrous/LectureNotes.html.

[82] Mark M. Wilde. *Quantum Information Theory*. Cambridge University Press, 2017.

[83] Holevo Alexander S. *Quantum Systems, Channels, Information, A Mathematical Introduction*. De Gruyter, 2012.

[84] Michael A. Nielsen and Isaac L. Chuang. *Quantum Computation and Quantum Information: 10th Anniversary Edition*. Cambridge University Press, New York, NY, USA, 10th edition, 2011.

[85] Cristhiano Duarte, Gabriel Dias Carvalho, Nadja K. Bernardes, and Fernando de Melo. Emerging dynamics arising from coarse-grained quantum systems. *Phys. Rev. A*, 96:032113, Sep 2017.

[86] Man-Duen Choi. Positive linear maps on c*-algebras. *Canadian Journal of Mathematics*, 24(3):520 – 529, 1972.

[87] A. Jamiolkowski. Linear transformations which preserve trace and positive semidefiniteness of operators. *Reports on Mathematical Physics*, 3(4):275 – 278, 1972.

[88] Man-Duen Choi. Completely positive linear maps on complex matrices. *Linear Algebra and its Applications*, 10(3):285 – 290, 1975.

[89] W. Forrest Stinespring. Positive functions on c*-algebras. *Proceedings of the American Mathematical Society*, 6:211 – 216, 1955.

[90] M. A. Neumark. On a representation of additive operator set functions. *Doklady Akademii Nauk SSSR*, 41:359 – 361, 1943.

[91] K Kraus. General state changes in quantum theory. *Annals of Physics*, 64(2):311 – 335, 1971.

[92] Peter Štelmachovič and Vladimír Bužek. Dynamics of open quantum systems initially entangled with environment: Beyond the kraus representation. *Phys. Rev. A*, 64:062106, Nov 2001.

[93] Hilary A. Carteret, Daniel R. Terno, and Karol Życzkowski. Dynamics beyond completely positive maps: Some properties and applications. *Phys. Rev. A*, 77:042113, Apr 2008.

[94] Francesco Buscemi and Nilanjana Datta. Equivalence between divisibility and monotonic decrease of information in classical and quantum stochastic processes. *Phys. Rev. A*, 93:012101, Jan 2016.

[95] A Rivas, SF Huelga, and MB Plenio. Quantum non-markovianity: characterization, quantification and detection. *Reports on progress in physics*, 77:094001, 2014.

[96] C. Cohen-Tannoudji, B. Diu, and F. Laloë. *Quantum Mechanics*. Hermann, Paris, 1977.

[97] J. A. Wheeler and W. Hubert Zurek, editors. *Quantum Theory and Measurement*. Princeton University Press, Princeton, NJ, 1983.

[98] Kurt Jacobs. *Quantum Measurement Theory and its Applications*. Cambridge University Press, first edition, 2014.

[99] E. Joos, H. D. Zeh, C. Kiefer, D. Giulini, J. Kupsch, and I. O. Stamatescu. *Decoherence and the Appearance of a Classical World in Quantum Theory*. Springer, 2003.

[100] W. H. Zurek. Decoherence and the transition from quantum to classical. *Physics Today*, 52:24, 1999.

[101] C. Brukner. On the quantum measurement problem. *ArXiv e-prints*, July 2015.

[102] Ibrahim Saideh, A. D. Ribeiro, Giulia Ferrini, Thomas Coudreau, Pérola Milman, and Arne Keller. General dichotomization procedure to provide qudit entanglement criteria. *Phys. Rev. A*, 92:052334, Nov 2015.

[103] M. Brune, S. Haroche, J. M. Raimond, L. Davidovich, and N. Zagury. Manipulation of photons in a cavity by dispersive atom-field coupling: Quantum-nondemolition measurements and generation of "schrödinger cat" states. *Phys. Rev. A*, 45:5193–5214, Apr 1992.

[104] Scott Hill and William K. Wootters. Entanglement of a pair of quantum bits. *Phys. Rev. Lett.*, 78:5022–5025, Jun 1997.

[105] William K. Wootters. Entanglement of formation of an arbitrary state of two qubits. *Phys. Rev. Lett.*, 80:2245–2248, Mar 1998.

[106] Ivan S. Oliveira, Tito J. Bonagamba, Roberto S. Sarthour, Jair C.C. Freitas, and Eduardo R. deAzevedo, editors. *NMR Quantum Information Processing*. Elsevier Science B.V., Amsterdam, 2007.

[107] David Poulin. Macroscopic observables. *Phys. Rev. A*, 71:022102, Feb 2005.

[108] H.P. Breuer and F. Petruccione. *The Theory of Open Quantum Systems*. Oxford University Press, 2002.

[109] Nadja K. Bernardes, Andre R. R. Carvalho, C. H. Monken, and Marcelo F. Santos. Coarse graining a non-markovian collisional model. *Phys. Rev. A*, 95:032117, Mar 2017.

[110] J. Eisert, M. Friesdorf, and C. Gogolin. Quantum many-body systems out of equilibrium. *Nature Physics*, 11(2):124 – 130, 2015.

[111] P. Faist. Quantum Coarse-Graining: An Information-Theoretic Approach to Thermodynamics. *ArXiv e-prints*, July 2016.

[112] Inés de Vega and Daniel Alonso. Dynamics of non-markovian open quantum systems. *Rev. Mod. Phys.*, 89:015001, Jan 2017.

[113] M. M. Wolf, J. Eisert, T. S. Cubitt, and J. I. Cirac. Assessing non-markovian quantum dynamics. *Phys. Rev. Lett.*, 101:150402, Oct 2008.

[114] Ángel Rivas, Susana F. Huelga, and Martin B. Plenio. Entanglement and non-markovianity of quantum evolutions. *Phys. Rev. Lett.*, 105:050403, Jul 2010.

[115] A. J. van Wonderen and K. Lendi. Virtues and limitations of markovian master equations with a time-dependent generator. *Journal of Statistical Physics*, 100(3):633–658, 2000.

[116] R. Alicki and K. Lendi. *Quantum Dynamical Semigroups and Applications*. Lecture Notes in Physics. Springer-Verlag Berlin Heidelberg, 1987.

[117] James Millen and André Xuereb. Perspective on quantum thermodynamics. *New Journal of Physics*, 18(1):011002, 2016.

[118] Sai Vinjanampathy and Janet Anders. Quantum thermodynamics. *Contemporary Physics*, 57(4):545–579, 2016.

[119] Adam M. Kaufman, M. Eric Tai, Alexander Lukin, Matthew Rispoli, Robert Schittko, Philipp M. Preiss, and Markus Greiner. Quantum thermalization through entanglement in an isolated many-body system. *Science*, 353(6301):794–800, 2016.

[120] V. Dunjko and M. Olshanii. Thermalization from the perspective of eigenstate thermalization hypothesis. *Annual Review of Cold Atoms and Molecules*, pages 443–471, 2013.

[121] Borivoje Dakić and Časlav Brukner. *The Classical Limit of a Physical Theory and the Dimensionality of Space*, pages 249–282. Springer Netherlands, Dordrecht, 2016.

[122] John T. Kent. The fisher-bingham distribution on the sphere. *Journal of the Royal Statistical Society. Series B (Methodological)*, 44(1):71–80, 1982.